

Aus der Klinik und Poliklinik für Dermatologie und Venerologie  
der Universität zu Köln  
Direktorin: Universitätsprofessorin Dr. med. E. R. von Stebut-Borschitz

**Analysis of skin myeloid cells in C57BL/6 and  
BALB/c mice following low-dose *Leishmania*  
*major* infection**

Inaugural-Dissertation zur Erlangung der ärztlichen Doktorwürde  
der Medizinischen Fakultät  
der Universität zu Köln

vorgelegt von  
Katharina Inga Inselmann

promoviert am 22. Mai 2025

Gedruckt mit Genehmigung der Medizinischen Fakultät der Universität zu Köln  
2025

Dekan: Universitätsprofessor Dr. med. G. R. Fink

1. Gutachterin: Universitätsprofessorin Dr. med. E. R. von Stebut-Borschitz
2. Gutachterin: Professorin Dr. PhD C. Niessen

## Erklärung

Ich erkläre hiermit, dass ich die vorliegende Dissertationsschrift ohne unzulässige Hilfe Dritter und ohne Benutzung anderer als der angegebenen Hilfsmittel angefertigt habe; die aus fremden Quellen direkt oder indirekt übernommenen Gedanken sind als solche kenntlich gemacht.

Bei der Auswahl und Auswertung des Materials sowie bei der Herstellung des Manuskriptes habe ich keine Unterstützungsleistungen erhalten.

Weitere Personen waren an der Erstellung der vorliegenden Arbeit nicht beteiligt. Insbesondere habe ich nicht die Hilfe einer Promotionsberaterin/eines Promotionsberaters in Anspruch genommen. Dritte haben von mir weder unmittelbar noch mittelbar geldwerte Leistungen für Arbeiten erhalten, die im Zusammenhang mit dem Inhalt der vorgelegten Dissertationsschrift stehen.

Die Dissertationsschrift wurde von mir bisher weder im Inland noch im Ausland in gleicher oder ähnlicher Form einer anderen Prüfungsbehörde vorgelegt.

Die dieser Arbeit zugrunde liegenden Experimente sind von mir mit Unterstützung von Frau Dr. rer. nat. Dominika Lukas und Herrn Dr. rer. nat. Nir Yogev und den biologisch-technischen Assistentinnen Frau Beate Lorenz und Frau Marion Reibetanz durchgeführt worden.

Die Isolierung der Leishmanien sowie die damit erfolgten intradermalen Infektionen der Versuchstiere und die Messung der Ohrläsionen wurden durch die biologisch-technische Assistentin Frau Beate Lorenz durchgeführt. Die Abtötung der Versuchstiere, die Isolierung von Einzelzellen, die anschließenden Zellfärbungen und die Färbungen der mittels Zytospin-Zentrifuge generierten Objektträger wurden nach erfolgter Anleitung durch Frau Dr. rer. nat. Dominika Lukas, Herrn Dr. rer. nat. Nir Yogev und Frau Beate Lorenz von mir selbstständig durchgeführt, ebenso wie die FACS-Analysen und die Messungen mittels ELISA. Die Datenanalyse erfolgte selbstständig durch mich unter Supervision durch Frau Univ.-Prof. Dr. med. Esther R. von Stebut-Borschitz sowie Herrn Dr. rer. nat. Nir Yogev.

Diese Arbeit wurde durch das „Köln Fortune Programm“ der Medizinischen Fakultät der Universität zu Köln gefördert.

## Erklärung zur guten wissenschaftlichen Praxis:

Ich erkläre hiermit, dass ich die Ordnung zur Sicherung guter wissenschaftlicher Praxis und zum Umgang mit wissenschaftlichem Fehlverhalten (Amtliche Mitteilung der Universität zu Köln AM 132/2020) der Universität zu Köln gelesen habe und verpflichte mich hiermit, die dort genannten Vorgaben bei allen wissenschaftlichen Tätigkeiten zu beachten und umzusetzen.

Köln, den 11.12.2024

Unterschrift:

## **Danksagung**

Für meinen Vater

# Table of contents

<b>TABLE OF CONTENTS</b>	<b>5</b>
<b>LIST OF ABBREVIATIONS</b>	<b>8</b>
<b>1. ZUSAMMENFASSUNG</b>	<b>12</b>
<b>2. INTRODUCTION</b>	<b>14</b>
2.1 Leishmaniasis	14
2.1.1. <i>Leishmania</i> life cycle	15
2.1.2. Cutaneous leishmaniasis	16
2.2 Immune system	16
2.2.1. Myeloid cells	17
2.2.2. Myeloid cells in the immune response in experimental murine CL ( <i>L. major</i> )	20
2.3 Host dependence of the immune response towards <i>L. major</i> infection	22
2.4 iNOS & arginase-1	23
2.5 Aim	25
<b>3. MATERIAL AND METHODS</b>	<b>26</b>
3.1 Material	26
3.1.1. <i>Leishmania</i> parasites	26
3.1.2. Mice	26
3.1.3. Instruments	26
3.1.4. Laboratory supplies	27
3.1.5. Reagents	28
3.1.6. Kits (ready-to-use)	30
3.1.7. Buffer and consumption solutions	30
3.1.8. Antibodies	32
3.1.9. Software	33
3.2 Methods	34
3.2.1. Animal experiments welfare certificate	34
3.2.2. Cultivation of <i>L. major</i> promastigotes	34
3.2.3. Intradermal infection of mice	35
3.2.4. Determination of ear lesion size	35

3.2.5.	Single cell isolation from ears by enzymatic and mechanical tissue digestion	35
3.2.6.	Counting viable cells	35
3.2.7.	Flow cytometry	36
3.2.8.	Cytospin centrifugation and DiffQuik hematoxylin and eosin staining	45
3.2.9.	LN cell preparation	45
3.2.10.	Antigen specific restimulation	46
3.2.11.	Cytokine quantification in supernatant of LN cells	46
3.2.12.	Statistical analysis	47
<b>4.</b>	<b>RESULTS</b>	<b>48</b>
4.1	Development of ear lesions in C57BL/6 vs. BALB/c mice after infection with <i>L. major</i>	48
4.2	Presence of parasites in ear lesions of mice after infection with <i>L. major</i>	49
4.3	IFN $\gamma$ release of LN cells at different time points after antigen-specific restimulation in <i>L. major</i> infection	51
4.4	Myeloid cells in ears of C57BL/6 and BALB/c mice in steady state and at different time points after infection with <i>L. major</i>	53
4.5	Distribution of myeloid ear cells based on CD11b and CD11c marker expression	55
4.5.1.	Identification of different cell subsets based on Ly6C and CD64 marker expression among myeloid ear tissue cells	58
4.5.2.	Expression of iNOS and arginase-1 in myeloid ear tissue cells	62
4.5.3.	Expression of iNOS and arginase-1 in different myeloid cell subsets in ear tissue	64
4.5.4.	Ly6C and CD11b expression among MHC II <sup>neg</sup> ear cells in C57BL/6 and BALB/c mice after infection with <i>L. major</i>	69
<b>5.</b>	<b>DISCUSSION</b>	<b>72</b>
5.1	Evolution of ear lesion size of <i>L. major</i> infected mice differs between C57BL/6 and BALB/c mice	72
5.2	<i>L. major</i> parasites found in ear tissue indicate successful (intra-dermal) infection	73
5.3	Comparison of IFN $\gamma$ release of LN cells after restimulation with SLA between C57BL/6 and BALB/c mice reflects their distinct immune reactions towards <i>L. major</i> infection	73
5.4	Gating strategy	74
5.5	Myeloid cells in C57BL/6 and BALB/c mice differ in their expression levels of Ly6C and CD64 at critical time points in the infection with <i>L. major</i>	75

5.5.1.	MHC II <sup>neg</sup> cells	75
5.5.2.	MHC II <sup>+</sup> cells	78
5.6	iNOS and Arginase-1 expression differs between C57BL/6 and BALB/c mice after infection with <i>L. major</i> , but is independent of cell type	84
5.7	Conclusion/Outlook	87
6.	REFERENCES	89
7.	APPENDIX	101
7.1	List of Figures	101
7.2	List of tables	101
8.	VORABVERÖFFENTLICHUNGEN VON ERGEBNISSEN	102

## List of Abbreviations

AF 700	Alexa Fluor 700
APC	Antigen presenting cell
APC	Allophycocyanin
Aqua dem.	Demineralized water
CD	Subset of differentiation
cDC	Conventional dendritic cells
cDC1	Conventional dendritic cells type 1
cDC2	Conventional dendritic cells type 2
CL	Cutaneous Leishmaniasis
CO <sub>2</sub>	Carbon dioxide
DC	Dendritic cells
dDC	Dermal dendritic cell
DN	Double negative
DNA	Desoxyribonucleic acid
DNase	Desoxyribonuclease
DP	Double positive
ELISA	Enzyme-linked immune sorbent assay
FACS	Fluorescence activated cell sorting
FCS	Fetal calf serum
FITC	Fluorescein isothiocyanate
FSC	Forward scatter

g	Standard acceleration due to gravity (1 g = 9,80665 m/s <sup>2</sup> )
h	Hour
Hi	High
H <sub>2</sub> O	Water
H <sub>2</sub> O <sub>2</sub>	Hydrogen peroxide
IFN <sub>γ</sub>	Interferon gamma
IL	Interleukin
iNOS	Inducible nitric oxide synthase
Int	Intermediate
l	Liter
LC	Langerhans cell
lin	Lineage
L. major	Leishmania major
LN	Lymph node
lo	Low
mg	Milligrams
ml	Milliliters
MFI	Mean fluorescence intensity
MHC	Major histocompatibility complex
min	Minute
Mo	Monocytes

Mo-DC	Monocyte-derived dendritic cells
Mo-MΦ	Monocyte-derived MΦ
MΦ	Macrophage
μg	Microgram
μl	Microliter
neg	Negative
ng	Nanogramm
NK	Natural Killer
nm	Nanometer
NO	Nitric oxide
PE	Phycoerythrin
PE-Cy7	Phycoerythrin cyanine 7
pg	Pikogramm
RT	Room temperature
SA-HRP	Streptavidin conjugated to horseradish-peroxidase
SEB	Staphylococcal enterotoxin B
SLA	Soluble Leishmania Antigen
SN	Single negative
SP	Single positive
SSC	Side scatter
Th	T-helper cells/lymphocytes
Th <sub>1</sub>	Type 1 T-helper cells/lymphocytes

---

Th <sub>2</sub>	Type 2 T-helper cells/lymphocytes
Th <sub>17</sub>	Type 17 T-helper cells/lymphocytes
TR	Tissue resident
VL	Visceral leishmaniasis
W	Week
WHO	World Health Organization
+	Positive

---

## 1. Zusammenfassung

Die kutane Leishmaniasis stellt eine Form der weltweit verbreiteten Leishmaniasis dar, die insbesondere in subtropischen Gebieten endemisch ist. Über einen Stich der Sandmücke kommt es zur Infektion mit *Leishmanien*, wobei die Parasiten zunächst myeloide Zellen, insbesondere Makrophagen, befallen und hier zu den sogenannten Amastigoten heranreifen und sich replizieren. Charakteristisch für die kutane Form der Leishmaniasis sind Hautulzerationen, die selbstlimitierend abheilen, sofern ein intaktes Immunsystem besteht. Die viszerale Leishmaniasis dagegen endet unbehandelt häufig letal. In den Maus-Genotypen C57BL/6 und BALB/c spiegelt sich das Phänomen unterschiedlicher Immunantworten mit konsekutiv differierender Krankheitsausprägung wider. Mäuse des Genotyps C57BL/6 zeigen nach Infektion mit *L. major* einen selbstlimitierenden Krankheitsverlauf mit spontaner Abheilung der Hautläsionen, wohingegen Mäuse des Genotyps BALB/c einen schwereren Verlauf mit nekrotisierenden Läsionen ohne spontane Abheilungstendenz aufweisen. Auch nach Ausheilung persistieren die Parasiten lebenslang im Wirt, wodurch die Gefahr einer erneuten Exazerbation unter Immunsuppression besteht. Derzeit gibt es kein verfügbares Vakzin.

Myeloide Zellen, insbesondere Makrophagen und Dendritische Zellen, aber auch Monozyten spielen in der Erkrankung eine zentrale Rolle. In den letzten Jahrzehnten hat sich durch die intensive Forschung das Bild einer diversen Zellpopulation geformt, wobei stetig neue Aspekte die Komplexität des myeloiden Netzwerks unterstreichen. Ziel dieser Arbeit war es, darzustellen, inwiefern die Ausprägung der Zellantwort auf Ebene myeloider Zellen je nach Immunitätslage des Individuums differiert und dabei insbesondere phänotypische, aber auch funktionelle Unterschiede dieser Zellen während verschiedener Krankheitsphasen mit einzubeziehen. Zunächst wurden dazu die Ohren von C57BL/6 und BALB/c Mäusen mit *L. major* Parasiten infiziert. Zu verschiedenen Zeitpunkten nach Infektion wurden die Tiere abgetötet, das Volumen der Ohrläsionen gemessen und das Ohrgewebe zu Einzelzellen aufgearbeitet. Mittels Durchflusszytometrie erfolgte die Analyse verschiedener Oberflächenantigene sowie intrazellulärer Antigene, anhand derer insgesamt zwölf Untergruppen myeloider Zellen unterteilt werden konnten. Der Anteil dieser verschiedenen Zellgruppen an der gesamten myeloiden Zellpopulation konnte so zwischen den Maus-Genotypen zu verschiedenen Krankheitszeitpunkten nach Infektion mit *L. major* verglichen werden. Insgesamt prägte sich in den ersten Wochen nach Infektion zunächst ein ähnliches Bild und es zeigten sich hinsichtlich der myeloiden Zellgruppen nur wenige Unterschiede zwischen den Maus-Genotypen. Der Hauptunterschied zeigte sich vornehmlich in Woche 9 nach Infektion, wobei in C57BL/6 Mäusen im Gegensatz zu BALB/c Mäusen ein signifikant höherer Anteil der Zellen die Marker Ly6C und CD64 exprimierte. Die Expression dieser Marker kann sowohl auf einen monozytären Ursprung, als auch auf eine pro-inflammatorische

Signatur der Zellen hindeuten. Der Zeitpunkt des Auftretens während der Heilungsphase der C57BL/6 Mäuse könnte auf eine wichtige Bedeutung dieser Zellen für die antiparasitäre Immunantwort schließen lassen. In der Population, welche mutmaßlich vorwiegend Monozyten beinhaltete zeigte sich zudem eine starke Dynamik in der Expression von Ly6C, was durch eine stetige Differenzierung sowie Ein- und Auswanderung der Zellen in bzw. aus dem Gewebe bedingt sein könnte. Die Daten sprechen insgesamt für eine wichtige Bedeutung der Monozyten und von diesen abgeleiteten Zellen für die Heilung in C57BL/6 Mäusen.

Anhand der iNOS- bzw. Arginase-1-Expression konnte das pro- bzw. anti-inflammatorische Milieu in den verschiedenen Genotypen dargestellt werden. Wie bereits anhand der Literatur antizipierbar, konnte bestätigt werden, dass in C57BL/6 Mäusen eine signifikant höhere Expression von iNOS stattfindet, als in BALB/c Mäusen. Es zeigten sich hier bezüglich der Enzymexpression jedoch keine spezifischen Tendenzen auf Zellebene, sondern lediglich vergleichend zwischen den Maus-Genotypen. Beispielsweise zeigten als von Monozyten abgeleitete Makrophagen definierte Zellen in C57BL/6 Mäusen eine signifikant höhere Expression von iNOS, wohingegen diese in BALB/c Mäusen signifikant mehr Arginase-1 produzierten.

Unsere Beobachtungen lassen daher vermuten, dass die Funktionalität von Zellen eher durch den Genotyp der entsprechenden Mäuse und die immunologische Prägung ihrer zellulären (Mikro-)Umgebung, wie z.B. durch pro-inflammatorische Zytokine bestimmt wird, als dass sie mit spezifischen phänotypischen Eigenschaften verbunden ist.

## 2. Introduction

### 2.1 Leishmaniasis

Leishmaniasis is an infectious vector-borne disease, caused by parasites of the genus *Leishmania*, which are transmitted to humans and other mammals by female sand flies.<sup>1-4</sup> As a neglected tropical disease, leishmaniasis causes an estimated 0.7 to 1 million new cases per year according to actual reports of the World Health Organization (WHO).<sup>5</sup> 12 million people are already infected, while 350 million people are at risk of infection.<sup>1,6,7</sup>

Three main forms of the disease can be distinguished: Visceral, (also termed kala-azar), cutaneous and mucocutaneous leishmaniasis.<sup>8</sup> With approximately 600.000 to 1 million new cases worldwide per year, cutaneous leishmaniasis (CL) is the most common form of the disease, while of visceral leishmaniasis (VL) 50.000 to 90.000 cases occur annually.<sup>5</sup> The majority of cases of CL is reported in the Americas, the Mediterranean basin, Middle East and Central Asia. VL mainly appears in Brazil, east Africa and India.<sup>5</sup> Whereas VL, associated with fever, anemia, weight loss and affection of liver and spleen, is fatal in over 95% of cases when left untreated, the cutaneous form results in ulcers that may leave permanent scars, disability or stigma.<sup>1,5</sup>

More than 20 *Leishmania* species are known to exist, with each of them having different impacts on form and severity of the disease.<sup>1,8</sup> One of the species leading to the cutaneous form is *L. major*.<sup>1</sup> In addition to parasite species, immune competence determines disease outcome.<sup>1</sup> Leishmaniasis is strongly linked to poverty and occurs predominantly in rural areas, where access to health care is limited.<sup>1,9</sup> However, although considered a tropical disease, leishmaniasis is becoming more and more relevant all over the world due to globalization and climatic changes. Therefore, in the future, cases of leishmaniasis might increase also in wealthier and better developed regions of the world.<sup>1,9,10</sup> Unfortunately, no vaccine is available so far.<sup>1</sup> Leishmaniasis is treatable and curable, however, drugs are expensive, show severe adverse effects and an increase in drug resistance is observed.<sup>1,11</sup> In addition, parasites cannot be fully eliminated from the body<sup>12</sup>, but may persist<sup>13-16</sup> live-long<sup>17</sup>, which might provide long-term memory and immunity against the disease<sup>18</sup>, but in contrast bears the risk of a relapse once immunosuppression occurs.<sup>1,5,13,19</sup>

### 2.1.1. *Leishmania* life cycle

*Leishmania* are obligate intracellular parasites that have different developmental stages.<sup>20-24</sup> Infection of female sand flies takes place during their blood meal of infected humans or other mammals<sup>21,25</sup>, where they take up amastigote life forms of the parasite.<sup>23,26</sup> When ingested in the sand fly gut, these life forms may transform into infective metacyclic promastigotes.<sup>20-24,27</sup> Transmission of the disease to another host takes place during the next bite of the sand fly<sup>2</sup>, whereby promastigotes are intradermally inoculated into the host's organism.<sup>23,24</sup> Neutrophils, macrophages (MΦ) and dendritic cells (DC) then phagocytose *Leishmania* promastigotes.<sup>28</sup> In MΦ, they locate to parasitophorous vacuoles (PV)<sup>29</sup>, which are formed by fusion of phagosomes and lysosomes<sup>30</sup> to transform into the intracellular amastigote life form<sup>31,32</sup> and replicate.<sup>24,30,33,34</sup> Finally, during another sand fly blood meal and consecutive parasite uptake, another cycle of transmission starts, (Figure 1).<sup>23</sup>

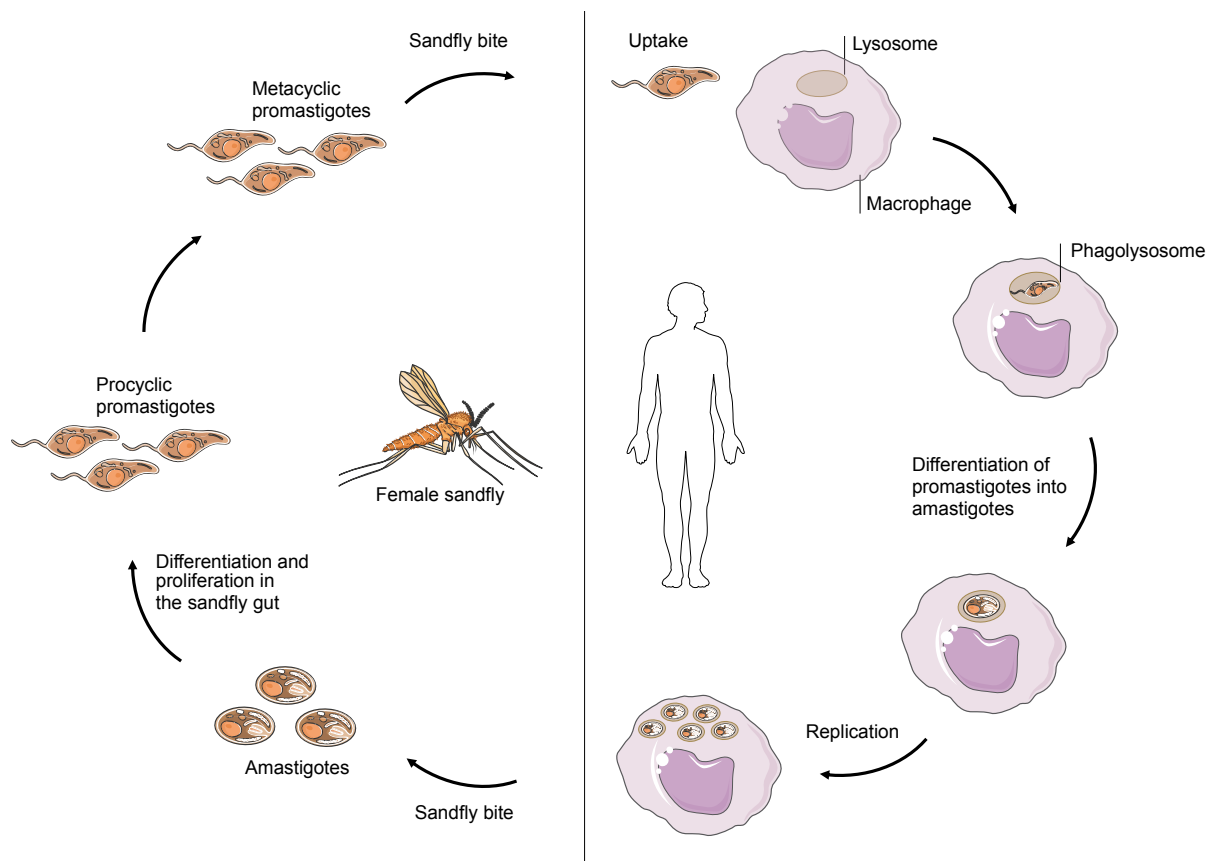


**Figure 1** *Leishmania* life cycle

Figure was modified after Sacks & Noben-Trauth<sup>23</sup> and created using Smart Servier Medical Art, no permission required.<sup>35</sup> Inoculation of *L. major* parasites takes place during the bite of a sand fly. MΦ take up promastigotes and phagolysosomes are formed. Inside these phagolysosomes, promastigotes differentiate into amastigotes and replicate. During another blood meal of the sand fly, amastigotes are taken up into the gut of female sand flies. Here, proliferation and differentiation into non-infectious procyclic promastigotes takes place. These forms are rapidly dividing and differentiate into non-dividing metacyclic promastigotes, which can be transmitted during another sand fly bite.<sup>23</sup>

### 2.1.2. Cutaneous leishmaniasis

CL is characterized by a lesion which occurs at the site of a sand fly bite. Lesions develop approximately 5 weeks after infection and their appearance correlates with the onset of parasite growth control.<sup>36-38</sup> CL can be subdivided into Old World vs. New World CL, which refers to location-dependent predominance of distinct *Leishmania* species in different parts of the world. Old World CL species are prevalent in regions of the Mediterranean Basin, the Middle east, the Horn of Africa, or the Indian subcontinent, while New world species are mainly found in Middle and South America. These forms also differ from each other by phenotype of lesions. *L. major* is one of the species that leads to Old World CL and is transmitted by the sand fly *Phlebotomus papatasi*.<sup>4,39</sup> Lesions heal spontaneously over the course of time, which may be supported by local therapy.<sup>1,40-42</sup> However, the infection may result in scars that persist live-long.<sup>1,5</sup> In addition, some cases of CL can develop into more serious manifestations, such as diffuse CL, disseminated CL, mucocutaneous leishmaniasis and leishmaniasis recidivans.<sup>11</sup>

## 2.2 Immune system

The immune system consists of two parts, the innate and the adaptive immune system, which both are crucially important to effectively initiate host defense responses.<sup>43-45</sup> In the dermis, an effective interaction between both parts is provided by the network of lymphatic and blood vessels, which support migration of immune cells in and out of the skin.<sup>46</sup>

Innate immunity not only includes physical, chemical and microbiological barriers, but more importantly consists of cells like neutrophils, monocytes, MΦ and natural killer (NK) cells as well as complement, cytokines and acute phase proteins. Altogether, these components constitute the initial host response, which is a rapid, but not very precise reaction towards an invading pathogen or toxin.<sup>43-45</sup>

By inducing and regulating T lymphocyte responses, DC perform a linking position between innate and adaptive immunity.<sup>45-52</sup>

Adaptive immunity is composed of T and B lymphocytes, which develop specific reactions when confronted with antigens, but take several days or weeks to evolve appropriate responses.<sup>43</sup> These specific reactions include B and T cell activation and differentiation pathways, leading to T cell homing towards site of inflammation and antibody release by B cells.<sup>43</sup> The type of activated T cell in response to antigen is determined by the major histocompatibility complex (MHC) molecule used for antigen presentation.<sup>43</sup> MHC class I molecules, which are expressed by all nucleated cells, present endogenous antigens, including virus and tumor antigens.<sup>43</sup> This results in activation of CD8<sup>+</sup> cytotoxic T cells, which then attack

marked cells.<sup>43</sup> Presentation of exogenous antigen via MHC class II molecules, which in steady-state are primarily expressed by professional antigen presenting cells (APCs) such as DC, MΦ and B cells, leads to activation of CD4<sup>+</sup> T cells.<sup>43</sup> These CD4<sup>+</sup> T helper (Th) cells may be further distributed into Th<sub>1</sub>, Th<sub>2</sub> and Th<sub>17</sub> cells,<sup>45</sup> which all display distinct effector functions.<sup>44</sup> In the following, by production of cytokines, T cells induce activation of additional cells in order to mount an effective response towards pathogen invasion.<sup>43</sup> Cytokine production also supports B cell growth, which then become mature cells able to secrete antibodies. In return, antibody production features a supportive function for T cells and serves the elimination process of toxins and pathogens.<sup>43</sup> Importantly, these responses provide immune memory, meaning that during a second confrontation with the same antigen, the reaction can be much faster and therefore more efficient.<sup>43-45</sup>

### **2.2.1. Myeloid cells**

Myeloid cells represent a heterogenic group of cells belonging to the leukocyte lineage and include MΦ, DC and monocytes.<sup>53-55</sup> These cells share the feature of being professional antigen-presenting cells and are part of the mononuclear phagocyte system.<sup>53-57</sup> Already in the 19<sup>th</sup> century, the phagocytosis theory was proposed by Elie Metchnikoff.<sup>58</sup> In the following, important characteristics and functions of these three cell groups are described.

#### **MΦ**

MΦ are considered important myeloid cells of the immune system, which are found in tissues all over the body. They possess one of the highest phagocytic capacities of all immune cells and act as host protectors that may adapt to different influences. Among their responsibilities lay diverse tasks, which include engulfment and neutralization of cellular debris and pathogens, as well as tissue homeostasis and repair. MΦ contribute to host-defense mechanisms with the ability to stimulate T cells, wound healing and resolution of inflammation. Importantly, MΦ are able to constantly switch their functional states from anti- to pro-inflammatory and reverse, which is important to stop inflammatory processes once pathogen elimination has taken place and keep tissue damage to a minimum. By producing signal molecules like chemokines and cytokines, MΦ also recruit additional immune cells to the site of inflammation. In return, MΦ also require supply of messengers by other immune cells in order to be activated. Therefore, the appropriate interplay between this cell network is important for an effective immune response with elimination of invading organisms as well as the restoration of tissue integrity.<sup>6,53-55,59-63</sup>

Historically, tissue MΦ and monocytes were grouped together and defined as mononuclear phagocytes. Moreover, MΦ were believed to arise from monocytes, as in 1968, van Furth et

al. defined a developmental series, in which monocytes were claimed to originate from promonocytes in the bone marrow, which after migration in the peripheral blood differentiated into MΦ found in the tissue.<sup>64</sup> On the basis of this and the knowledge until that time point, the mononuclear phagocyte system was established.<sup>56</sup> In contrast, later, the embryonic origin of MΦ was shown in experiments of Naito et al. (1989, 1990). Immature MΦ, which afterwards were found to differentiate into fetal MΦ, developed in the yolk sac even before monocytes or promonocytes were found here. Also, no differentiation of monocytes or promonocytes into fetal MΦ was obtained. This indicated fetal MΦ derived directly from hematopoietic stem cells. However, a second monocyte-derived MΦ (mo-MΦ) population was found to originate from the yolk sac and therefore, it was concluded that two different MΦ populations are derived in the yolk sac.<sup>65</sup> In addition, as hematopoiesis continues in the fetal liver, also a fetal MΦ population, as well as a monocyte/MΦ population were found here. Their origin was suspected to be either from hematopoietic stem cells emerging in the fetal liver or by blood supply from the yolk sac.<sup>66</sup> Later, it became clear, that MΦ can maintain themselves through self-renewal and longevity and therefore are independent of monocyte supply.<sup>67</sup> This was also confirmed in experiments by Hashimoto et al. (2013), since after depletion of MΦ, local proliferation of MΦ took place in order to repopulate the tissue.<sup>68</sup> The supply of MΦ by circulatory Ly6C<sup>med/hi</sup> monocytes was found to be important especially during inflammation, where monocytes infiltrate affected tissues and develop into pro-inflammatory MΦ.<sup>69,70</sup>

## Monocytes

The rapid recruitment of monocytes is made possible due to their circulation in the peripheral blood.<sup>64</sup> Monocytes can be categorized according to different expression levels of the surface marker Ly6C which correlate with different functionality.<sup>47,69</sup> Despite different functionality, there is evidence that nonclassical Ly6C<sup>lo</sup> monocytes evolve from classical Ly6C<sup>hi</sup> monocytes.<sup>67,69</sup> When developed into Ly6C<sup>lo</sup> monocytes, they lose the ability to migrate, whereas classical Ly6C<sup>hi</sup> monocytes still possess this feature.<sup>69</sup> Ly6C<sup>lo</sup> monocytes have a longer half-life than Ly6C<sup>hi</sup> monocytes<sup>47</sup> and while they maintain homeostasis, Ly6C<sup>hi</sup> monocytes rather take action in inflammatory processes.<sup>47,59,69,71</sup> Besides development into Ly6C<sup>lo</sup> monocytes and MΦ, classical Ly6C<sup>+/hi</sup> monocytes also have the ability to differentiate into other myeloid cell types, such as DC.<sup>69,72-77</sup> However, they are not only precursor cells, but do have phagocytic capacity themselves<sup>78</sup> and may even engage in activities like migration to lymph nodes (LN) and antigen presentation that usually correspond to other myeloid cell types like tissue-MΦ and DC.<sup>79</sup>

## DC

DC rank among the most potent APCs to induce T cell immunity. By patrolling in the tissue, they act as immune sentinels.<sup>80</sup> Once they capture foreign antigens or potential hazardous material, DC rapidly react and induce immune responses. Thereby, they perform key functions in the induction and regulation of immunity.<sup>43,55,80,81</sup>

The term “DC” was coined in 1973, when Steinman et al. described “a novel cell type” in peripheral lymphoid organs, which they named “DC”.<sup>82</sup> These cells originated from bone marrow as well as spleen.<sup>83</sup> They expressed major histocompatibility complex (MHC) linked alloantigens<sup>84</sup> and it was observed that DC were the most potent cells in inducing a mixed leukocyte reaction. Therefore it was assumed, that these cells were critical for generating immune responses.<sup>48</sup> In line with this, it was shown that coculture of DC and T cells resulted in T cell proliferation<sup>49</sup> and in contrast, stimulating capacity was reduced when DC numbers were diminished.<sup>51</sup> Moreover, in 1981, Nussenzweig et al. analyzed surface antigens of DC, which led to the assumption of DC being separate from other leukocytes and “part of a unique Ia-rich leukocyte differentiation pathway”. Also, they came to the conclusion that it was unlikely for DC to be monocyte-derived.<sup>85</sup> Already then they observed less phagocytic capacity in DC than in typical MΦ<sup>86</sup>, whereas MΦ were less potent than DC in stimulating T cell proliferation.<sup>49</sup> DC are found in lymphoid and non-lymphoid tissues. Especially during inflammation, DC migrate towards lymphoid organs, where they present peptides on their MHCs towards T lymphocytes. T lymphocytes then become activated, expand and produce cytokines. The ability to migrate constitutes one of the differences to MΦ.<sup>43,55,80,81,87</sup> Furthermore, their role not only includes the initiation of pathogen fighting responses, but also the elimination of autoreactive T lymphocytes, which can be identified when confronted with self-antigen presenting DCs.<sup>55,87,88</sup>

Today, several different DC subtypes are known, which are defined by distinct phenotypical and functional properties and also seem to differ in their origins: In general, it was shown that DC arise from pre-DC in the bone marrow.<sup>89-91</sup> Common dendritic progenitors (CDP) responsible for maintaining the pDC as well as cDC population were described by Onai et al. (2007).<sup>92</sup> Also, a MΦ and DC progenitor (MDP) has been described, which gives rise to several subsets of MΦ, specific types of DC and monocytes.<sup>93</sup> In contrast to this, DC may also be monocyte-derived: Several authors showed that in inflammation, monocytes can differentiate into DC, whereby they acquire typical DC markers.<sup>47,75,77</sup> It has been shown that these monocyte-derived-DC (mo-DC) might possess distinct features than other DC subtypes.<sup>74,75</sup>

In the skin, DC can be further subdivided into Langerhans cells (LC) found in the epidermis and DC found in the dermis, also termed dermal DC (dDC).<sup>94</sup> In the dermis, Henri et al. (2010) separated four different dDC subsets based on their expression of the markers Langerin (CD207), CD11b and CD103. Among these subsets, Langerin<sup>neg</sup>, CD11b<sup>high</sup>, CD103<sup>neg</sup> dDC

made up the most frequent cells with  $\approx 66\%$ , whereas the other three cell subsets were found in lower percentages: Langerin<sup>neg</sup>, CD11b<sup>neg/low</sup>, CD103<sup>neg</sup> dDC made up  $\approx 16\%$  and Langerin<sup>pos</sup>, CD11b<sup>low</sup> dDC that consisted of CD103<sup>pos/neg</sup> dDC made up  $\approx 3\%$  each.<sup>94</sup>

In order to better identify and classify DC, in 2014, Guilliams et al. proposed a new nomenclature, where they subdivided classical DC (cDC) into cDC1 (e.g. CD207<sup>+</sup>, CD11b<sup>neg</sup>, CD8alpha<sup>+</sup> and CD103<sup>+</sup>) and cDC2 (e.g. CD207<sup>neg</sup>, CD11b<sup>+</sup> and CD172a<sup>+</sup>).<sup>57</sup> Interestingly, Schlitzer et al. (2015) described that subset priming towards either cDC1 or cDC2 takes place already in the BM.<sup>95</sup> These cDC1 and cDC2 were described to differ in their T cell stimulatory capacity with regard to Th cell priming in different directions. As early as 1999, Moldonado-Lopez et al. described the role of the DC subclass in promoting Th<sub>1</sub> or Th<sub>2</sub> polarization, as antigen presentation by CD11b<sup>+</sup> (DC2-like) cells lead to Th<sub>2</sub> answers, whereas presentation by CD11b<sup>dull/neg</sup> (DC1-like) cells lead to Th<sub>1</sub> answers.<sup>96</sup> This dichotomy was further substantiated by several other studies.<sup>97-102</sup> In a study by Sulczewski et al. (2020) splenic cDC1s were shown to promote Th<sub>1</sub> polarization.<sup>102</sup> In contrast, Plantinga et al. (2013) found, that CD11b<sup>+</sup> cDCs induced Th<sub>2</sub> cell immunity, while CD103<sup>+</sup> cDCs were unable to do so.<sup>98</sup> Also, in other studies it was shown that during helminth infection, mainly CD11b<sup>+</sup> cDCs accumulate in the mesenteric lymph nodes (MLN) and stronger induce Th<sub>2</sub>-associated cytokines such as IL-5 and IL-13.<sup>99</sup>

In conclusion, myeloid cells form a very heterogeneous yet closely interlinked group, due to their different differentiation pathways and origins, as well as divergent roles and specialisations in immunity and therefore are a very complex cell network to study.

### **2.2.2. Myeloid cells in the immune response in experimental murine CL (*L. major*)**

In the early phase of *Leishmania* infection, the immune system does not respond in an appropriate manner towards pathogen invasion. This phase during the first 4-5 weeks of infection is referred to as “silent phase”, as host responses towards infection like production of cytokines like IL-12 or IFN $\gamma$  are not present and parasite growth takes place.<sup>36</sup> Here, among myeloid cells, M $\Phi$  take over a special role: They allow parasites to reside, replicate and differentiate within them. Especially in dermal M $\Phi$ , the intracellular survival of *L. major* parasites was shown to be greater than in other M $\Phi$  analyzed, e.g. mo-M $\Phi$  or peritoneal M $\Phi$ .<sup>32</sup> However, especially in immunodeficient mice, other cell types, such as neutrophils, eosinophils and dendritic leukocytes have also been observed to harbor parasites.<sup>36</sup> Also, a study by Leon et al. (2007) showed, that next to monocytes and M $\Phi$ , dermal mo-DC and LN mo-DC were predominantly infected with *L. major*.<sup>75</sup>

Phagocytosis of *Leishmania* is enabled by complement activation with conversion of C3b to C3bi and fixation of the MΦ receptor CR3.<sup>103</sup> This process inhibits the release of IL-12, a cytokine which is important for the induction of protective Th<sub>1</sub> cell responses.<sup>104-108</sup> In the infection with *Leishmania*, IL-12 is released by infected DC, but not by infected MΦ.<sup>109</sup> Von Stebut et al. (1998) showed that although MΦ ingest parasites, they do not become activated by infection<sup>109</sup> and the ability of *L. major*-MΦ to produce IL-12 was shown to be suppressed in various studies.<sup>110,111-113</sup> Next to this, there are several other strategies which *Leishmania* use to avoid usual host-defense mechanisms: For example, in a study by Locksley et al. (1988), no respiratory burst machinery was detectable in *L. major*-infected dermal MΦ, a mechanism by which parasites presumably are enabled to hide and differentiate within dermal MΦ.<sup>6,32</sup> Another strategy is the inactivation of C3b by the *Leishmania* surface protease gp63, thereby leading to increased resistance against complement.<sup>114</sup> Also, impaired IFN $\gamma$ -gamma mediated signaling in *Leishmania* infected cells has been reported.<sup>115</sup>

After the initial “silent phase”, several immune cells are recruited towards lesion site, including neutrophils, eosinophils, MΦ, DC and lymphocytes, and lesion formation takes place.<sup>36,116</sup> MΦ eventually become activated via cytokines, especially IFN $\gamma$ <sup>117-120</sup> and TNF- $\alpha$ <sup>121-124</sup> and MΦ activation then leads to pathogen-killing<sup>118,125</sup> in an NO-dependent manner and lesion resolution<sup>6,126-128</sup> For the induction of such protective immunity against *Leishmania*, DC are important: Although, compared to MΦ, DC are less efficient in phagocytosis of *L. major* parasites, DC are important initiators of T cell responses with consecutive MΦ activation.<sup>6,18,109</sup> LC and DC have been shown to ingest the parasites at the site of infection and migrate towards skin-draining LN.<sup>129,130</sup> Parasite-specific antigens then are presented towards T lymphocytes<sup>18,129,130</sup>, inducing T cell proliferation and an antigen-specific immune response.<sup>18,129,130</sup> In contrast to infection of MΦ, infection of DC with *L. major* leads to upregulation of the activation marker MHC I as well as induction of IFN $\gamma$  production by CD8<sup>+</sup> T cells.<sup>6,38,109</sup> Also, MHC II upregulation was found to be stronger in infected DC than in infected MΦ, therefore leading to earlier priming of CD4<sup>+</sup> T cells towards effector Th<sub>1</sub> cells by DC than by MΦ.<sup>6,109</sup> However, DC immigration into lesional tissue is delayed until approximately 5 weeks after parasite inoculation.<sup>36</sup>

At least five different DC subsets were shown to be involved following *L. major* infection. In a study by Baldwin et al. (2004), among these different DC, the most prominent subsets found in skin lesions were LC and dDC. Those cells also contained the highest parasite counts.<sup>131</sup> As already described earlier, during inflammatory processes, Ly6C<sup>hi</sup> monocytes are recruited towards sites of inflammation and may differentiate into MΦ or DC, while during steady state, they mature in the circulation and begin to down-regulate the expression of Ly6C.<sup>69</sup> Also, in the infection with *L. major*, monocytes are recruited towards lesion site, infiltrate the tissue and may

differentiate into monocyte-derived cells.<sup>75,132,133</sup> Previous studies showed that these monocyte-derived cells, together with monocytes and MΦ are predominantly infected by *L. major* parasites. Also, they very likely take action in the induction of protective Th<sub>1</sub> responses.<sup>75</sup>

### **2.3 Host dependence of the immune response towards *L. major* infection**

The infection with *L. major* is handled differently dependent on the individual immune system and genetic background of the host, which clinically appears as non-healing progressive lesions, that can even lead to systemic disease vs. lesion resolution. C57BL/6 and BALB/c mice are two different mouse strains that are known to develop these distinct immune responses towards the infection with *L. major*. In experimental immunology settings, C57BL/6 mice resemble resistant hosts and control *L. major* infection similar to immune-competent humans, which in this case is self-limiting. Control of parasite growth takes place approximately 5-6 weeks after infection. Contrary to this, BALB/c mice represent a strain susceptible to infection, that is not resolving, but rather presenting continuous lesion formation that even results in more severe complications such as systemic disease. Thus, BALB/c resemble immune-compromised patients and are used as a model for non-healing disease forms.<sup>15,23,36,38,131,134-138</sup> Distinct T cell responses seem to be involved in these differences.<sup>136,139</sup> Thereby, the type of T cells is a key factor for disease direction.<sup>108</sup> Th<sub>1</sub> cells were shown to produce IFN $\gamma$  and IL-2, while Th<sub>2</sub> cells produce IL-4, IL-5 and IL-10 (Mosmann et al. 1986, cited by Sommer et al.1998).<sup>140</sup>

Resistance was found to be associated with IL-12 driven Th<sub>1</sub> cell responses. When treating otherwise susceptible BALB/c mice with IL-12, a shift from a Th<sub>2</sub> predominant response towards a Th<sub>1</sub> response was observed, which was accompanied with resolution of disease.<sup>108</sup> In line with this, other studies showed that healing in resistant mice correlates with increased IFN $\gamma$  secretion and decrease of IL-4 secretion.<sup>141,140</sup> Susceptibility towards disease is associated with IL-4 mediated Th<sub>2</sub> cell<sup>136,139,142</sup> responses and failure to downmodulate IL-4.<sup>113,140</sup> Thereby, high IL-4 levels correlate with severity of disease.<sup>143</sup> Moreover, treatment of IL-4 expressing susceptible BALB/c mice with anti-IL-4 antibody led to attenuation of the disease progress.<sup>142</sup> Also, in a study by Kopf et al. (1996), BALB/c mice deficient in IL-4 eventually became resistant against the disease, whereas IL-4 competent BALB/c mice developed progressive and necrotic lesions.<sup>144</sup> Also, IL-17 has been identified as a cytokine involved in disease progress, as its levels were found to be higher in infected BALB/c than in infected C57BL/6 mice and in addition, IL-17 deficient mice developed significant smaller lesion volumes, which remained stable for several weeks.<sup>145</sup> In addition, in investigations of Belkaid et al. (2002), resistant C57BL/6 mice

contained higher numbers of parasite-specific CD8<sup>+</sup> T cells compared to those found in susceptible BALB/c mice.<sup>38</sup>

Conclusively, these two strains show opposing immune reactions to the infection, in terms of susceptibility and resistance, mimicking human disease in immunocompetent vs. immunodeficient conditions and therefore are two very common genetic backgrounds used as an experimental tool to study anti-*Leishmania* immunity and to compare disease outcome.<sup>131,135</sup>

## 2.4 iNOS & arginase-1

Although the enzymes inducible nitric oxide synthase (iNOS/NOS2) and arginase-1 use the same substrate, L-arginine, for their activities,<sup>146,147</sup> their roles in the disease are very contrary.

Inducible nitric oxide synthase (iNOS/NOS2) is found in a variety of cells, including MΦ, DC and NK cells.<sup>148-155</sup> iNOS is one of the three isoforms of the NO synthase<sup>148-151,156-163</sup> and its product, NO, performs diverse functions, including host-protective antiviral and antimicrobial effects, as well as involvement in wound healing.<sup>126,164-166</sup> Its induction depends on Th<sub>1</sub> cell associated inflammatory cytokines, such as IFN $\gamma$  and TNF- $\alpha$ <sup>147,167-169</sup> and microbial products and is mainly regulated through transcriptional mechanisms.<sup>170,171</sup> In the infection with *L. major*, iNOS activity has been shown to be important for the cure of the disease: Several studies found a correlation between iNOS expression and lesion resolution as well as parasite control.<sup>126,172,173</sup> Also, a study by Belkaid et al. (2000) showed, that deficiency in iNOS leads to faster progressing dermal lesions, which eventually become necrotic.<sup>36</sup>

In contrast to iNOS is the enzyme arginase-1: It is expressed by various cells, e.g. MΦ, DC<sup>168</sup> fibroblasts<sup>174</sup> and keratinocytes<sup>175,176</sup> and its expression has been found to be increased by Th<sub>2</sub> cytokines, such as IL-4, IL-10 and IL-13.<sup>147,168,177</sup> Arginase-1 is part of the urea cycle, where it converts L-arginine into L-ornithine and urea<sup>178-180</sup>, a step important for the detoxification of ammonia<sup>179</sup> and the supply with ornithine.<sup>146,181,182</sup> The latter of which can be further converted to prolin and polyamines, which are then used for collagen synthesis<sup>183,184</sup> and cell proliferation.<sup>146,182,185</sup> In line with this, expression of MΦ-derived arginase-1 has also been shown to be important for wound healing.<sup>175</sup> However, in *L. major* infected mice, healing was shown to be independent of arginase-1.<sup>186</sup> Moreover, mice susceptible to disease, which showed progressive lesions before, developed significantly smaller skin swellings in the absence of arginase-1<sup>187</sup> or when arginase-1 activity was inhibited.<sup>188</sup> Importantly, *Leishmania* parasites require arginase-derived polyamines for replication, and it has been shown that the activity of arginase correlates with parasite growth.<sup>188</sup> Importantly, since NO-production by

iNOS is dependent on its substrate arginine, arginase-1 might also be capable to reduce substrate supply of iNOS.<sup>147,189-191</sup>

## 2.5 Aim

The interplay between *Leishmania* parasites and host cells is complex and several strategies of the parasite have been shown to be important for the ability to manipulate host defense mechanisms.<sup>6,32,103,104,109-115</sup>

The assumption that the group of MΦ, DC and monocytes, which play a central role in the disease, is more heterogenic than was thought before, has evolved over the past years.<sup>69,75,80,94</sup> Distinct types of cells in terms of ontogeny and subset identity accumulate in infected tissue and perform different functions during immunogenic processes.<sup>36,75</sup> However, concerning the role of different DC subsets in *L. major* infection, much of the information about these cells in *Leishmania* infection has been investigated prior to the increasing knowledge about subset heterogeneity.<sup>131</sup> Therefore, it is not completely clear, whether different subgroups of these myeloid cells might play a role in the infection and possibly also contribute to distinct functionality.

In leishmaniasis, progression and severity of disease differ between distinct genotypes of mice.<sup>23,36,38,131,134-137</sup> Therefore, the working hypothesis of this thesis is that myeloid cell subset distribution differs between the two genotypes of mice, as well as corresponding functionality of these cells.

Within this thesis, I wanted to address the following aims:

- 1) The first aim is to characterize different myeloid cell subsets of potentially distinct origins on the basis of specific marker expression. This characterization strategy will be repeated at different infectious stages to gain knowledge about myeloid cell kinetics during progression of the disease.
- 2) The second aim is to compare myeloid cell subset appearance and distribution between the two genotypes, C57BL/6 and BALB/c mice.
- 3) To describe the overall tendency towards pro- or anti-inflammatory actions, as well as the contribution of specific cell subsets, the third aim is to analyze myeloid cell functionality with regard to iNOS and arginase-1 expression.

### 3. Material and Methods

#### 3.1 Material

##### 3.1.1. *Leishmania* parasites

*Leishmania major* (*L. major*), clone V1 (MHOM/IL/80 Institute Pasteur, Paris, France (MHOM/IL/80/Friedlin)

##### 3.1.2. Mice

For this analysis, C57BL/6J mice and BALB/c mice, all between 7-25 weeks old at time point of infection, were used.

##### 3.1.3. Instruments

Centrifuge Heraeus Megafuge 40R	Thermo Fisher Scientific
Cytocentrifuge Cellspin I Centrifuge (Cytospin)	THARMAC, VWR
FACS Attune NxT Acoustic Focusing Cytometer	Invitrogen by Thermo Fisher Scientific
Fluorescence microscope	Keyence Deutschland GmbH
Freezer -20°C	Bosch economic-froster
Freezer -80°C	VWR International
Fridge	Liebherr, MediLine
GasDocUnit for CO <sub>2</sub> euthanasia	Medres – medical research GmbH
GentleMACS Octo Dissociator	Miltenyi Biotec
Incubator Heraeus Heracell 150	Thermo Fisher Scientific
Microscopes	Zeiss Primo Star/Nikon
Microscope Slides (Menzel-Gläser Superfrost)	Thermo Fisher Scientific
Multichannel pipette	Integra
Multimode plate reader VICTOR Nivo	PerkinElmer

Pipetgirl	INTEGRA Biosciences
Vortex	Heidolph Instruments
Water bath	PolyScience

### 3.1.4. Laboratory supplies

Caliper	VWR International
Cannula	Omnican-F, B. Braun
Cell Culture Multiwell Plate, 6 well, PS Cellstar®	Greiner Bio-One
Cell strainers 70 µm	Corning Incorporated
Deep well microplate 96-well	VWR International
Dispenser	VWR International
ELISA maxi sorp 96-well plate	Thermo Fisher Scientific
ELISA plate sealers	G-Bioscience (VWR International)
FACS tubes	Falcon; Corning
Finntip pipette	Thermo Fisher Scientific
Finntip pipette tips	VWR International
GentleMACS™ C Tubes	Miltenyi Biotec
Gloves	Ansell Limited
Microplates, 6-; 96-well, flat bottom	Greiner Bio-One
Microplates, 96 well, PS, U-Bottom	Greiner Bio-One
Microplates, 96 well, V-shaped	Thermo Fisher Scientific
Neubauer counting chamber	Marienfeld (VWR International)
Parafilm laboratory film	Heathrow (VWR International)

Pipette (5; 10; 25 ml)	CELLSTAR Greiner Bio-One
Pipette filter tips (0.2-12.,5; 125; 300; 1250 µl)	INTEGRA Biosciences
Pipette Racks (for 12.5; 125; 300; 1250 µl)	INTEGRA Biosciences
Reaction tubes (0.5; 1.5; 2; 5 ml)	Eppendorf Hamburg
Tubes Cellstar ® (15; 50 ml)	Greiner Bio-One
Tubes 50 ml	THGeyer

### 3.1.5. Reagents

ACK Lysing Buffer	Lonza BioWhittaker
Aqua dem.	Arium SterilePlus (Sartopore 2 150), Sartorius
Attune Bleach	Invitrogen by Thermo Fisher Scientific
Attune Performance Tracking Beads	Invitrogen by Thermo Fisher Scientific
Attune Wash solution	Life technologies
Attune 1X Focusing Fluid	Life technologies
Attune 1X Shutdown Solution	Invitrogen by Thermo Fisher Scientific
BSA	Sigma
Collagenase Type I	Worthington Biochemical Corporation
Color Reagent A (H <sub>2</sub> O <sub>2</sub> )	BD Biosciences
Color Reagent B (Tetramethylbenzidine)	BD Biosciences
DMEM High Glucose w/ L-Glutamine, w/Sodium Pyruvate	Biowest
DNase I	Roche Germany

Ethanol 70%	Merck
Fetal calf serum (FCS)	Sigma Aldrich
Fixable Viability Dye eF780	Invitrogen by Thermo Fisher Scientific
Helipur H plus N	B. Braun
HEPES	Carl Roth GmbH
H <sub>3</sub> PO <sub>4</sub>	Roth
Liberase LT	Roche
L-Glutamine 100X sterile filtered 200mM	Biowest
MEM Non-Essential-Amino-Acids 100X	Biowest
M199 Medium (1X)	Gibco, Invitrogen
M199 Medium (10X)	Gibco, Invitrogen
Normal Goat Serum	Sigma Aldrich
PBS tablets	Gibco, Life Technologies, Thermo Fisher Scientific
Penicillin-Streptomycin Solution 100X sterile filtered	Biowest
RPMI-1640 medium without L-Glutamine	Lonza, BioWhittaker
Staphylococcus Enterotoxin B	Sigma
Streptavidin eFluor 780	BioLegend
Streptavidin-HRP	R&D Systems
Trypan blue	Sigma Aldrich
Tween 20 (Polysorbat 20)	Caesar & Loretz GmbH
2-Mercaptoethanol	Sigma Aldrich

### 3.1.6. Kits (ready-to-use)

AbC Total Antibody Compensation Kit	<ul style="list-style-type: none"> <li>• AbC™ Total capture beads</li> <li>• Negative beads</li> </ul>	Invitrogen by Thermo Fisher Scientific
Foxp3/Transcription Factor Staining Buffer Set	<ul style="list-style-type: none"> <li>• Permeabilization Buffer 10X</li> <li>• Fixation/Permeabilization Concentrate</li> <li>• Fixation/Perm Diluent</li> </ul>	Invitrogen by Thermo Fisher Scientific
RAL DIFF-QUIK Staining Kit	<ul style="list-style-type: none"> <li>• RAL Diff-Quik Fixative solution (methanol based solution)</li> <li>• RAL Diff-Quik Solution I (Xanthene solution) = buffered solution of Eosin Y (anionic dye)</li> <li>• RAL Diff-Quik Solution II = buffered solution of thiazine dyes (cationic dyes), consisting of methylene blue and Azure A</li> </ul>	RAL Diagnostics by Siemens Healthineers
Mouse IFN-gamma DuoSet ELISA	<ul style="list-style-type: none"> <li>• Capture Antibody</li> <li>• Detection Antibody</li> <li>• Recombinant Standard</li> <li>• Streptavidin conjugated to horseradish-peroxidase</li> </ul>	R&D Systems

### 3.1.7. Buffer and consumption solutions

Collagenase Type I	400 U/ml in DMEM high glucose
Digestion medium	50 µl DNase (20 mg/ml) 500 µl Collagenase Type I (400 U/ml) 9,5 ml DMEM high glucose medium
DNase	20 mg/ml in RPMI

ELISA assay diluent	10% FCS in PBS
ELISA block buffer	1% BSA in PBS
ELISA capture antibody	4,0 µg/ml in PBS
ELISA coating puffer	7.13 g Na <sub>2</sub> HCO <sub>3</sub> + 1.59 g Na <sub>2</sub> CO <sub>3</sub> + 1l PBS; pH 9,5
ELISA detection antibody	600 ng/ml in ELISA reagent diluent
ELISA reagent diluent	0.1% BSA, 0.05% Tween 20 in PBS
ELISA stop solution	1 M H <sub>3</sub> PO <sub>4</sub>
ELISA substrate solution	1:1 mixture of Color reagent A (H <sub>2</sub> O <sub>2</sub> ) & Color reagent B (Tetramethylbenzidine)
ELISA wash buffer	0.05% Tween 20 in PBS
Fixation Solution	¼ eBioscience Fixation/Permeabilization Concentrate ¾ eBioscience Fixation /Perm Diluent
HEPES 1M	200 ml PBS + 47.66 g HEPES sterile filtered, 4°C, pH 7.4
<i>Leishmania</i> Medium	70% M199 Gibco (1x) 20% FCS 4% HEPES 1 M 2.85% M199 10x 1% Adenine 10 mM 1% L-Glutamine, (1%) 1% Penicillin / Streptomycin (100 U/ml) 0.2% Hemine (0.25%)
PBS 1X	1 PBS tablet in 500 ml aqua dem.

RPMI complete Medium	5% FCS (5%) 1% HEPES 1M 1% Non-Essential Amino-Acids 1% Penicillin / Streptomycin 1% L-Glutamine 0.1% 50mM 2-Mercaptoethanol in RPMI-1640
Soluble <i>Leishmania</i> Antigen	1:100 in RPMI
Staphylococcus Enterotoxin B	10 µg/ml in PBS
Wash buffer	1 part Permeabilization Buffer 10X 9 parts aqua dem.
2-Mercaptoethanol 50mM	400 µl + 100 ml aqua dem.

### 3.1.8. Antibodies

Anti-Mouse Arginase 1 APC, Clone A1exF5	Thermo Fisher Scientific
Anti-Mouse CD11b PE-Cy7, Clone M1/70	Thermo Fisher Scientific /eBioscience
Anti-Mouse CD11c Alexa Fluor 700, Clone	BioLegend
Anti-CD16/32 (FC block), Clone 93	Invitrogen by Thermo Fisher Scientific
Anti-Mouse CD19 Biotin, Clone 6D5	BioLegend
Anti-Mouse CD45 BV421, Clone 30-F11	BioLegend
Anti-Mouse CD49b Biotin, Clone DX5	BioLegend
Anti-Mouse CD64 (Fc $\gamma$ RI) FITC , Clone X54-5/7.1	BioLegend
Anti-Mouse CD90.2 / Thy-1.2 Biotin, Clone 30-H12	Thermo Fisher Scientific

Anti-Mouse I-A/I-E BV510, Clone M5/114.15.2	BioLegend
Anti-Mouse iNOS PE, Clone CXNFT	Thermo Fisher Scientific
Anti-Mouse Ly6C BV711, Clone HK1.4	BioLegend
Anti-Mouse Ly6G Biotin, Clone 1A8	BioLegend
Anti-Mouse NK1.1 Biotin, Clone PK136	BioLegend

### 3.1.9. Software

FACS Software	Thermo Fisher Scientific
FlowJo Version 9.9.5	FlowJo™ Software, Ashland, USA
GraphPad Prism Version 8.4.0	GraphPad Software, San Diego, CA, USA

## 3.2 Methods

### 3.2.1. Animal experiments welfare certificate

Mice were bred under *specific pathogen free* conditions, according to North Rhine-Westphalia authority guidelines. Animal care was provided by the animal care takers of the Tierhaltungsnetzwerk der Medizinischen Fakultät, Universität zu Köln. Infection and euthanization as well as organ extraction was carried out according to legal regulations. For the mice used and the procedures performed in this study the experimental reference number is: (AZ) 81-02.04.2019.A234.

**Table 1** Number of mice analyzed per time point and strain

Week	Strain	
	C57BL/6	BALB/c
0 (naive)	12	10
1.5	10 / 10	10 / 10
3	5 / 5 / 5	5 / 5 / 5
6	5 / 8 / 5	4 / 5 / 5
9	5 / 5 / 5	5 / 5 / 5
12	5 / 5 / 6	-

### 3.2.2. Cultivation of *L. major* promastigotes

*L. major* promastigotes were prepared by a laboratory technician at Universitätsklinikum Köln.  $1-2 \times 10^7$  freshly isolated amastigotes were plated in 5 ml *Leishmania* medium. The bottle was sealed airtight and incubated at 27°C. After 2-3 days, 5 ml of fresh medium was added to dilute the culture 1:2. After a further 3-5 days, the cells were split for the first time (1:5, sometimes 1:2) and then split two or three times a week at a ratio of 1:10, depending on the density. Every 6 to 8 weeks, new medium with *L. major* amastigotes ( $1-2 \times 10^7/5$  ml) was prepared.

### **3.2.3. Intradermal infection of mice**

Infection of mice was achieved by low-dose intradermal inoculation of approximately  $10^3$  high-infectious metacyclic promastigotes in DMEM into each ear of both, C57BL/6 and BALB/c mice. Inoculation was performed by a technician of the lab.

### **3.2.4. Determination of ear lesion size**

Ear lesion size was measured three-dimensional (ear thickness, width and length of lesion) using a caliper and the volume was calculated using the following formula:  $[(a/2 \times b/2 \times c/2) \times 4/3 \times \pi]$ .

### **3.2.5. Single cell isolation from ears by enzymatic and mechanical tissue digestion**

At the required time points, mice were euthanized by CO<sub>2</sub> euthanasia and afterwards disinfected using 70% ethanol. Ears were harvested and transferred into cell culture 6-well plates containing 5 ml PBS per well. Ears were collected separately per animal. To achieve efficient digestion, each ear was split to ventral and dorsal dermal sheet and was then dermis down transferred into a cell culture 6-well plate containing digestion medium. Tissue was incubated for 1 h at 5% CO<sub>2</sub> and 37°C. Digestion was stopped by addition of 2 ml RPMI complete solution to each well. For mechanical digestion, each ear was transferred into a gentleMACS C tube, containing 5 ml RPMI complete solution. Tissue was homogenized using the gentleMACS Dissociator. To separate cells from the remaining tissue material, each cell suspension was transferred through a 70 µm cell strainer into a 50 ml tube. Remaining digestion medium of each ear was also passed through the strainer into the corresponding tube. GentleMACS C tubes were washed using 10 ml RPMI complete solution and content was also transferred through the cell strainers into the tubes.

To separate cells from their medium, all samples were centrifuged at 300 g, 4°C, for 10 min. Supernatant was discarded and cell pellets were resuspended in defined volumes of PBS in order to be ready for cell counting.

### **3.2.6. Counting viable cells**

Viable cells were counted using Neubauer Chambers. Cell pellets were resuspended in defined volumes of PBS and diluted with trypan blue in a specific concentration according to cell pellet volumes. Only viable, unstained cells were counted. 4 squares (16 chambers each)

and only top and left borders were counted. To calculate total cell counts per organ, the following formula was used:

- Total cell counts per organ = mean count of 4 squares x dilution of trypan blue x  $10^4$  (chamber factor) x total volume in ml

### **3.2.7. Flow cytometry**

#### **Surface staining**

Fluorescence-activated cell sorting (FACS) is a common method used to analyze and characterize cells by their phenotypic appearance. After single cell isolation and counting of cells, cells were centrifuged at 300 g, 4°C, 10 min. to gain cell pellets, supernatant was discarded and cell pellets were resuspended in defined volumes of PBS to gain  $3 \times 10^6$  cells per 200  $\mu$ l (if total cell counts were below this, lower numbers were taken). Cells were transferred to a 96-well plate for staining. The plate was centrifuged at 300 g, 4°C, 4 min. to gain cell pellets, supernatant was discarded and cell pellets were resuspended in 50  $\mu$ l of anti-FC-block (anti-CD16/-CD32) each and incubated at 4°C in the dark for 30 min. Anti-FC-block incubation was stopped by adding 150  $\mu$ l clean PBS to each sample. Cells were centrifuged at 300 g, 4°C, 4 min., supernatant was discarded and cells were washed by centrifugation with 150  $\mu$ l of PBS.

In preliminary experiments (data not shown), different antibody concentrations and markers were tested to determine optimal antibody panels for the staining.

Cell pellets were resuspended in 50  $\mu$ l of surface staining containing the following antibodies in the concentrations shown in Table 2: Anti-mouse Alexa Fluor 700-linked CD11c, Biotin-linked-CD19, -CD49b, -CD90.2, -Ly6G, and -NK1.1, BV421-linked CD45, BV510-linked I-A/I-E, BV711-linked Ly6C, FITC-linked CD64 and PE-Cy7-linked CD11b.

Staining was incubated at 4°C in the dark for 30 min. and stopped by adding 150  $\mu$ l PBS to each well. The plate was centrifuged at 300 g, 4°C, 4 min., supernatant was discarded and cells were washed twice with 150  $\mu$ l clean PBS followed by centrifugation at 300 g 4°C for 4 min. Cell pellets were resuspended in 50  $\mu$ l of APC-eFluor 780-linked-Streptavidin and incubated at 4°C in the dark for 30 min. Incubation of staining was stopped by adding 150  $\mu$ l clean PBS. The plate was centrifuged, supernatant was discarded and cells were again washed by centrifugation with clean PBS as previously described.

**Table 2 Antibody panel used for surface staining**

Laser/Channel	Fluorochrome	Surface	Dilution in PBS
		FC Block	1:100
BL1	FITC	CD64	1:100
RL2	Alexa Fluor 700	CD11c	1:200
RL3	APC eFluor 780	Streptavidin	1:400
RL3	APC eFluor 780	Viability	1:1000
RL3	Biotin	CD19	1:400
RL3	Biotin	CD49b	1:250
RL3	Biotin	CD90.2	1:1000
RL3	Biotin	Ly6G	1:500
RL3	Biotin	NK1.1	1:500
VL1	BV421	CD45	1:400
VL2	BV510	MHC II	1:150
VL4	BV711	Ly6C	1:600
YL4	PE-Cy7	CD11b	1:400

## Fixation & intracellular staining

For fixation of cells, the eBioscience fixation kit was used. Per cell pellet, 100 µl of fixation solution was used. Each cell pellet was resuspended in 100 µl of fixation solution and then incubated at 4°C in the dark for 45 min. After 45 min., the fixation process was stopped by adding 100 µl of wash buffer.

After cell fixation, cells were washed twice by centrifugation at 400 g 4°C for 5 min. using 150 µl wash buffer. For intracellular staining, cell pellets were resuspended in 50 µl of intracellular staining solution, which consisted of wash buffer containing PE-linked anti-iNOS and APC-linked anti-Arginase 1 antibodies in the concentrations shown in Table 3. The cells were incubated with staining solution at 4°C in the dark for 45 min. The incubation was stopped by adding 100 µl wash buffer and cells were centrifuged at 400 g 4°C, 5 min. Cells were washed with 150 µl of wash buffer by centrifugation at 400 g 4°C for 5 min. and afterwards, cell pellets were resuspended in 100 µl of wash buffer.

**Table 3 Antibody panel used for intracellular staining**

Laser/Channel	Fluorochrome	Surface	Dilution in eBioscience kit wash buffer (permeabilization solution)
RL1	APC	Arginase	1:100
YL1	PE	iNOS	1:200

## Acquisition

Stained cell samples were acquired with the FACS Attune NxT Acoustic Flow Cytometer by Invitrogen/Thermo Fisher Scientific using the NxT Attune Software. Prior to acquisition, automatic compensation was performed with single cell staining or beads using appropriate fluorochromes. Where necessary, manual compensation was performed additionally afterwards. Analysis and manual compensation of data was performed using FlowJo Software, version 9.9.5.

## Myeloid cell gating strategy in ear samples

Isolated ear tissue cells obtained from naïve mice and mice at week 1.5, 3, 6, 9 and 12 after infection with *L. major* were stained with surface staining in order to characterize different myeloid cell subsets based on their phenotypical appearance using flow cytometry. Since cell

numbers obtained from ear tissue of naïve mice and mice at early time points after infection were very low, here, 2-4 ear samples from different mice were pooled to generate detectable values.

After excluding doublets, a specific gating strategy was used to enrich for myeloid cells (Figure 2). First, by using lineage markers specific for B cells (CD19), T cells (CD90.2), NK cells (CD49b/DX-5 and NK1.1) and neutrophil granulocytes (Ly6G), myeloid cells were identified as lineage negative ( $\text{lin}^{\text{neg}}$ ) and  $\text{CD45}^+$  cells (Figure 2A+B).<sup>47,55,72,73,79,85,87,192,193</sup>

Next, MHC class II-expressing cells were selected (Figure 2C). Regarding the subtype of cells expressing MHC II, different types of these cells are possible:

It was shown, that DC express constitutively high levels of MHC II on their surface<sup>61,85,194,195</sup> which is well accepted by today (e.g. reviewed in Merad et al. (2013) and Kashem et al. (2017)).<sup>55,87</sup> In contrast, on M $\Phi$  and monocytes, this marker was only found in a minority of cells, when kept under specific-pathogen-free (SPF) conditions. However, when these cells were kept under non-SPF conditions or injected with bacille Calmette-Guérin (BCG), MHC II levels were similar to those obtained on DC.<sup>85</sup> Specifically, in the infection with *L. major*, MHC II upregulation was found to be stronger in infected DC than in infected M $\Phi$ .<sup>109</sup> In addition, there is evidence, that upon differentiation of monocytes into M $\Phi$  or DC, MHC class II is upregulated.<sup>47,72,73,75,76</sup>

In our population of cells, subsumed as “MHC II<sup>+</sup> cells”, cells with both, intermediate and high expression levels of MHC II were included. Therefore, cells expressing MHC II were thought to be composed mainly of DC and mo-DC as well as M $\Phi$  and mo-M $\Phi$ .

In addition to tissue-resident or tissue-infiltrating myeloid cells, blood cells from the circulation might be included in this population. Furthermore, this might be an explanation for the number of MHC II<sup>neg</sup> cells found throughout all weeks post-infection in ear dermis, since mouse blood monocytes are mainly described to be MHC II negative.<sup>47,72,73,76,196,197</sup>

Therefore, monocytes were suspected to make up the majority of MHC II<sup>neg</sup> cells. To differentiate between them and other myeloid cells, the population of cells identified as  $\text{CD45}^+$ ,  $\text{lin}^{\text{neg}}$ , first was further separated into MHC II<sup>neg</sup> and MHC II<sup>+</sup> cells. MHC II<sup>neg</sup> and MHC II<sup>+</sup> myeloid cells were then further analyzed using different markers. These markers included CD11b, CD11c, CD64 and Ly6C.

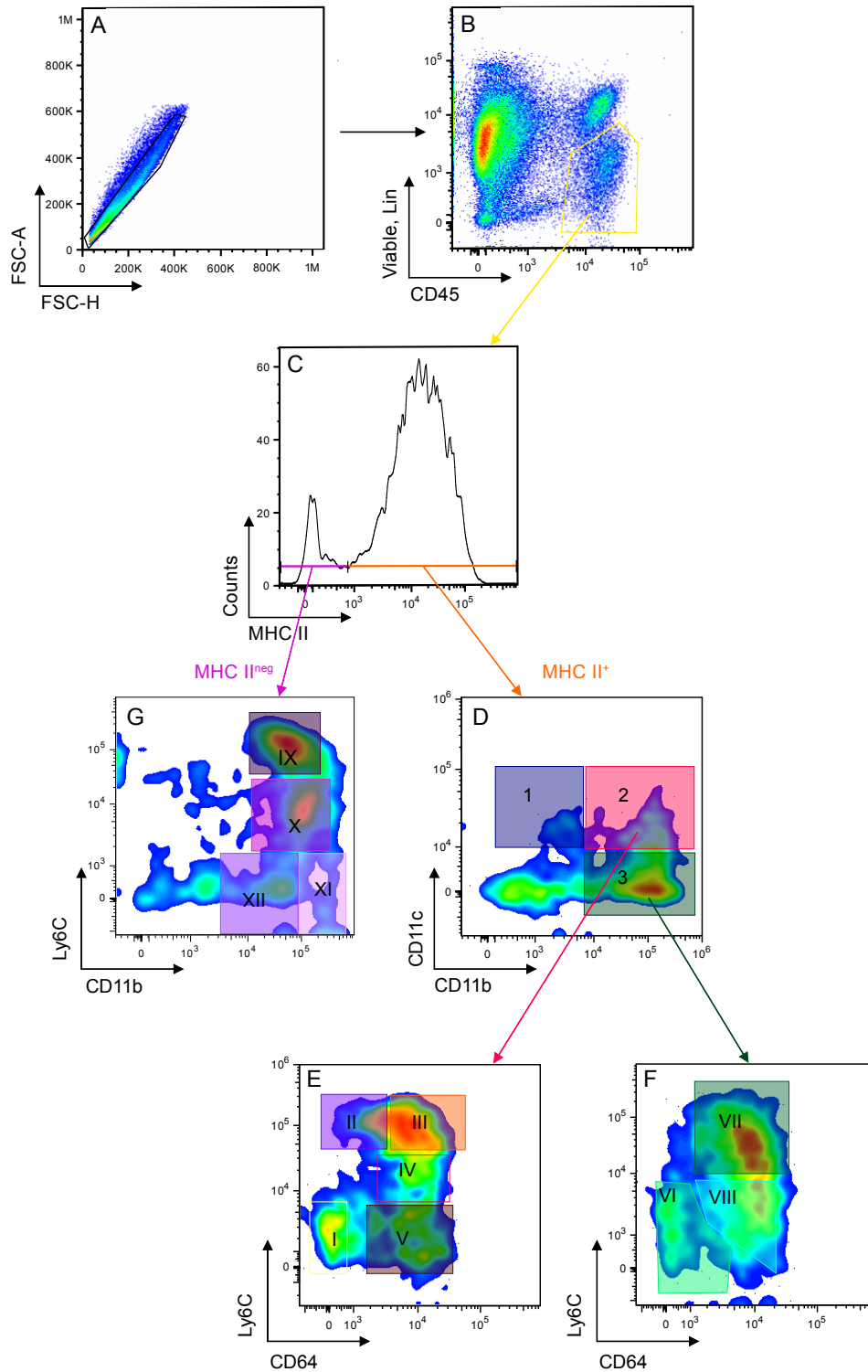


**Figure 2 Gating strategy**

Representative FACS density plots for the gating strategy used to identify myeloid cell subsets in ear tissue. A) Doublets were excluded in side and forward scatter (shown is forward scatter, FSC-A and FSC-H). B) A gate was set for viable, lineage<sup>neg</sup> and CD45<sup>+</sup> cells. C) Resulting cells were separated into MHC II<sup>neg</sup> vs. MHC II<sup>+</sup> cells. The gating strategy was applied to all experiments and adjusted accordingly. D) MHC II<sup>+</sup> cells were further subdivided in group 1, 2 and 3 according to the expression of the markers CD11b and CD11c. E) CD11b<sup>+</sup>/CD11c<sup>+</sup> (group 2) and F) CD11b<sup>+</sup>/CD11c<sup>neg</sup> cells (group 3) were then analyzed for the expression of Ly6C and CD64 and subdivided into eight subsets. G) MHC II<sup>neg</sup> cells were further analyzed for the expression of the markers CD11b and Ly6C and subdivided into four subsets.

Many years ago, the marker CD11c was detected and its expression was found especially on DC.<sup>194,195</sup> Today, it is well accepted that this marker is expressed on DC.<sup>87,94,192,198</sup> When differentiating into DC, monocytes upregulate CD11c.<sup>47</sup> In addition, CD11c can be found on monocytes and M $\Phi$ .<sup>195,199-201</sup> Also mo-M $\Phi$  may express CD11c, which has been observed in the gut.<sup>72</sup>

CD11b (M1/70) is expressed on (dermal) M $\Phi$ <sup>61,192,194,202,203</sup> as well as monocytes<sup>47,69,203</sup> and DC.<sup>61,194,195</sup> It should be noted, that subtypes of DC differ in their expression of CD11b. Specifically among dDC, Henri et al. (2010) showed, that the majority of dDC can be subdivided into two subsets and distinguished by expression of CD11b vs. absence of CD11b.<sup>94</sup> In other sources, these cells are also referred to as cDC1 and cDC2.<sup>55,57,102</sup>

According to the different marker expression of CD11b and CD11c, three myeloid cell groups (1-3) were identified among MHC II<sup>+</sup> cells (Figure 2D): Group 1 expressed MHC II and CD11c, but lacked expression of CD11b. Since absence of CD11b is a feature of cDC1, and MHC II<sup>+</sup><sup>61,85</sup> together with CD11c expression<sup>94,192,194,195,198</sup> also fits to the DC-like cell type, these cells were considered as cDC1.<sup>55,57,87</sup> Due to the previously described features, group 2 (MHC II<sup>+</sup>/CD11b<sup>+</sup>/CD11c<sup>+</sup>) was thought to be constituted of M $\Phi$  or DC of any origin, therefore named Mo/M $\Phi$ /DC, whereas group 3 (MHC II<sup>+</sup>/CD11b<sup>+</sup>/CD11c<sup>neg</sup>) most likely contributed to different M $\Phi$  subsets, possibly also including mo-M $\Phi$  and were termed Mo/M $\Phi$ .

The separation and identification of M $\Phi$  vs. DC by only the above described markers is not necessarily sufficient, since markers often are not exclusive for the different cell types, marker expression within groups defined as M $\Phi$  or DC may differ, and especially during inflammation, additional cells infiltrate the tissue.<sup>57,87,196,197</sup> Therefore, we made an attempt to categorize the cell subsets present in mouse dermis, by adding markers that helped to define the different myeloid cell types more conclusively. Since technical conditions only allowed usage of a limited antibody panel, we selected two additional surface markers, CD64 and Ly6C. Based on the literature, these markers, in combination with traditional markers, such as MHC II, CD11b or CD11c, can help to make more definitive categorizations of myeloid cell subsets<sup>72-76,98,196,197,204</sup> In the following it is described, how the identification and subdivision of myeloid cells into eight different myeloid cell subsets was performed using the additional surface markers Ly6C and CD64.

Gautier et al. (2012) identified a group of mRNA transcripts which are more powerful for the aim of distinguishing M $\Phi$  from DC.<sup>196</sup> Among these genes, one of them encodes the high-affinity Fc $\gamma$  receptor I, CD64, which is expressed on M $\Phi$  and partially on monocytes<sup>196</sup> and can be used to distinguish dDC from mo-DC and M $\Phi$ .<sup>72,73,98,196,204</sup>

Therefore, we added the marker CD64 to our antibody panel (Figure 2E+F). After the analysis of CD11b and CD11c expression, we further examined Mo/MΦ/DC (group 2, Figure 2E) and Mo/MΦ (group 3, Figure 2F), which only differed by their expression of CD11c, for the expression of the markers CD64 and Ly6C. Ly6C is a monocyte marker expressed on monocytes in low to high amounts and may indicate a monocytic origin of DC and MΦ. However, it should be noticed, that Ly6C can be downregulated upon differentiation of monocytes into DC and MΦ.<sup>69,72,73,75,76,98,197</sup>

cDC1 (group 1) were not further analyzed for their expression of Ly6C and CD64, since these cells could be categorized as cDC1 due to their expression of MHC II and CD11c, as well as absence of CD11b<sup>55,57,61,85,87,94,192,194,195,198</sup> and, in addition, made up very low percentages.

Among the Mo/MΦ/DC (group 2, MHC II<sup>+</sup>, CD11b<sup>+</sup>, CD11c<sup>+</sup>), five different cell subsets were separated: I (Ly6C<sup>neg</sup>/CD64<sup>neg</sup>), II (Ly6C<sup>+/hi</sup>/CD64<sup>lo/+</sup>), III (Ly6C<sup>+/hi</sup>/CD64<sup>+/hi</sup>), IV (Ly6C<sup>+</sup>/CD64<sup>+/hi</sup>) and V (Ly6C<sup>neg</sup>/CD64<sup>+/hi</sup>), (Figure 7).

In a study by Tamoutounour et al. (2012), among CD11b<sup>+</sup> cells, the identification of intestinal DC by their CD11c<sup>hi</sup>, CD64<sup>neg</sup> phenotype was described.<sup>72</sup> Furthermore, in another study, Tamoutounour et al. (2013) separated a population of CD11b<sup>+</sup> dermal cells into two groups: 1) Ly6C<sup>neg</sup> CD64<sup>neg</sup> (Flt3L-dependent, CCR2-independent) dermal (conventional) DC and 2) Ly6C<sup>lo to hi</sup> CD64<sup>lo to hi</sup> (Flt3L-independent, CCR2-dependent) “CD11b<sup>+</sup> non-DCs”.<sup>73</sup> The characterization of conventional DC (cDC) applied to our subset I with expression of MHC II, CD11b and CD11c and low expression or absence of Ly6C and CD64. We also defined these cells as cDC, but further characterized them as cDC2 based on their expression of CD11b.<sup>55,57,73</sup>

In contrast, subset II resembled mo-DC, defined by high expression of Ly6C and low to positive expression of CD64, similar to the investigation of Tamoutounour et al. (2013), where a population characterized by marker expression MHC II<sup>lo to +</sup>, CD11b<sup>+</sup>, CD11c<sup>neg to lo</sup>, Ly6C<sup>lo to hi</sup> and CD64<sup>lo to +</sup> were considered mo-DC.<sup>73</sup> In addition, Chow et al. (2016) also described mo-DC in the spleen as CD11c<sup>int</sup>, CD11b<sup>high</sup>, MHC II<sup>+</sup>, Ly6C<sup>+</sup> and CD64<sup>+</sup>.<sup>74</sup> Importantly, also in a study by Leon et al. (2007), in *L. major* infected mice, the description of mo-DC correlated with our subset II.<sup>75</sup>

In addition, these cells phenotypically also resembled cells, defined by Serbina et al. as “TipDCs”, which are characterized by their monocytic origin, as well as their expression of iNOS.<sup>205,206</sup>

When Tamoutounour et al. (2013) analyzed the “CD11b<sup>+</sup> non-DC” population in mouse skin, they found two populations resembling the features of tissue MΦ. Those populations both were CD64<sup>+</sup> and Ly6C<sup>lo</sup>, but could be distinguished into MHC II<sup>neg</sup> and MHC II.<sup>73</sup> The phenotypic

appearance of the population expressing MHC II fitted to subset V in this investigation, which also expressed MHC II and CD11b. Although MΦ and DC may express CD11c<sup>196</sup>, we characterized these cells as MΦ rather than mo-DC or cDC. This was based on their higher levels of CD64 expression, compared with CD64 levels in cells defined as mo-DC or cDC, which is in accordance with the study by Tamoutounour et al. (2013), where MΦ were defined as CD64<sup>hi</sup>, whereas mo-DC were CD64<sup>lo/+</sup> and DCs were CD64<sup>neg</sup>.<sup>73,196</sup>

Because we additionally found cells which showed similar high expression levels of CD64, compared to those obtained in subset V, but differed in their expression of Ly6C, we separated three subsets: III (Ly6C<sup>+/hi</sup>), IV (Ly6C<sup>+</sup>) and V (Ly6C<sup>neg</sup>), which were speculated to be tissue-infiltrating monocytes, developing into MΦ. This speculation was based on several studies: A study by Crane et al. using a model of sterile wound healing indicated, that Ly6C<sup>hi</sup> inflammatory monocytes are recruited from the circulation towards tissue, where they undergo a transition to Ly6C<sup>lo</sup> MΦ, possibly displaying MΦ involved in tissue repair. This transition, however, is not immediate.<sup>207</sup> Also in other studies, a transition from monocytes to MΦ in inflamed tissue has been described: Bain et al. (2013) showed, that in the gut, Ly6C<sup>hi</sup> monocytes give rise to MΦ, which was associated with upregulation of MHC II and CD64, and downregulation of Ly6C and functional markers such as iNOS. This was a continuous process, where distinct differentiation stages could be obtained. Interestingly, during inflammation, this maturation process with full differentiation from Ly6C<sup>hi</sup> inflammatory monocytes into resident MΦ was partly disrupted, leading to accumulation of early stages of their differentiation continuum.<sup>197</sup> Furthermore, Tamoutounour et al (2012) described the transition of Ly6C<sup>hi</sup> monocytes to MΦ in the gut in a waterfall-shaped manner. This was named the “Mo-waterfall”, which summarizes a differentiation process from Ly6C<sup>hi</sup> blood-monocytes towards MΦ-like cells upon tissue entry, accompanied by downregulation of Ly6C, and upregulation of markers such as MHC II, CD64 and CD11c. Importantly, during inflammation, this waterfall primarily consisted of Ly6C<sup>int to hi</sup> cells, with very few Ly6C<sup>lo</sup> cells, and blood monocytes primarily differentiated into MΦ that displayed a Ly6C<sup>int to hi</sup>MHC II<sup>+</sup>CD64<sup>+</sup> phenotype.<sup>72</sup> In group 2, subsets III, IV and V phenotypically represented these differentiation stages in terms of Ly6C downregulation, although they all already expressed MHC II, CD11c and CD64.<sup>72</sup> Subset III phenotypically was the closest to the stage of monocytes, with high expression of Ly6C, and already high expression of CD64 and were therefore considered as mo-MΦ (“mo-MΦ”).<sup>72</sup> Subset V possibly displayed the stage closest to a MΦ (“MΦ”) with expression of CD64, but low expression of Ly6C,<sup>72</sup> while subset IV seemed to be an intermediate stage between subset III and V (“mo-MΦ/MΦ”).

Interestingly, a similar phenomenon as observed in Mo/MΦ/DC (group 2) was also found among Mo/MΦ (group 3). These cells, which were defined by expression of MHC II, CD11b

and absence of CD11c expression, were separated into three different subsets: VI (Ly6C<sup>neg</sup>/CD64<sup>neg/+</sup>), VII (Ly6C<sup>+</sup>/CD64<sup>+/hi</sup>) and VIII (Ly6C<sup>neg</sup>/CD64<sup>+/hi</sup>). Although lacking CD11c expression, subset VII and VIII possibly also resembled the waterfall-like differentiation process from tissue-infiltrating monocytes towards MΦ.<sup>72</sup> Subset VII rather resembled subset III, therefore named “CD11c<sup>neg</sup> mo-MΦ”, whereas subset VIII rather resembled subset V (“CD11c<sup>neg</sup> MΦ”). However, in this group no real intermediate stage was found.

Subset VI, next to expression of CD11b and absence of CD11c, was defined by absence of Ly6C and no to low expression of CD64. Expression of MHC II and CD11b and absence of CD11c and Ly6C were in line with the definition as tissue-resident MΦ (TR-MΦ) by Bain et al. (2013).<sup>197</sup> However, they additionally characterized these cells by the expression of F4/80, a marker we did not include in our study, and also, CD64 expression was lower than described by Bain et al. (2013).<sup>197</sup> Yet, these cells did also not exactly fit to the phenotype of DCs, since they did not express CD11c<sup>87,194,195,198</sup>, although they partly resembled cells described by Tamoutounour et al. (2013) as “CD11b<sup>+</sup> DCs”, which amongst other markers were CD11b<sup>+</sup>, CD64<sup>neg</sup>, Ly6<sup>neg</sup>, MHC II<sup>+</sup> and CD11c<sup>lo to +</sup>.<sup>73</sup> Therefore, it was not exactly clear, whether subset VI cells rather resembled the described TR-MΦ or CD11b<sup>+</sup> DCs.<sup>73,197</sup> Eventually, we defined these cells as TR-MΦ, because of their absence of CD11c, which conflicted with the usual characterization of DC<sup>87,194,195,198</sup>, and second, because cDCs are described to be CD64<sup>neg</sup><sup>72,73,98,196,204</sup>, but in fact, low expression of this marker was found in these cells.

Finally, we analyzed the MHC II<sup>low</sup> population in more detail (Figure 2G): As already mentioned, the population of myeloid cells (CD45<sup>+</sup>, lin<sup>neg</sup>), that did not express MHC II was believed to be constituted mainly of monocytes.<sup>47,72,73,76,196,197</sup> To further confirm the monocytic phenotype of these cells, they were analyzed for the expression of the marker Ly6C, which can be up- and downregulated during differentiation processes of monocytes and is therefore found on the surface of monocytes in low to high amounts.<sup>69</sup> Another marker that fits to the phenotype of blood monocytes is CD11b.<sup>69,72,76,203,208</sup> According to expression levels of Ly6C and CD11b, the population was further subdivided into four different subsets in order to better visualize the differences of marker expression of these cells as well as their distinct behavior over time after infection with *L. major*: IX (Ly6C<sup>hi</sup>, CD11b<sup>+</sup> monocytes), X (Ly6C<sup>int</sup>, CD11b<sup>+</sup> monocytes), XI (Ly6C<sup>lo/neg</sup>, CD11b<sup>+</sup> monocytes), XII (Ly6C<sup>lo/neg</sup>, CD11b<sup>lo/+</sup> monocytes).

### **Determination of total cell numbers per ear**

Due to limited channels available, we used the same FACS channel for the fixable viability dye and the lineage markers. Therefore, to determine total cell numbers per ear, a gate was set on

viable cells in all ear samples and this was conferred to as 100% of viable cells obtained by microscopic cell counting with trypan blue dye exclusion.

Cell numbers of each subset were then calculated by using percentages obtained by our gating strategy (frequency of parent). When analyzing cell subsets, samples with very low cell numbers or no identifiable cell subsets were excluded.

### **3.2.8. Cytospin centrifugation and DiffQuik hematoxylin and eosin staining**

Cytospin technique is a method to separate cells from a fluid medium and layer them on microscope slides. Layering of cells is achieved by centrifugation of the material in a specific centrifuge containing chambers and corresponding microscope slides for each sample.<sup>209</sup> Cytospin centrifugation was performed on cell suspensions generated from infected ear tissue, in order to be able to analyze intracellular and paracellular content of infected ear tissue microscopically. Per cytospin centrifugation tube, cells from one ear sample were used.

20  $\mu$ l of each ear sample were taken and filled up to a volume of 200  $\mu$ l using PBS. Therefore, if cell numbers reached  $3 \times 10^6$ , approximately  $0.3 \times 10^6$  cells of each sample were taken. If cell numbers were below  $3 \times 10^6$ , 10% of each sample was used for cytospin centrifugation.

Cell suspensions were filled into cytospin centrifugation tubes. Each tube was connected with one microscope slide. Cells were centrifugated in the Cytocentrifuge Cellspin I (Cytospin) by THERMAL using the default program of the centrifuge. The resulting cells smeared on microscope slides were stained with DiffQuik hematoxylin and eosin (H&E) staining, using the DIFF-QUIK kit by RAL Diagnostics.<sup>210</sup> As per the instruction manual, each slide was first dipped into the fixation solution for one min. Following this, each slide was dipped into Solution I for two min. and then finally dipped into Solution II for one min. Slides were washed in H<sub>2</sub>O and left to dry. Afterwards, they were examined microscopically for the presence of *L. major* parasites.

### **3.2.9. LN cell preparation**

Cervical lymph nodes were digested mechanically by mashing them through a 70  $\mu$ m cell strainer using the plunger of a syringe. Cell strainers were washed with 1 ml PBS and content of each well was transferred into a 15 ml tube. Each well was washed with 1 ml PBS to collect remaining cells and the solution was also transferred into the corresponding tube. Samples were centrifuged at 300 g, 4°C for 10 min. to separate the cells from their medium. Supernatant was discarded and cell pellets were resuspended in defined volumes of PBS in order to be ready for cell counting. After counting of cells, cells were centrifuged again at 300 g, 4°C, 10

min. to gain cell pellets, supernatant was discarded and cell pellets were resuspended in defined volumes of PBS.

### **3.2.10. Antigen specific restimulation**

To assess in vitro cytokine release levels of lymph node cells in response to *L. major* contact, lymph node cells were restimulated with isolated soluble *Leishmania* antigen (SLA).

SLA was prepared by a laboratory technologist at Universitätsklinikum Köln.<sup>211</sup>

After preparation of single cells of cervical lymph nodes, in a 96-well plate, per well, 200 µl RPMI medium containing  $1 \times 10^6$  cells were plated in restimulation medium. In week three, for each restimulation only  $0,5 \times 10^6$  cells were used, because cell counts were low.

For restimulation, the following media were applied

- $1 \times 10^6$  cells:
  - 10 µl SLA
  - RPMI complete medium; negative control
  - 20 µl Staphylococcus Enterotoxin B (SEB); positive control
- $0,5 \times 10^6$  cells:
  - 5 µl SLA
  - RPMI complete; negative control
  - 10 µl SEB; positive control

To reduce technical errors, per LN sample, up to three replicates were performed (three wells à  $10^6$  cells) for SLA and RPMI medium, respectively, and up to two replicates (two wells à  $10^6$  cells) for SEB medium, if cell counts allowed. After resuspension in the corresponding medium, cells were incubated at 5% CO<sub>2</sub>, 37°C for 48 h.

After 48 h, cells were centrifuged at 300 g, 4°C for 4 min. Supernatant was collected and pooled per medium, then distributed onto 96 well plates and stored at -20°C.

### **3.2.11. Cytokine quantification in supernatant of LN cells**

To quantify the amount of IFN $\gamma$  in supernatant of LN samples after antigen specific restimulation, the sandwich-ELISA “Mouse IFN-gamma DuoSet ELISA” kit by R&D Systems was used. Supernatants of technical repetitions were pooled per lymph node and medium. ELISA was performed according to manufacturer’s instructions:

A 96-well maxi-sorp plate was coated with 100 µl of anti-cytokine capture antibody and incubated overnight at 4°C. For each incubation, the maxi-sorp plate was covered with a plate

sealer. The next day, the plate was washed three times with ELISA wash buffer. After the last washing step, the plate was inverted and blotted against a paper towel to remove any remaining buffer. Per well, 300  $\mu$ l of ELISA block buffer was applied and incubated on a shaker for 1.5 h at room temperature (RT). After incubation, the plate was washed three times with ELISA wash buffer and afterwards, remaining buffer was removed using the described technique. Standard dilution was prepared, and standard concentrations, as well as samples in 100  $\mu$ l reagent diluent each were added to the plate and incubated on a shaker for 1.5 h at RT. After incubation, the plate was washed three times with ELISA wash buffer. Per well, 100  $\mu$ l of detection antibody was added and incubated on a shaker for 1.5 h at RT. After incubation, the plate was washed three times with wash buffer. 100  $\mu$ l of SA-HRP-solution was added per well and incubated for 20 min. at RT protected from light. Afterwards, the plate was washed three times with ELISA wash buffer and remaining fluid was removed. 100  $\mu$ l of ELISA substrate solution was added to each well and incubated for 5-20 min. at RT protected from light. The reaction was stopped by adding 50  $\mu$ l of ELISA stop solution per well. Optical density of each well was determined immediately using the Victor Nivo reading machine set to 450 nm. The blank values were subtracted from the calculated values and a standard curve was then created. Afterwards the values were corrected according to the dilution factors.

### **3.2.12. Statistical analysis**

For all statistical analyses the GraphPad Prism software, version 8.4.0 was used.

For statistical analysis of significance of difference between C57BL/6 and BALB/c mice at corresponding time points, Mann-Whitney-Test was used. For some groups, also a classical t-test would have applied, but since not in all groups normal distribution applied, Mann-Whitney-Test was used for all groups. To find out whether not only differences between means but also differences between distribution of values in the two groups were present, after performing Mann-Whitney-test, also Kolmogorov-Smirnov-test was performed at time points at which significant differences between groups were found. Here, in the majority of subsets and time points tested, the distribution also differed between the two mouse types. Subsets/time points where no statistically significant difference in the distribution was found, despite significant differences in means, are highlighted in the text.

## 4. Results

### 4.1 Development of ear lesions in C57BL/6 vs. BALB/c mice after infection with *L. major*

In order to generate a cutaneous infection with *L. major*, C57BL/6 and BALB/c mice were inoculated intradermally with low doses of *L. major* promastigotes into each ear. First, ear lesion sizes of mice from one independent experiment were measured at different time points after parasite inoculation (Figure 3) to display successful infection and to compare progress of disease between both genotypes of mice.

In C57BL/6 mice, lesion volumes increased until week 6 and had already decreased when measured in week 9. In contrast, in BALB/c mice, lesion volume constantly increased until week 9. Differences of lesion sizes between both genotypes were statistically significant in weeks 6 and 9, where BALB/c mice showed bigger lesions than C57BL/6 mice ( $p$  values  $<0.01$  and  $<0.0001$ ).

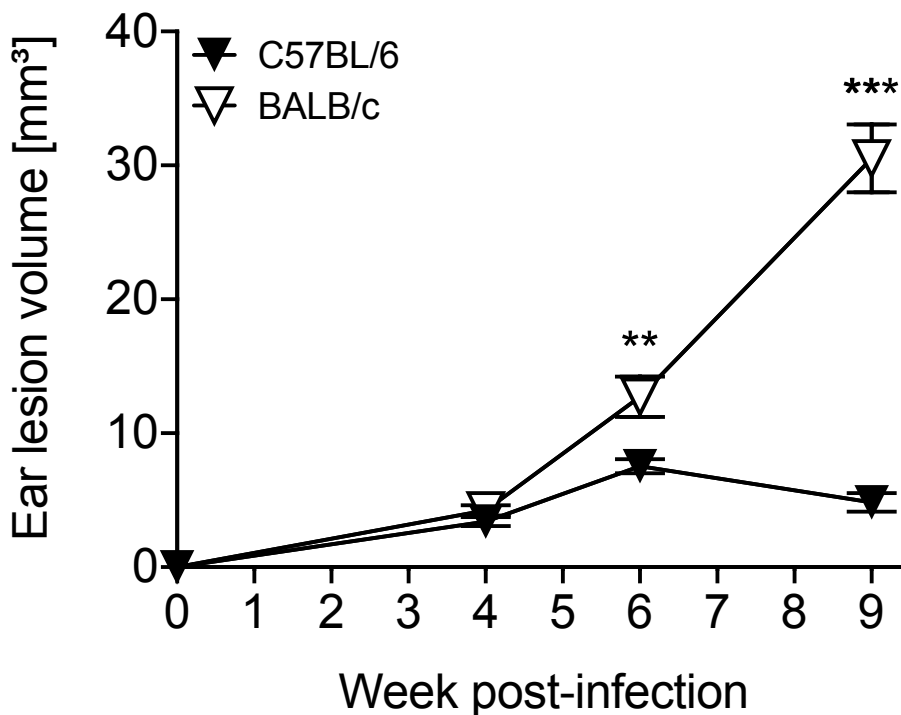


**Figure 3 Ear lesion curve**

Ear lesions of C57BL/6 (▼) and BALB/c mice (▽) were measured in weeks 4 and 6 and weeks 4 and 9 after infection with *L. major*, with  $n \geq 4$  ( $\geq 8$  ears) per time point and strain from one independent experiment. Per mouse, both ears were measured separately, and the mean lesion volume was calculated per mouse. Values represent mean lesion volume in mm<sup>3</sup>  $\pm$  Standard Error of the Mean (SEM). Significance of difference between values in C57BL/6 and BALB/c mice was determined using Mann-Whitney test, with  $\alpha = 0.05$ ; \*\* =  $p < 0.01$ ; \*\*\* =  $p < 0.001$ .

#### 4.2 Presence of parasites in ear lesions of mice after infection with *L. major*

After the inoculation of low doses of *L. major* promastigotes into the ear of C57BL/6 and BALB/c mice, ear tissue was harvested at different time points after infection. Single cell suspensions were prepared from ear tissue by enzymatic and mechanical digestion. To identify *L. major* parasites in single cell suspensions, cytospin centrifugation was performed per cell suspension of each ear sample. Figure 4 shows a section of one Diff Quik-stained slide showing a M $\Phi$  infected with *L. major* amastigotes.

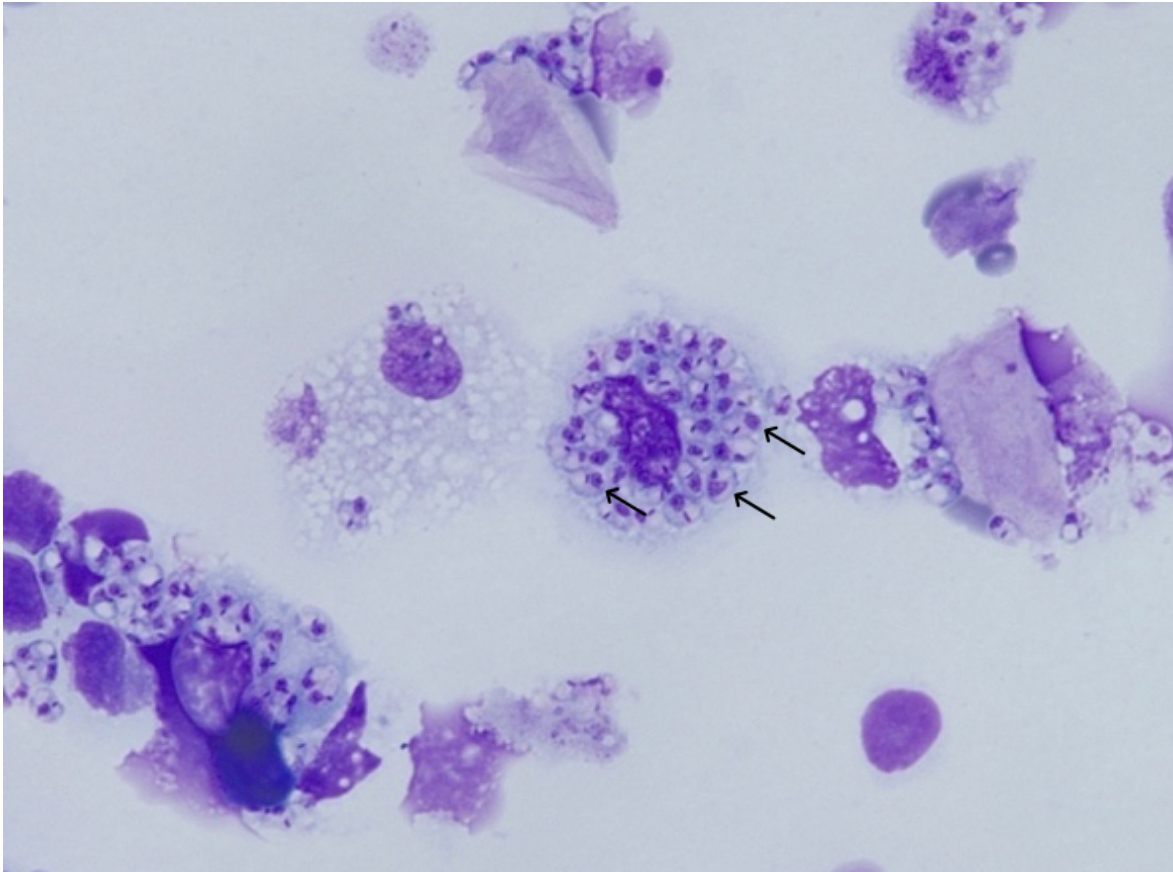


**Figure 4** Parasite uptake into a M $\Phi$  isolated from infected ear tissue

Shown are *L. major* infected cells obtained from an ear sample of a BALB/c mouse in week 9 post-infection. The picture shows representative data from one of three independent experiments at this time point with  $n \geq 4$  ( $\geq 8$  ears) per mouse strain. Ear tissue of C57BL/6 and BALB/c mice was harvested at different time points post-infection with *L. major*. Single cell suspensions were generated from each ear by enzymatic and mechanical digestion. Cytospin centrifugation was performed on each cell suspension isolated from one infected ear. Slides were stained using DiffQuik H&E staining to visualize parasite invasion into cells. In the center of the picture, a M $\Phi$  containing *L. major* parasites can be seen. Arrows mark *Leishmania* amastigotes.

Each slide was screened for the presence of parasites (Table 4). In addition to ear lesion measurements, this served as an additional control for successful infection with *L. major*. In week 3, the overall cell density found on microscope slides was very low and only few slides contained *L. major* parasites (7/30 and 2/30 slides in C57BL/6 and BALB/c mice, respectively). Parasite presence increased towards week 6 in both mice, where all slides contained *L. major* parasites. In BALB/c mice, parasites were present in all ears screened in week 9. In contrast, in C57BL/6 mice, a slight decrease in the number of slides containing parasites was obtained over time (26/30 slides in week 9 and 23/32 slides in week 12).

**Table 4 Presence of *L. major* amastigotes in ear tissue of C57BL/6 and BALB/c mice at different time-points after infection with *L. major***

Week	Strain	
	C57BL/6	BALB/c
	Slides containing parasites	Slides containing parasites
0	n.d.	n.d.
1.5	n.d.	n.d.
3	7/30	2/30
6	36/36	28/28
9	26/30	30/30
12	23/32	n.d.

Ear tissue of C57BL/6 and BALB/c mice was harvested at different time points after infection with *L. major*. Single cell suspensions were generated from each ear by enzymatic and mechanical digestion. Cytospin centrifugation was performed per cell suspension isolated from one infected ear. The resulting cells smeared on a microscope slide were stained using DiffQuik H&E staining to visualize parasite invasion into tissue cells. Values represent the numbers of microscope slides containing *L. major* amastigotes out of the total number of slides examined per mouse strain and time point, with  $n \geq 4$  ( $\geq 8$  ears) from three independent experiments. N.d. = not determined.

### **4.3 IFN $\gamma$ release of LN cells at different time points after antigen-specific restimulation in *L. major* infection**

In addition to ear tissue of *L. major* infected mice, the ear draining cervical LN of these mice were also harvested at different time points after infection. LN tissue was digested mechanically to isolate single cells. The resulting cell suspension was analyzed for cells capable of IFN $\gamma$  release in response to *L. major* exposure, which was achieved by antigen specific restimulation performed with SLA, (Figure 5). Cells isolated in weeks 3, 6 and 9 post-infection from both genotypes and in week 12 from C57BL/6 mice were restimulated with SLA for 48 h. Afterwards, levels of IFN $\gamma$  in supernatant of LN samples were assayed using sandwich-ELISA. Positive controls, which were performed by stimulation of cells with SEB all revealed high IFN $\gamma$  levels, indicating viable cell preparations containing APC and T cells (data not shown).

Unstimulated samples showed low IFN $\gamma$  production throughout all weeks post-infection in C57BL/6 mice. In BALB/c mice, a small increase in IFN $\gamma$  was observed over time. Release levels in unstimulated samples of C57BL/6 and BALB/c mice did not differ significantly in weeks 3 and 6 but did in week 9 ( $p$  value < 0.0001).

In SLA-stimulated samples of C57BL/6 LN cells, IFN $\gamma$  release increased over time starting in week 3 with  $7.5 \pm 0.7$  ng/ml and reaching maximum levels in week 9 ( $35.6 \pm 7.4$  ng/ml) and week 12 ( $37.3 \pm 10.5$  ng/ml). In contrast, in BALB/c mice, significantly lower levels of IFN $\gamma$  were found in week 3 with  $3.3 \pm 0.1$  ng/ml. Also in week 9, IFN $\gamma$  levels were lower ( $28.7 \pm 4.2$  ng/ml), although not statistically significant.

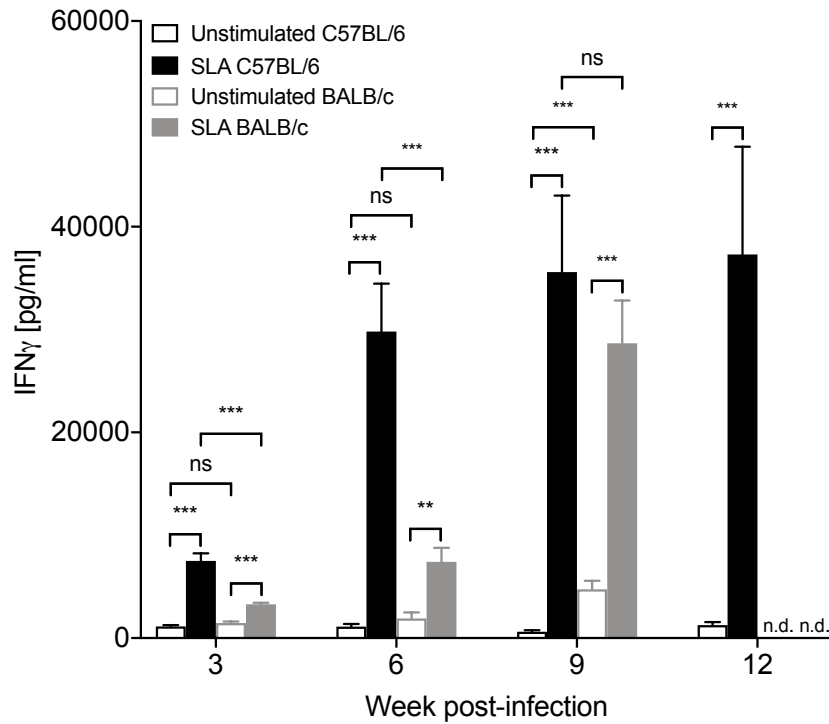


**Figure 5 IFN $\gamma$  quantification in supernatant of LN cells restimulated with SLA at different time points after infection with *L. major***

Cervical LN from C57BL/6 (black) and BALB/c mice (grey) were harvested in weeks 3, 6, 9 and 12 after infection with *L. major*. LN were pooled per mouse and single cells were obtained by mechanical digestion. LN cells were restimulated with SLA or left untreated. IFN $\gamma$  levels assessed by ELISA performed on supernatant of cervical LN are shown in pg/ml, with  $n \geq 4$  of three independent experiments per time point and strain. Error bars show means  $\pm$  SEM. Significance of differences between values in C57BL/6 and BALB/c mice was determined using Mann-Whitney test, with  $\alpha = 0.05$ ; \* =  $p < 0.05$ ; \*\* =  $p < 0.01$ ; \*\*\* =  $p < 0.001$ .

#### 4.4 Myeloid cells in ears of C57BL/6 and BALB/c mice in steady state and at different time points after infection with *L. major*

Isolated ear tissue cells obtained from naïve mice and mice at week 1.5, 3, 6, 9 and 12 after infection with *L. major* were stained with surface staining in order to characterize different myeloid cell subsets based on their phenotypical appearance using flow cytometry. Since cell numbers obtained from ear tissue of naïve mice and mice at early time points after infection were very low, here, 2-4 ear samples from different mice were pooled in order to generate detectable values.

By using a dumping channel including different lineage markers we aimed to gate out all non-myeloid cells. Figure 6 shows percentages and total cell numbers of viable, CD45<sup>+</sup> and lineage (CD19, CD90.2, CD49b/DX-5, NK1.1 and Ly6G) negative cells over time after infection in ear samples of C57BL/6 and BALB/c mice.

Percentages and cell numbers increased over time after infection in both mice, with a slight decrease seen in week 6. In week 3, statistically significant higher percentages were found in BALB/c mice than in C57BL/6 mice ( $p = 0.000077$ ), whereas in week 9 after infection, statistically significant higher percentages of myeloid cells were found in C576BL/6 than in BALB/c mice ( $p = 0.000161$ ).

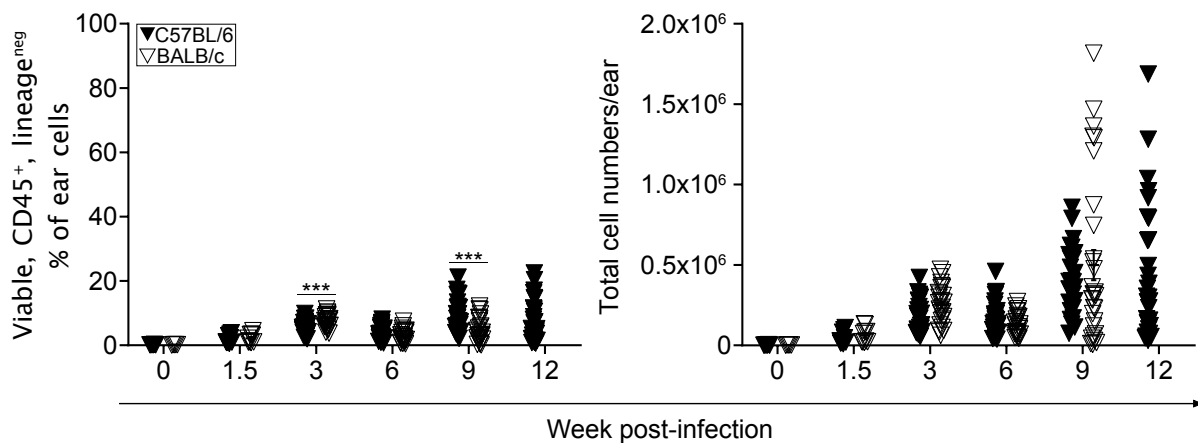


**Figure 6** Viable, CD45<sup>+</sup>, lineage<sup>neg</sup> myeloid cells in naïve mice and after infection with *L. major*

Ear tissue of C57BL/6 (▼) and BALB/c (▽) mice was harvested at different time points after infection with *L. major*, with  $n \geq 4$ , ( $\geq 8$  ears) from three independent experiments per time point and strain. Single cell suspensions were generated from each ear by enzymatic and mechanical digestion. At weeks 0 (naïve mice) and 1.5, 2-4 ear samples were pooled to enrich cells to generate more valuable results. Cells were stained with surface staining and antigen expression of cells was assessed using flow cytometry. Myeloid cells were identified by expression of the surface marker CD45<sup>+</sup> and absence of the lineage markers CD19, CD90.2, CD49b/DX-5, NK1.1 and Ly6G, (lin<sup>neg</sup>). Shown is the development of percentages and total cell numbers per ear of these myeloid cells over time after infection with *L. major* in C57BL/6 and BALB/c mice. Significance of differences between values in C57BL/6 and BALB/c mice was determined using Mann-Whitney test, with  $\alpha = 0.05$ ; \* =  $p < 0.05$ ; \*\* =  $p < 0.01$ ; \*\*\* =  $p < 0.001$ .

After defining myeloid cells, we separated between MHC II<sup>pos</sup> and MHCII<sup>neg</sup> myeloid cells. Figure 7 shows percentages and total cell numbers per ear of MHC II<sup>+</sup> and MHC II<sup>neg</sup> myeloid cells over time after infection. Percentages and total cell counts of MHC II<sup>+</sup> myeloid cells increased over time after infection in both, C57BL/6 and BALB/c mice with a slight decrease in week 6 after infection and an increase afterwards. Statistically significant differences between mice were found in percentages of uninfected mice ( $p = 0.004329$ ), as well as in weeks 3 ( $p = 0.000783$ ), 6 ( $p = 0.000012$ ) and 9 ( $p < 0.000001$ ) after infection with *L. major*. In MHC II<sup>neg</sup> myeloid cells, percentages slightly decreased towards week 1.5 and week 3 after infection, then showed an increase in week 6 after infection in both mice. In week 9 after infection, percentages had decreased in both mice, again, however this decrease was stronger in C57BL/6 mice than in BALB/c mice. In percentages, statistically significant differences between mice were found in naïve mice ( $p = 0.004329$ ), as well as in weeks 3 ( $p = 0.000783$ ), 6 ( $p = 0.000012$ ) and 9 ( $p < 0.000001$ ) after infection with *L. major*. Total cell numbers per ear increased towards week 3 after infection in both mice, then decreased in week 6 after infection, followed by increasing cell numbers again in weeks 9 and 12 after infection with *L. major*. Statistically significant differences between mice were found in week 3 after infection ( $p = 0.000035$ ).

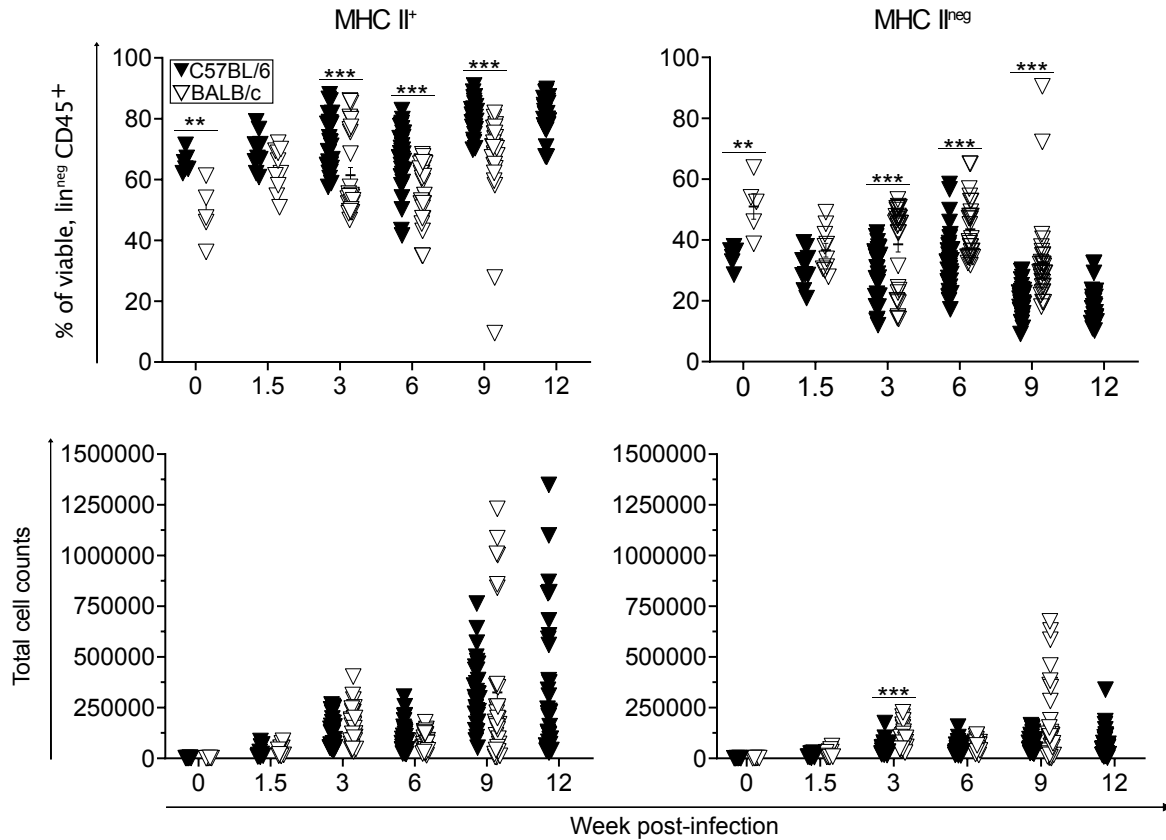


**Figure 7 MHC II<sup>+</sup> and MHC II<sup>neg</sup> myeloid ear tissue cells in naïve mice and after infection with *L. major***

Ear tissue of C57BL/6 (▼) and BALB/c (▽) mice was harvested at different time points after infection with *L. major*, with  $n \geq 4$ , ( $\geq 8$  ears) from three independent experiments per time point and strain. Single cell suspensions were generated from each ear by enzymatic and mechanical digestion. At weeks 0 (naïve mice) and 1.5, 2-4 ear samples were pooled to enrich cells to generate more valuable results. Cells were stained with surface staining and antigen expression of cells was assessed using flow cytometry. Myeloid cells were identified by expression of the surface marker CD45<sup>+</sup> and absence of the lineage markers CD19, CD90.2, CD49b/DX-5, NK1.1 and Ly6G, (lin<sup>neg</sup>). Shown is the development of percentages and total cell numbers per ear of MHC II<sup>+</sup> and MHC II<sup>neg</sup> myeloid cells over time after infection with *L. major* in C57BL/6 and BALB/c mice. Significance of differences between values in C57BL/6 and BALB/c mice was determined using Mann-Whitney test, with alpha = 0.05; \* =  $p < 0.05$ ; \*\* =  $p < 0.01$ ; \*\*\* =  $p < 0.001$ .

#### 4.5 Distribution of myeloid ear cells based on CD11b and CD11c marker expression

CD45<sup>+</sup>, lin<sup>neg</sup>, MHC II<sup>+</sup> cells were further separated by the markers CD11b and CD11c and according to this subdivided into group 1 (cDC1; MHC II<sup>+</sup>, CD11b<sup>neg</sup>, CD11c<sup>+</sup>), group 2 (Mo/MΦ/DC; MHC II<sup>+</sup>/CD11b<sup>+</sup>/CD11c<sup>+</sup>) and group 3 (Mo/MΦ; MHC II<sup>+</sup>/CD11b<sup>+</sup>/CD11c<sup>neg</sup>).

In Figure 8a, the development of these groups is shown in a representative FACS density plot in week 3 after infection vs. in steady state. Furthermore, the distribution and development of the three myeloid cell groups in ear samples of C57BL/6 and BALB/c mice is shown in percentages and cell numbers per ear over time after infection with *L. major* (Figure 8b) as well as in mean percentages per time point and strain (Figure 8c).

cDC1 (CD11b<sup>neg</sup>, CD11c<sup>+</sup>) (group 1) showed the lowest percentages and cell numbers among the three cell subsets. No increase in percentages was obtained over time. In cell numbers, a small increase was seen due to the overall increasing cell numbers with weeks post-infection with *L. major*.

Percentages of Mo/MΦ/DC (CD11b<sup>+</sup>, CD11c<sup>+</sup>) (group 2) were low in naïve mice (mean of 3% and 4% in C57BL/6 and BALB/c mice, respectively), and had only increased towards a mean of 8% in both mice in week 3. Highest percentages in this group were obtained in BALB/c mice in week 9 and in C57BL/6 mice in week 12 with 12% and 15%, respectively. Total cell numbers increased over time after infection with statistically significant difference between mice found only in week 6 ( $p = 0.0207$ ).

Mo/MΦ (CD11b<sup>+</sup>, CD11c<sup>neg</sup>) (group 3) made up the highest percentages at all time points. In week 1.5, a peak in percentages of these cells was obtained. Afterwards, in week 3, percentages dropped to lower percentages. Percentages remained at relatively stable levels in weeks 6, 9 and 12; similar to those obtained in naïve mice. Total cell numbers, however, increased, thus the total number of these cells increased over time after infection with *L. major*.

Surprisingly, cellular distribution and timing of appearance of the three cell groups were quiet similar in both mice, except for week 3, where statistically significant higher percentages of Mo/MΦ (group 3) were found in BALB/c mice than in C57BL/6 mice, ( $p < 0.001$ ).

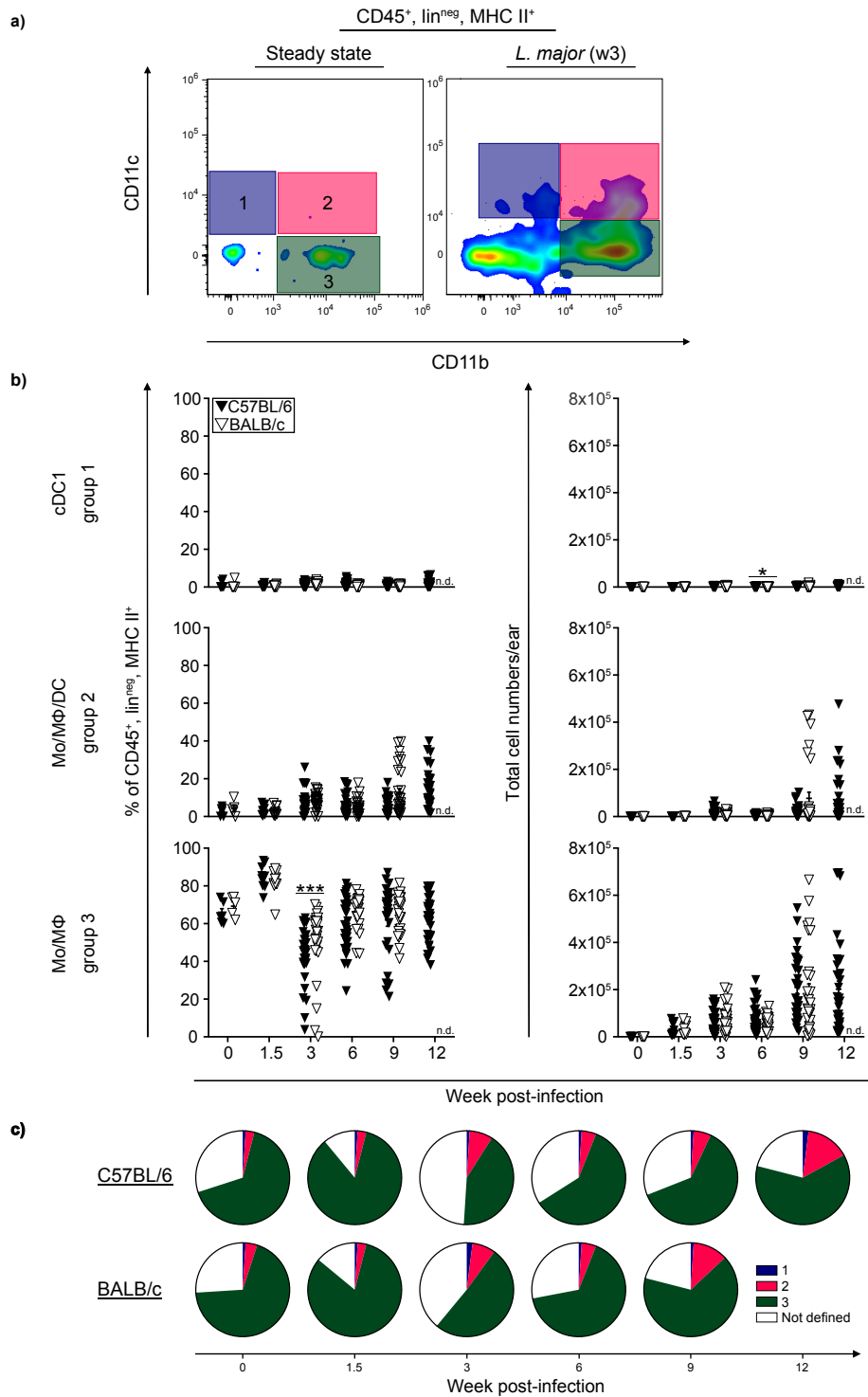


**Figure 8 Analysis of myeloid ear tissue cells in naïve mice and after infection with *L. major* based on CD11b and CD11c expression**

Ear tissue of C57BL/6 ( $\blacktriangledown$ ) and BALB/c ( $\blacktriangledown$ ) mice was harvested at different time points after infection with *L. major*, with  $n \geq 4$ , ( $\geq 8$  ears) from three independent experiments per time point and strain. Single cell suspensions were generated from each ear by enzymatic and mechanical digestion. At weeks 0 (naïve mice) and 1.5, 2-4 ear samples were pooled to enrich cells to generate more valuable results. Cells were stained with surface staining and antigen expression of cells was assessed using flow cytometry. Myeloid cells were identified by expression of the surface marker  $CD45^+$  and absence of the lineage markers  $CD19$ ,  $CD90.2$ ,  $CD49b/DX-5$ ,  $NK1.1$  and  $Ly6G$ , ( $lin^{neg}$ ). Among  $MHC II^+$  cells, three myeloid cell groups (1-3) were identified based on the expression of the markers  $CD11b$  and  $CD11c$ . a) Representative FACS density plots for the gating strategy used to subdivide three myeloid cell groups (1, 2 and 3) among  $MHC II^+$  cells, based on their expression of  $CD11b$  and  $CD11c$  in ear tissue of naïve mice (steady-state) and 3 weeks after infection with *L. major* (w3) in BALB/c mice. b) Development of percentages and total cell numbers per ear of myeloid cell groups 1-3 over time after infection with *L. major* in C57BL/6 and BALB/c mice. c) Mean percentages of group 1, 2 and 3 of all  $CD45^+ lin^{neg}, MHC II^+$  cells per time point and strain. Significance of differences between values in C57BL/6 and BALB/c mice was determined using Mann-Whitney test, with  $\alpha = 0.05$ ; \* =  $p < 0.05$ ; \*\* =  $p < 0.01$ ; \*\*\* =  $p < 0.001$ .

#### 4.5.1. Identification of different cell subsets based on Ly6C and CD64 marker expression among myeloid ear tissue cells

In Figure 9a, representative FACS density plots for the described subsets I-V identified among Mo/MΦ/DC (group 2) isolated from infected ear tissue of C57BL/6 mice are shown in week 12 after infection vs. in steady state. Also shown is the development of these subsets in ear tissue of C57BL/6 and BALB/c mice in percentages and total cell numbers per ear over time after infection with *L. major* (Figure 9b), as well as mean percentages per time point and strain (Figure 9c). Since in weeks 0 and 1.5 very low cell numbers were found in all cell subsets of group 2, which did not lead to valid values, these time points were excluded from the analysis, (n.a. = not analyzed). Among group 2, cDC2 (subset I) were dominant in week 3 in both mice. Percentages were higher in C57BL/6 mice than in BALB/c mice and the difference between both mice was statistically significant ( $p = 0.0140$ ). In week 3, percentages of cDC2 were followed by those obtained in mo-DC (subset II). In week 6, when compared to week 3, cDC2 and mo-DC (subset I and II) had decreased in both mice, but especially in BALB/c mice, reappeared from week 6 onwards. In week 6, an influx of mo-MΦ/MΦ and MΦ (subset IV and V) was seen, with highest percentages obtained in MΦ (subset V) (40% and 34% in C57BL/6 and BALB/c mice, respectively). Mo-MΦ (subset III) started to appear in week 9 and further increased towards week 12 in C57BL/6 mice.

Overall, the onset of cell subset appearance and distribution was very similar in both mice. Only in week 9, stronger differences between C57BL/6 and BALB/c mice were observed. Here, percentages of CD64<sup>+/hi</sup> mo-MΦ/MΦ and MΦ (subsets IV and V) were higher in C57BL/6 mice than in BALB/c mice. Differences between both mouse strains were statistically significant in Mo-MΦ/MΦ (IV) and MΦ (V), with percentages in C57BL/6 mice being higher than those obtained in BALB/c mice ( $p < 0.001$ , respectively). In contrast, percentages of CD64<sup>neg to +</sup> subsets cDC2 and mo-DC (subsets I and II) were higher in BALB/c mice than in C57BL/6 mice. In mo-DC, a statistically significant difference between both mice was found at this time point ( $p = 0.0165$ ).

In general, in both strains, percentages of CD64<sup>neg to +</sup> (subsets I and II together) were higher in week 3, whereas in week 6, percentages of CD64<sup>+/hi</sup> mo-MΦ, mo-MΦ/MΦ and MΦ (subsets III, IV and V together) were higher. Differences appeared in week 9, where the ratio between mo-MΦ, mo-MΦ/MΦ and MΦ (subsets III, IV and V) vs. cDC2 and mo-DC (subsets I and II) shifted towards mo-MΦ, mo-MΦ/MΦ and MΦ (III, IV and V) in C57BL/6 mice, but towards cDC2 and mo-DC (I and II) in BALB/c mice.

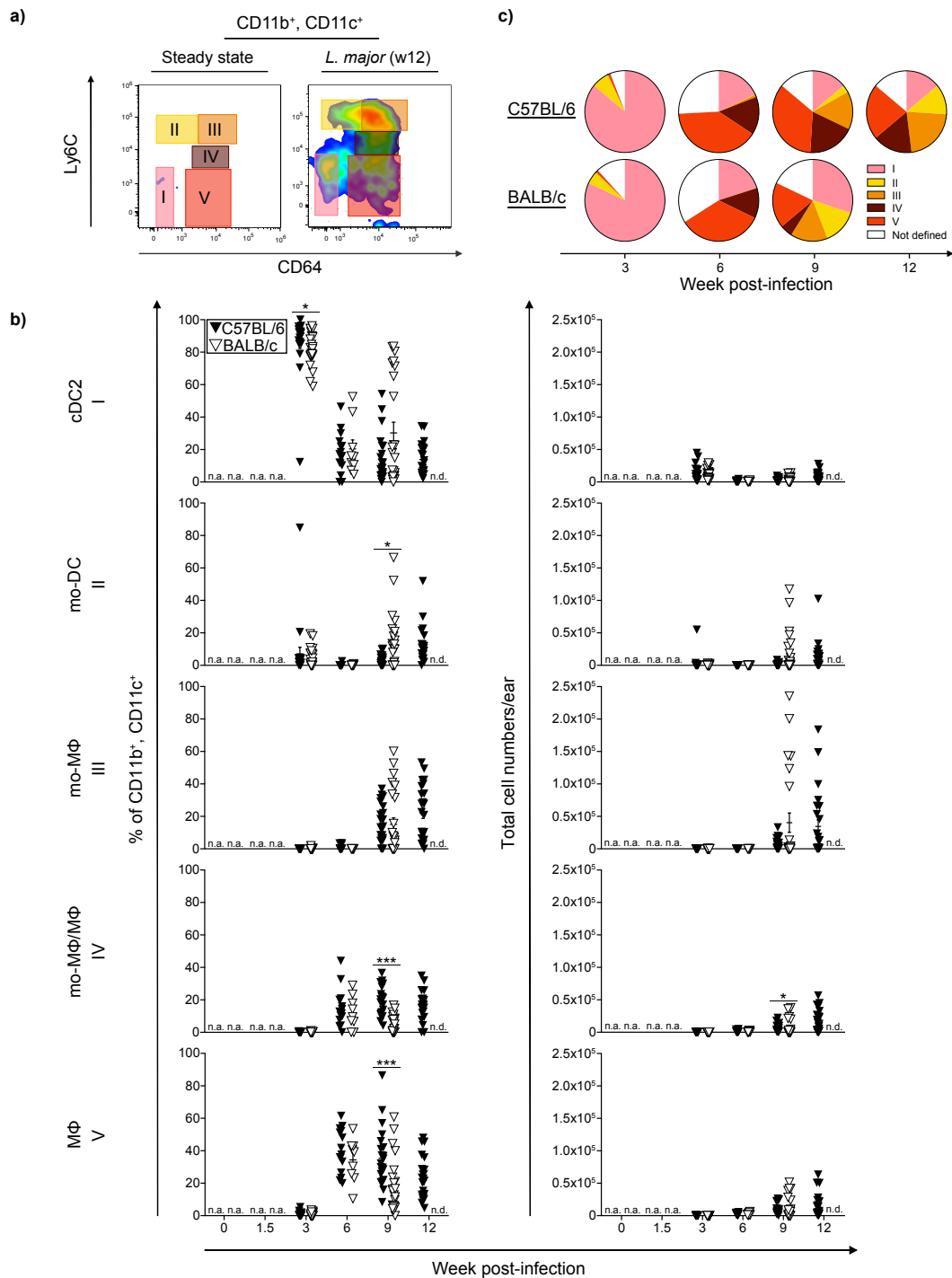


**Figure 9 Analysis of Ly6C and CD64 expression among myeloid cell group 2 in ear tissue of naïve mice and after infection with *L. major***

Ear tissue of C57BL/6 (▼) and BALB/c (▽) mice was harvested at different time points after infection with *L. major*, with  $n \geq 4$ , ( $\geq 8$  ears) from three independent experiments per time point and strain. Single cell suspensions were generated from each ear by enzymatic and mechanical digestion. At w0 (naïve mice) and w1.5, ear samples of two mice were pooled to enrich cells in to generate more valuable results. Cells were stained with surface staining and antigen expression of cells was assessed using flow cytometry. Myeloid cells were identified by expression of the surface marker CD45 and absence of the lineage markers CD19, CD90.2, CD49b/DX-5, NK1.1 and Ly6G, (lin<sup>neg</sup>). Based on the expression of the markers CD11b and CD11c, three myeloid cell groups (1-3) were identified among MHC II<sup>+</sup> cells. By analyzing the expression of the surface markers Ly6C and CD64, groups 2 and 3 were further subdivided into different myeloid cell subsets. **a)** Representative FACS density plots for the gating strategy used to subdivide group 2 into five myeloid cell subsets (I-V) in ear tissue of naïve mice (steady state) and 12 weeks after infection with *L. major* (w12) in C57BL/6 mice. **b)** Development of percentages and total cell numbers of subsets I-V in C57BL/6 and BALB/c mice over time after infection with *L. major*. At week 0 and 1.5 very low cell numbers were obtained and therefore, these time points were excluded (n.a. = not analyzed). **c)** Mean percentages of subsets I-V of all CD45<sup>+</sup> lin<sup>neg</sup>, MHC II<sup>+</sup>, CD11b<sup>+</sup>, CD11c<sup>+</sup> cells per time point and strain. Significance of differences between values in C57BL/6 and BALB/c mice was determined using Mann-Whitney test, with  $\alpha = 0.05$ ; \* =  $p < 0.05$ ; \*\* =  $p < 0.01$ ; \*\*\* =  $p < 0.001$ .

Figure 10a shows representative FACS density plots for the described subsets VI-VIII identified among Mo/MΦ (group 3) in infected ear tissue of C57BL/6 mice in week 12 after infection vs. in steady state. In Figure 10b, development of percentages and total cell numbers per ear of these subsets (VI-VIII) is shown. Mean percentages per time point and strain are shown in Figure 10c.

Among all three subsets, TR-MΦ (subset VI) made up the highest percentages in naïve mice. In naïve C57BL/6 mice, significant higher percentages were found already than in naïve BALB/c mice ( $p = 0.0043$ ). CD11c<sup>neg</sup> mo-MΦ (subset VII) then were dominant in week 1.5 in both mice, but these cells were possibly short-lived, as they disappeared in week 3. Here, again TR-MΦ (subset VI) showed the highest percentages. From week 3 onwards, CD11c<sup>neg</sup> mo-MΦ (subset VII) repopulated the tissue, accompanied by CD11c<sup>neg</sup> MΦ (subset VIII). In BALB/c mice, in week 3 statistically significant higher percentages of CD11c<sup>neg</sup> MΦ (subset VIII) were obtained than in C57BL/6 mice ( $p < 0.0001$ ). However, in BALB/c mice, a decrease in percentages of CD11c<sup>neg</sup> mo-MΦ (subset VII) was obtained in week 9, whereas TR-MΦ (subset VI) now had increased in percentages and made up the majority of all three cell subsets. This was not observed in C57BL/6 mice, which led to a difference in mean percentages of CD11c<sup>neg</sup> mo-MΦ (subset VII) and TR-MΦ (subset VI) between both mice, with TR-MΦ (subset VI) being higher in BALB/c mice and CD11c<sup>neg</sup> mo-MΦ (subset VII) being higher in C57BL/6 mice. Differences between percentages of these subsets in C57BL/6 and BALB/c mice at this time point were statistically significant ( $p < 0.0001$ , respectively). Interestingly, this resembled the behavior obtained in Mo/MΦ/DC (group 3), where higher percentages of CD64<sup>+/hi</sup> subsets were found in C57BL/6 mice in week 9, whereas in BALB/c mice, CD64<sup>neg to +</sup> subsets were more present at this time point. However, differences in the distribution between cell numbers of subset VII in week 9 after infection were not statistically significant (using Kolmogorov-Smirnov-Test).

Also, in BALB/c mice, mean percentages of TR-MΦ, CD11c<sup>neg</sup> mo-MΦ and CD11c<sup>neg</sup> MΦ (subset VI, VII and VIII) were rather similar in week 9, whereas in C57BL/6 mice, CD11c<sup>neg</sup> mo-MΦ (subset VII) made up much higher percentages than those found in TR-MΦ and CD11c<sup>neg</sup> MΦ (subset VI and VIII).

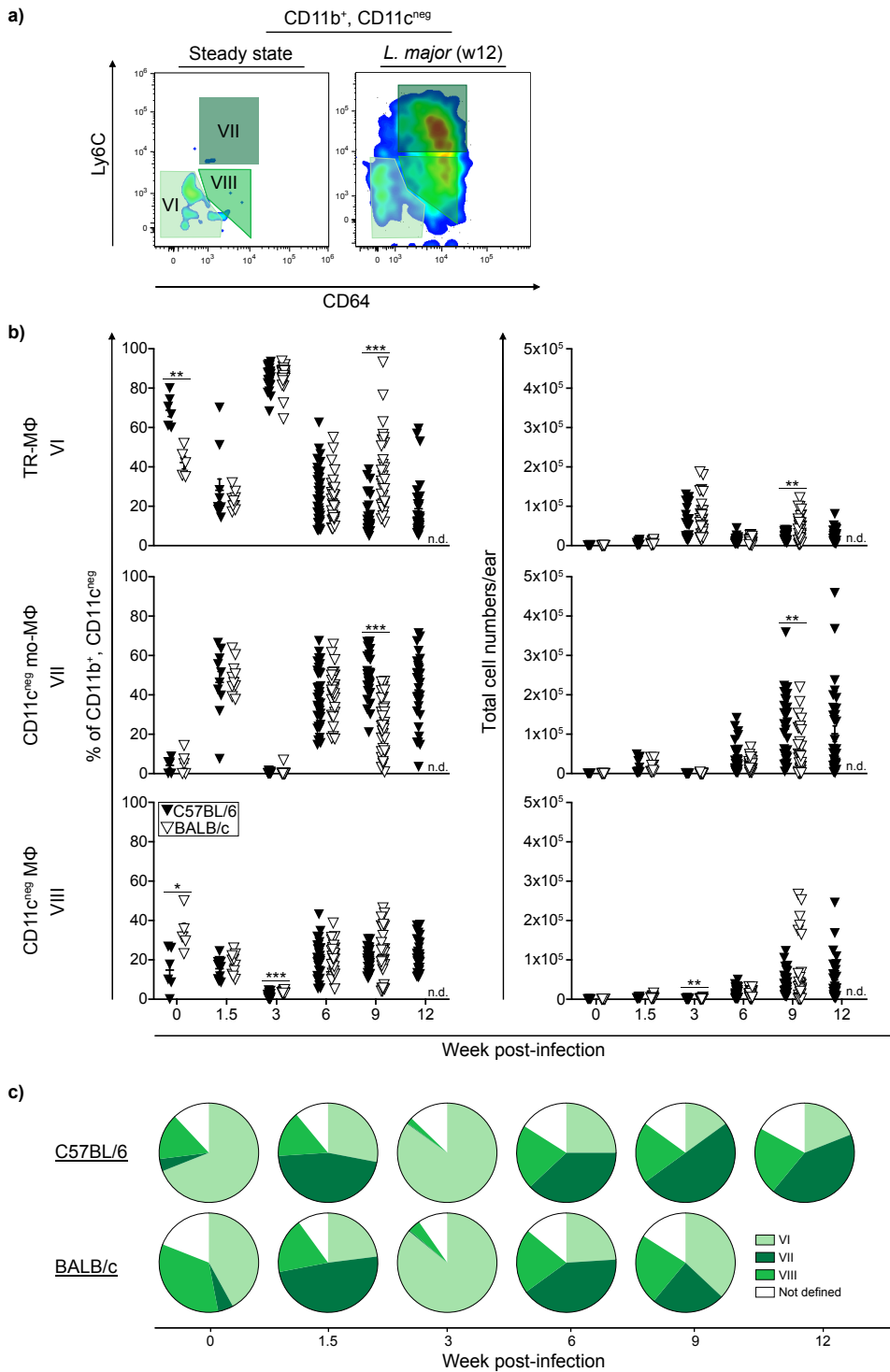


**Figure 10 Analysis of Ly6C and CD64 expression among myeloid cell group 3 in ear tissue of naïve mice and after infection with *L. major***

Ear tissue of C57BL/6 (▼) and BALB/c (▽) mice was harvested at different time points after infection with *L. major*, with  $n \geq 4$ , ( $\geq 8$  ears) from three independent experiments per time point and strain. Single cell suspensions were generated from each ear by enzymatic and mechanical digestion. At week 0 (naïve mice) and 1.5, ear samples of two mice were pooled to enrich cells to generate more valuable results. Cells were stained with surface staining and antigen expression of cells was assessed using flow cytometry. Myeloid cells were identified by expression of the surface marker CD45 and absence of the lineage markers CD19, CD90.2, CD49b/DX-5, NK1.1 and Ly6G, ( $lin^{neg}$ ). Based on the expression of the markers CD11b and CD11c, three myeloid cell groups (1-3) were identified among MHC II<sup>+</sup> cells. By analyzing the expression of the surface markers Ly6C and CD64, group 2 and 3 were further subdivided into different myeloid cell subsets. **a)** Representative FACS density plots for the gating strategy used to subdivide group 3 into three myeloid cell subsets (VI-VIII) in ear tissue of naïve mice (steady-state) and 12 weeks after infection with *L. major* (w12) in C57BL/6 mice. **b)** Development of percentages and total cell numbers per ear of subsets VI-VIII in C57BL/6 and BALB/c mice over time after infection with *L. major*. **c)** Mean percentages of subsets VI-VIII of all CD45<sup>+</sup>  $lin^{neg}$ , MHC II<sup>+</sup>, CD11b<sup>+</sup>, CD11c<sup>neg</sup> cells per time point and strain. Significance of differences between values in C57BL/6 and BALB/c mice was determined using Mann-Whitney test, with  $\alpha = 0.05$ ; \* =  $p < 0.05$ ; \*\* =  $p < 0.01$ ; \*\*\* =  $p < 0.001$ .

#### 4.5.2. Expression of iNOS and arginase-1 in myeloid ear tissue cells

To analyze functionality of myeloid ear tissue cells, the antibody panel used for flow cytometry staining also included anti-iNOS and anti-arginase-1 antibodies for intracellular staining. First, all MHC II<sup>+</sup> myeloid cells, composed of group 1, 2 and 3, were analyzed for their expression of iNOS and arginase-1. Figure 11 shows representative FACS histograms for the expression of iNOS in C57BL/6 (Figure 11a) and arginase-1 in BALB/c mice (Figure 11b) in steady-state vs. week 3 and week 9 after infection, respectively. In Figure 11c, percentages of MHC II<sup>+</sup> myeloid cells positive for iNOS or arginase-1 are shown over time after infection with *L. major*.

Percentages of iNOS expressing myeloid cells had increased in week 1.5 after infection in C57BL/6 and BALB/c mice. Mean percentages remained relatively stable until week 6. From week 6 onwards, percentages of iNOS expressing myeloid cells strongly increased, especially in C57BL/6 mice, with statistically significant higher values found in C57BL/6 mice than in BALB/c mice in weeks 6 and 9 ( $p = 0.0099$  and  $p = 0.0001$ , respectively). Percentages in C57BL/6 mice further increased towards week 12. However, in total cell numbers, in week 9 significant higher numbers of iNOS expressing myeloid cells were found in BALB/c mice than in C57BL/6 mice ( $p = 0.0274$ ).

Percentages of arginase-1 expressing myeloid cells remained very low until week 3, but had increased in week 6 in both mice. In BALB/c mice, percentages further increased towards week 9. In contrast, in C57BL/6 mice, percentages had decreased in weeks 9 and 12 compared to week 6. Percentages of arginase-1 expressing myeloid cells were statistically significant higher in BALB/c than in C57BL/6 mice in weeks 6 and 9 ( $p = 0.0284$  and  $p < 0.0001$ , respectively).

Interestingly, at later time points, such as week 6 and week 9, in C57BL/6 mice, a higher percentage of myeloid cells expressed iNOS than in BALB/c mice. In contrast, the percentage of myeloid cells expressing arginase-1 was higher in BALB/c mice than in C57BL/6 mice. Also, the development of percentages of arginase-1 expressing myeloid cells differed between the mice, with decreasing percentages in C57BL/6 mice from week 6 to week 9, but increasing percentages in BALB/c mice.

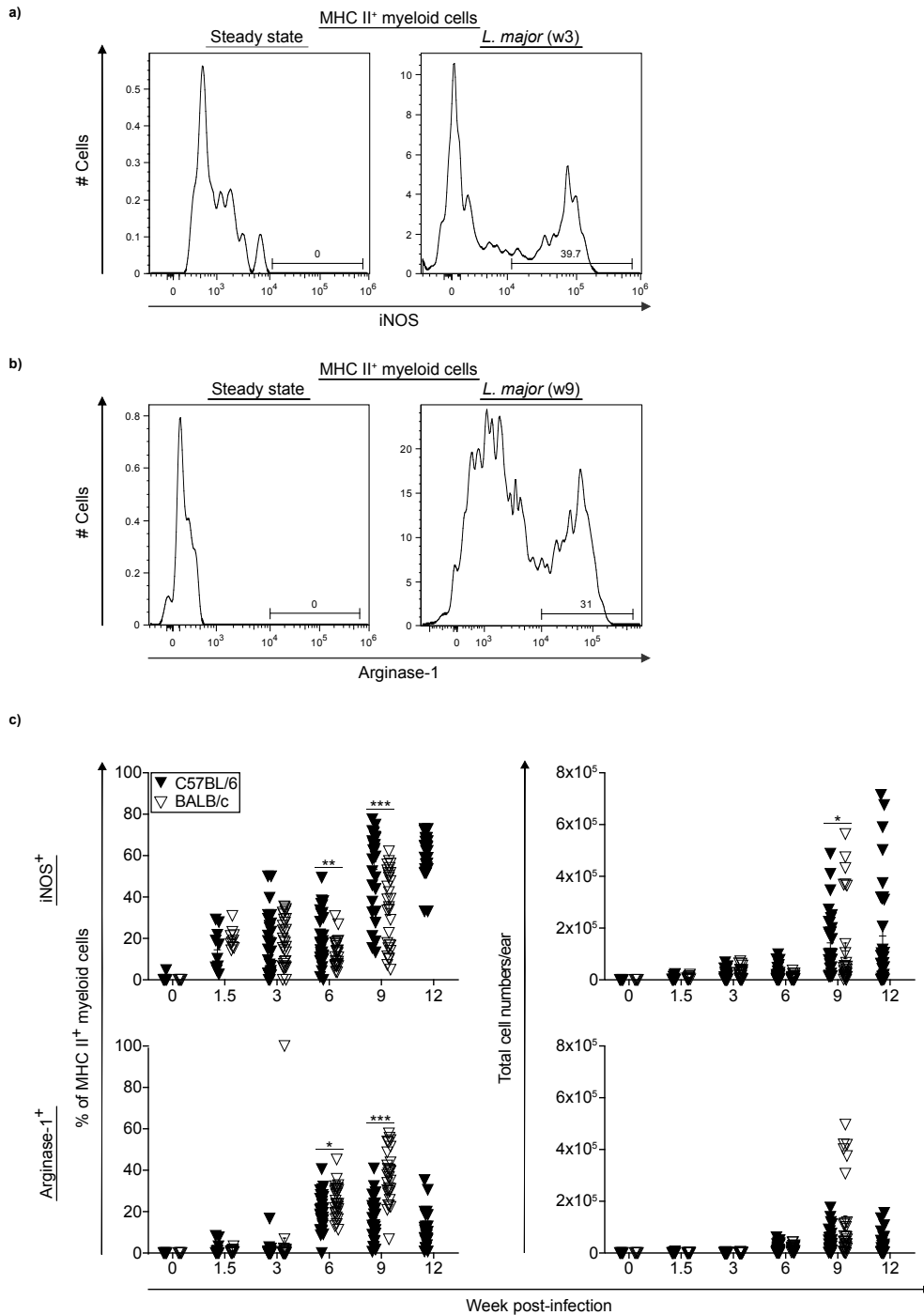


**Figure 11** iNOS and/or arginase-1 expression in MHC II<sup>+</sup> myeloid cells (1, 2 and 3) in ear tissue of naïve mice and after infection with *L. major*

Ear tissue of C57BL/6 (▼) and BALB/c (▽) mice was harvested at different time points after infection with *L. major*, with  $n \geq 4$ , ( $\geq 8$  ears) from three independent experiments per time point and strain. Single cell suspensions were generated from each ear by enzymatic and mechanical digestion. At weeks 0 (naïve mice) and 1.5, ear samples of two mice were pooled to enrich cells to generate more valuable results. Cells were stained with surface and intracellular staining and antigen expression of cells was assessed using flow cytometry. Myeloid cells were identified by expression of the surface marker CD45<sup>+</sup> and absence of the lineage markers CD19, CD90.2, CD49b/DX-5, NK1.1 and Ly6G, (lin<sup>neg</sup>) and MHC II<sup>+</sup> cells were further subdivided into three myeloid cell groups (1, 2 and 3) based on their expression of the markers CD11b and CD11c. Intracellular staining was used to identify intracellular expression of the enzymes iNOS and/or arginase-1 in myeloid ear tissue cells. **a)** Representative FACS histograms for iNOS expression in steady state vs. week 3 after infection with *L. major* (w3) in C57BL/6 mice. **b)** Representative FACS histograms for arginase-1 expression in steady state vs. week 9 after infection with *L. major* (w9) in BALB/c mice. **c)** Percentages and total cell numbers per ear  $\pm$  SEM of iNOS positive and arginase-1 positive myeloid cells (group 1, 2 and 3) in C57BL/6 and BALB/c mice at different time points after infection with *L. major*. Significance of differences between values in C57BL/6 and BALB/c mice was determined using Mann-Whitney test, with  $\alpha = 0.05$ ; \* =  $p < 0.05$ ; \*\* =  $p < 0.01$ ; \*\*\* =  $p < 0.001$ .

#### 4.5.3. Expression of iNOS and arginase-1 in different myeloid cell subsets in ear tissue

In addition to overall expression of iNOS and arginase-1 in myeloid ear tissue cells after infection with *L. major*, the proportion of cells expressing both, iNOS and arginase-1 or only one marker was analyzed. Furthermore, the cell subsets in Mo/MΦ/DC (group 2) and Mo/MΦ (group 3) were analyzed for their expression of iNOS and arginase-1. Figure 12 shows representative FACS density plots for the expression of iNOS and arginase-1 among CD11c<sup>neg</sup> mo-MΦ (subset VII) in C57BL/6 and BALB/c mice at weeks 6 and 9 after infection with *L. major*, (Figure 12a), as well as the percentages of myeloid ear tissue cells, which express iNOS or arginase-1 or both, iNOS and arginase-1 (Figure 12b).

Percentages of myeloid cells, expressing both, iNOS and arginase-1 differed between both mice in week 3, ( $p = 0.0394$ ), with higher values found in C57BL/6 than in BALB/c mice. From week 3 onwards, percentages of these cells increased until week 9 with similar values obtained in both genotypes. Percentages of myeloid cells expressing only iNOS were similar in both genotypes until week 6, where percentages had slightly decreased in both mice and afterwards started to increase again towards weeks 9 and 12. In weeks 6 and 9, percentages of only iNOS expressing myeloid cells were statistically significant higher in C57BL/6 mice than in BALB/c mice ( $p = 0.0004$  and  $p < 0.0001$ , respectively). Percentages in C57BL/6 mice further increased towards 49% in week 12. Percentages of myeloid cells expressing only arginase-1 increased in both genotypes until week 6. From week 6 to week 9, percentages did not further increase in BALB/c mice, but decreased in C57BL/6 mice from week 6 towards week 12 to a mean percentage of 2%. Percentages of only arginase-1 expressing myeloid cells were statistically significant higher in BALB/c mice than in C57BL/6 mice in weeks 3, 6 and 9, ( $p = 0.0073$ ,  $p < 0.0001$  and  $p < 0.0001$ , respectively).

Furthermore, the cell subsets in Mo/MΦ/DC (group 2) and Mo/MΦ (group 3) were analyzed for their expression of iNOS and arginase-1 (Figure 13). In week 6, mo-DC and mo-MΦ (subsets II and III) were excluded from the analysis, because cell numbers were too low.

In week 6 and 9, in all subsets (I-VIII), higher percentages of iNOS single positive cells were found in C57BL/6 mice in comparison to those found in BALB/c mice. In week 6, in CD11c<sup>neg</sup> mo-MΦ (subset VII) and CD11c<sup>neg</sup> MΦ (subset VIII) difference between mice was statistically significant ( $p < 0.0001$  and  $p = 0.0013$ , respectively). In week 9, except for cDC2 (subset I), difference between mice was statistically significant in all subsets.

Percentages of only arginase-1 expressing cells were higher in BALB/c mice than in C57BL/6 mice in week 6 in mo-MΦ/MΦ, MΦ, CD11c<sup>neg</sup> mo-MΦ (subsets IV, V, VII) ( $p < 0.0001$ ) and CD11c<sup>neg</sup> MΦ (subset VIII), ( $p = 0.0028$ ). However, in cDC2 and TR-MΦ (subsets I and VI),

percentages of arginase-1 single positive cells were higher in C57BL/6 than in BALB/c mice, with difference being statistically significant in TR-M $\Phi$  (subset VI), ( $p = 0.0361$ ). In week 9, in all subsets, statistically significant higher percentages of arginase-1 expressing cells were found in BALB/c mice than in C57BL/6 mice.

In week 6, in all subsets, except for TR-Mac (subset VI), percentages of cells expressing both, iNOS and arginase-1 were higher in C57BL/6 mice than in BALB/c mice. However, this shifted in week 9, where percentages were higher in BALB/c mice than in C57BL/6 mice in cDC2, mo-DC, M $\Phi$ , TR-M $\Phi$ , CD11c<sup>neg</sup> mo-M $\Phi$  and CD11c<sup>neg</sup> M $\Phi$  (subsets I, II, V, VI, VII and VIII). Difference between mice was statistically significant in CD11c<sup>neg</sup> mo-M $\Phi$  and CD11c<sup>neg</sup> M $\Phi$  (subsets VII and VIII) in week 6, ( $p = 0.0040$  and  $p=0.0240$ , respectively) and in cDC2, mo-DC, M $\Phi$  and TR-M $\Phi$  (subsets I, II, V, and VI) in week 9 ( $p < 0.0001$ ,  $p = 0.0191$ ,  $p= 0.0041$  and  $p < 0.0001$ , respectively).

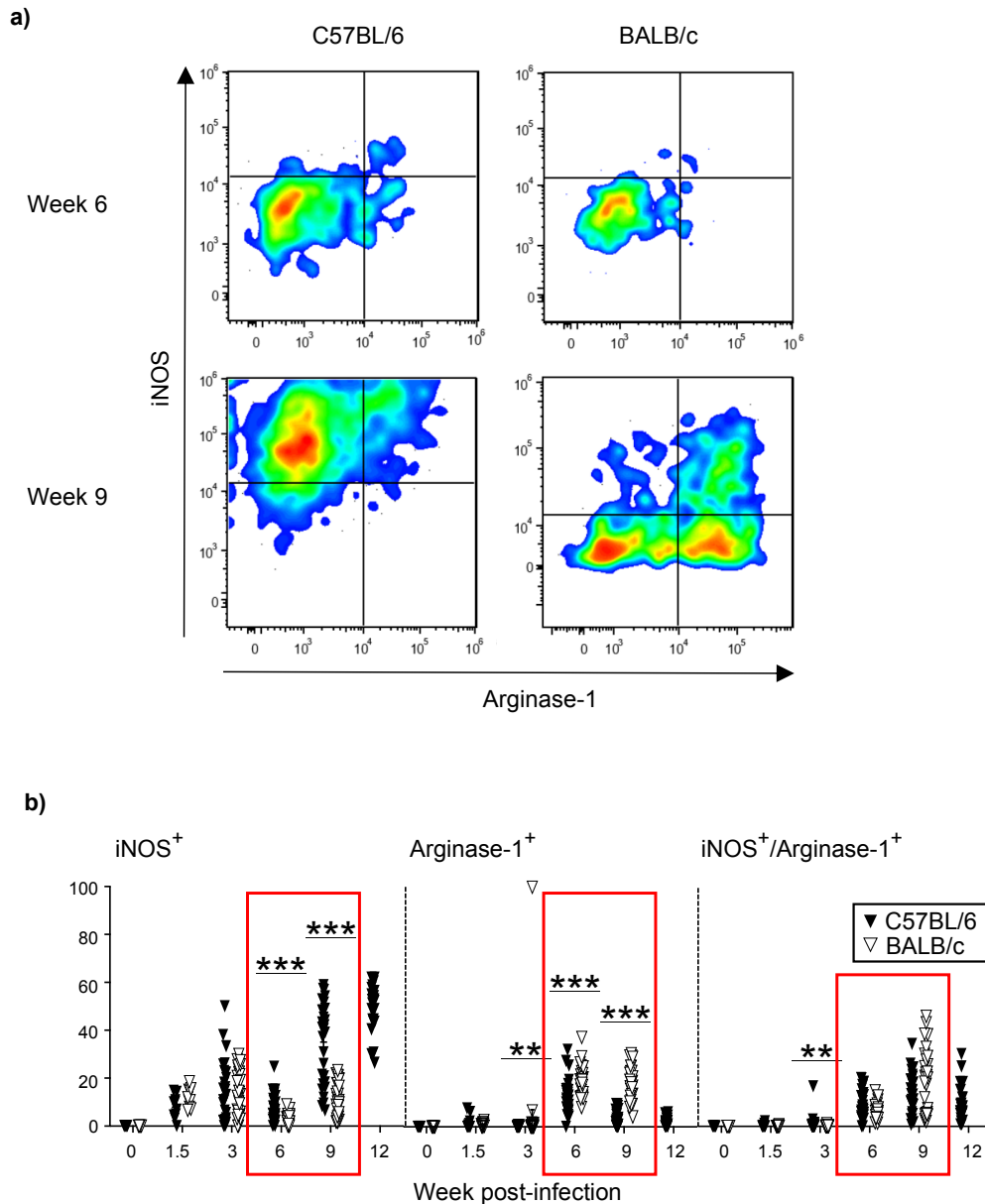
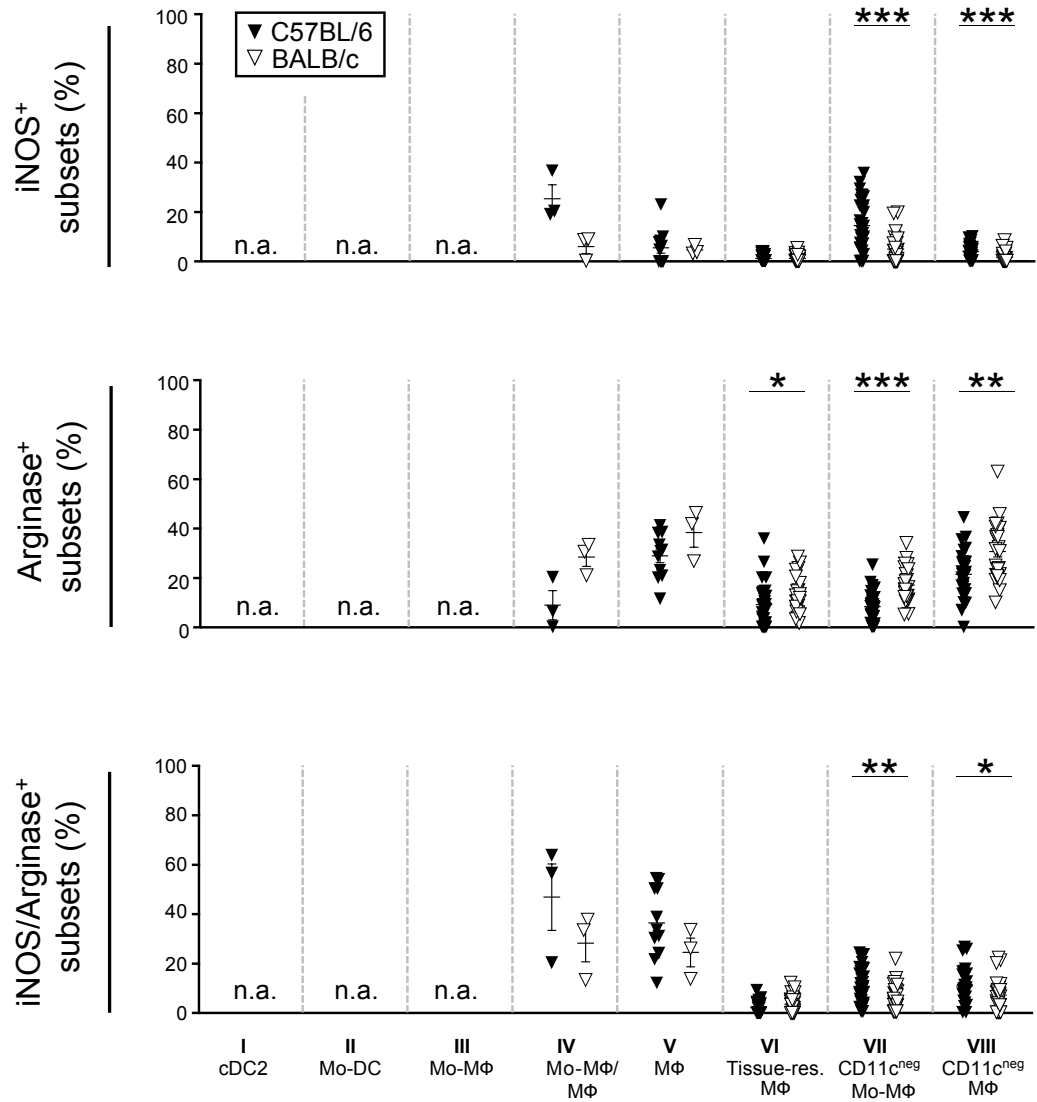


**Figure 12** iNOS and arginase-1 expression in MHC II<sup>+</sup> myeloid cells in ear tissue of naïve mice and after infection with *L. major*, specifically distributed into cells positive for iNOS and/or Arginase-1 expression

Ear tissue of C57BL/6 (▼) and BALB/c (▽) mice was harvested at different time points after infection with *L. major*, with  $n \geq 4$ , ( $\geq 8$  ears) from three independent experiments per time point and strain. Single cell suspensions were generated from each ear by enzymatic and mechanical digestion. At weeks 0 (naïve mice) and 1.5, ear samples of two mice were pooled to enrich in cells in order to generate more valuable results. Cells were stained with surface and intracellular staining and antigen expression of cells was assessed using flow cytometry. Myeloid cells were identified by expression of the surface marker CD45<sup>+</sup> and absence of the lineage markers CD19, CD90.2, CD49b/DX-5, NK1.1 and Ly6G, (*lin*<sup>neg</sup>) and MHC II<sup>+</sup> cells were further subdivided into three myeloid cell groups (1, 2 and 3) based on their expression of the markers CD11b and CD11c. Intracellular staining was used to identify intracellular expression of the enzymes iNOS and arginase-1 in myeloid cells. **a)** Representative FACS density plots for iNOS and arginase-1 expression among MHC II<sup>+</sup> myeloid cell subset VII at week 6 and 9 after infection with *L. major* in C57BL/6 and BALB/c mice. **b)** Percentages  $\pm$  SEM of MHC II<sup>+</sup> myeloid ear tissue cells (group 1, 2 and 3), expressing only iNOS, only Arginase-1, or both, iNOS and arginase-1 in C57BL/6 and BALB/c mice at different time points after infection with *L. major*. Significance of differences between values in C57BL/6 and BALB/c mice was determined using Mann-Whitney test, with  $\alpha = 0.05$ ; \* =  $p < 0.05$ ; \*\* =  $p < 0.01$ ; \*\*\* =  $p < 0.001$ .

## Week 6



## Week 9

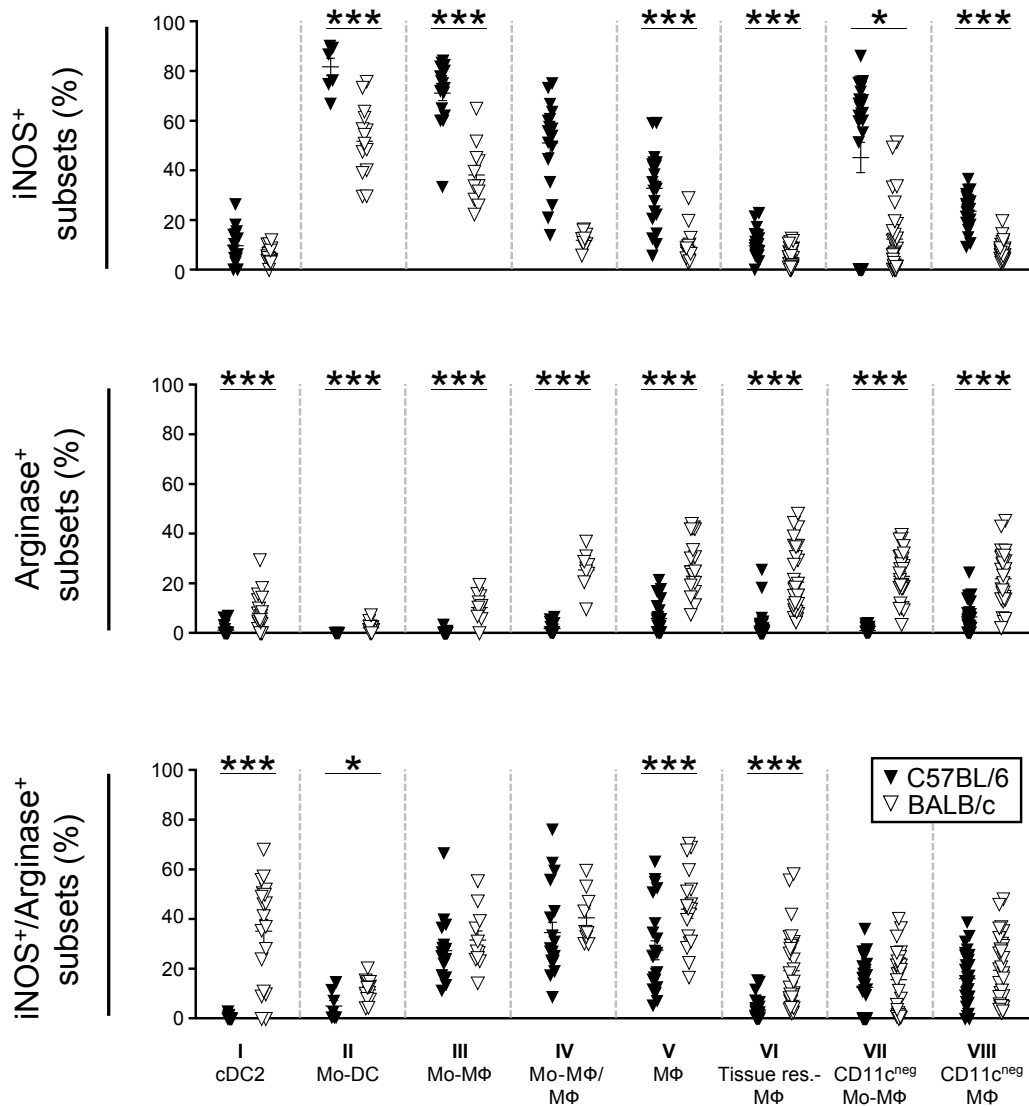


**Figure 13** iNOS and arginase-1 expression in MHC II<sup>+</sup> myeloid cells subsets (I-VIII) in ear tissue of C57BL/6 and BALB/c mice at week 6 and 9 after infection with *L. major*, specifically distributed into cells expressing either iNOS or arginase-1 or both, iNOS and arginase-1

Ear tissue of C57BL/6 (▼) and BALB/c (▽) mice was harvested at different time points after infection with *L. major*, with  $n \geq 4$ , ( $\geq 8$  ears) from three independent experiments per time point and strain. Single cell suspensions were generated from each ear by enzymatic and mechanical digestion. At weeks 0 (naïve mice) and 1.5, ear samples of two mice were pooled to enrich in cells in order to generate more valuable results. Cells were stained with surface and intracellular staining and antigen expression of cells was assessed using flow cytometry. Myeloid cells were identified by expression of the surface marker CD45<sup>+</sup> and absence of the lineage markers CD19, CD90.2, CD49b/DX-5, NK1.1 and Ly6G, (lin<sup>neg</sup>) and MHC II<sup>+</sup> cells were further subdivided into three myeloid cell groups (1, 2 and 3) based on their expression of the markers CD11b and CD11c. By analyzing the expression of the surface markers Ly6C and CD64, group 2 and 3 were further subdivided into different myeloid cell subsets (I-VIII). Intracellular staining was used to identify intracellular expression of the enzymes iNOS and arginase-1 in myeloid cells. **a)** Percentages  $\pm$  SEM of MHC II<sup>+</sup> myeloid ear tissue cell subsets I-VIII in week 6, expressing only iNOS or only arginase-1 or both markers in C57BL/6 and BALB/c mice in week 6 and 9 after infection with *L. major*. Subsets I, II and III were excluded from the analysis in week 6 (not analyzed = n.a.), because cell numbers were too low. Significance of differences between values in C57BL/6 and BALB/c mice was determined using Mann-Whitney test, with  $\alpha = 0.05$ ; \* =  $p < 0.05$ ; \*\* =  $p < 0.01$ ; \*\*\* =  $p < 0.001$ .

#### 4.5.4. Ly6C and CD11b expression among MHC II<sup>neg</sup> ear cells in C57BL/6 and BALB/c mice after infection with *L. major*

Figure 14a shows representative FACS density plots for subsets IX-XII in C57BL/6 mice in steady state vs. week 12 after infection with *L. major*. Development in percentages and total cell numbers per ear of these subsets over time after infection with *L. major*, as well as mean percentages per time point and strain are shown in Figure 14b and 14c, respectively. MHC II<sup>neg</sup> cells presented a range of different Ly6C expression levels throughout the different time points after infection. The percentages of Ly6C<sup>hi</sup>, CD11b<sup>+</sup> monocytes (Ly6C<sup>hi</sup>, CD11b<sup>+</sup> mo; subset IX), which expressed the highest levels of Ly6C of all four subsets, already differed between naïve C57BL/6 and BALB/c mice, ( $p = 0.0043$ ). Percentages then increased shortly after infection, with a peak in week 1.5 after infection. This influx of cells of Ly6C<sup>hi</sup>, CD11b<sup>+</sup> mo (subset IX) was stronger in C57BL/6 than in BALB/c mice ( $p = 0.0015$ ). Also in week 3, a statistically significant difference was found between C57BL/6 and BALB/c mice ( $p < 0.0001$ ). Ly6C<sup>hi</sup>, CD11b<sup>+</sup> mo (subset IX) had already decreased in week 3 after infection, to increase again in week 6. Here, in total cell numbers, a statistically significant difference was found between mice, with higher numbers in BALB/c than in C57BL/6 mice ( $p = 0.0233$ ), however no statistically significant difference was found in the distribution. Also, in Ly6C<sup>lo/neg</sup>, CD11b<sup>lo/+</sup> mo (subset XII), which was defined by low expression/absence of Ly6C and low to positive expression of CD11b, a fluctuation of percentages was found over time after infection with *L. major*. Overall, in Ly6C<sup>int</sup>, CD11b<sup>+</sup> mo (subset X) and Ly6C<sup>lo/neg</sup>, CD11b<sup>lo/+</sup> mo (subset XII), higher percentages were found in C57BL/6 than in BALB/c mice at all time points, except for week 9 after infection, where percentages were higher in BALB/c mice than in C57BL/6 mice. The difference in percentages between mice was statistically significant in subset X in weeks 1.5, 3 and 6 after infection ( $p = 0.0232$ ,  $p = 0.0411$  and  $p = 0.0092$ , respectively) and in Ly6C<sup>lo/neg</sup>, CD11b<sup>lo/+</sup> mo (subset XII) in week 6 after infection, ( $p = 0.0004$ ). Percentages of Ly6C<sup>hi</sup>, CD11b<sup>+</sup> mo (subsets IX), Ly6C<sup>int</sup>, CD11b<sup>+</sup> mo (subset X) and Ly6C<sup>lo/neg</sup>, CD11b<sup>lo/+</sup> mo (subset XII) were relatively similar in weeks 6, 9 and 12, whereas Ly6C<sup>lo/neg</sup> CD11b<sup>+</sup> mo (subset XI) was not present and only showed a small increase in percentages in week 3. At this time point in Ly6C<sup>lo/neg</sup> CD11b<sup>+</sup> mo (subset XI), in total cell numbers, a statistically significant difference was found between mice, with higher numbers in BALB/c than in C57BL/6 mice ( $p = 0.0095$ ). Also, in Ly6C<sup>lo/neg</sup>, CD11b<sup>lo/+</sup> mo (subset XII), regarding total cell numbers per ear, higher numbers were found in BALB/c than in C57BL/6 mice ( $p = 0.0092$ ) in week 3 after infection.

Overall, the expression of Ly6C in MHC II<sup>neg</sup>, CD11b<sup>+</sup> cells was dynamic over time, with an influx of Ly6C<sup>hi</sup> cells in week 1.5, towards mostly Ly6C<sup>neg</sup> cells in week 3, followed by a mix of cells expressing no, intermediate or high levels of Ly6C. However, without fate-mapping tools

and the limited antibody panel, we were not able to differentiate between blood monocytes and tissue-infiltrating cells and therefore, this population was not further analyzed.

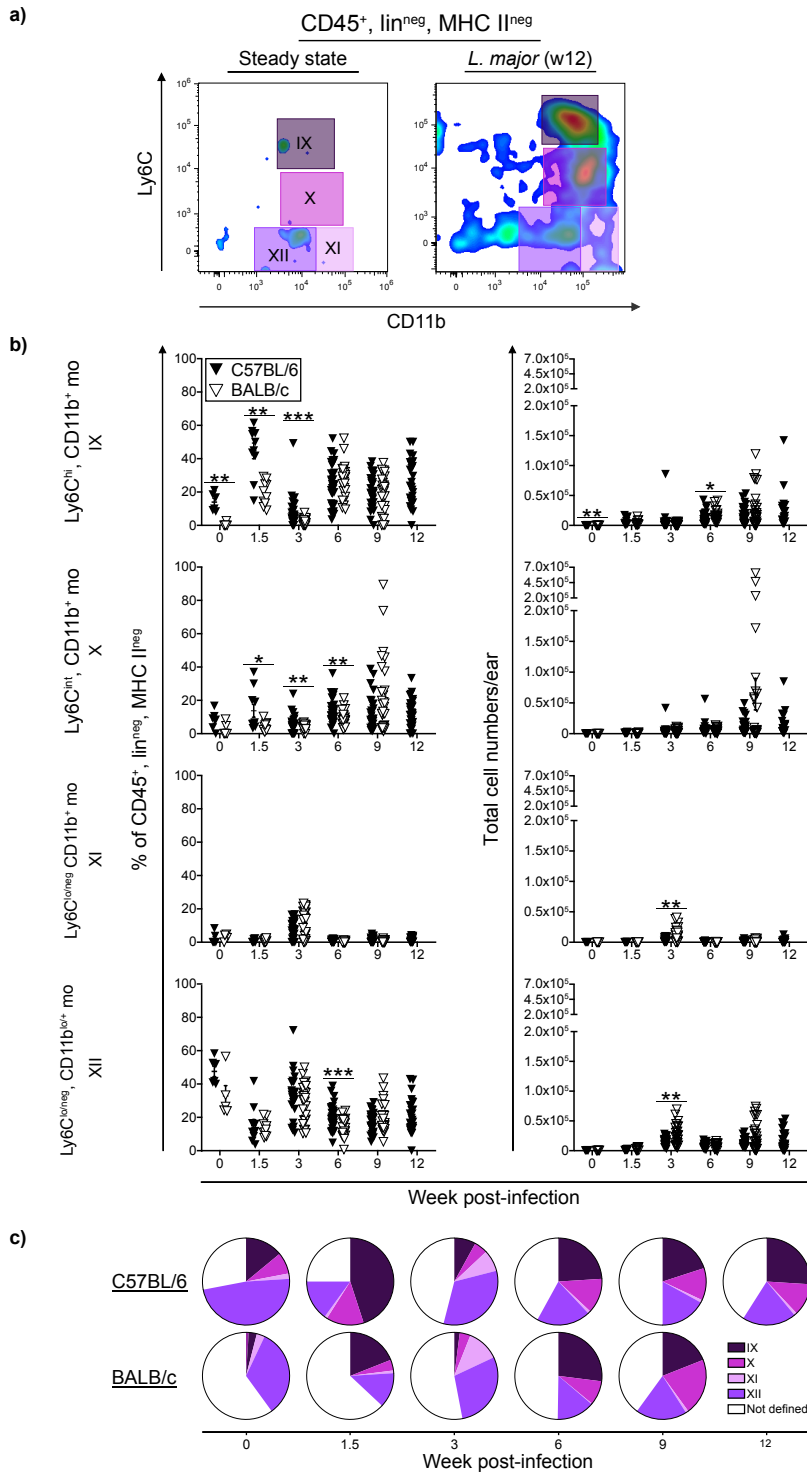


**Figure 14 Analysis of CD11b and Ly6C expression in MHC II<sup>neg</sup> ear tissue cells in naïve mice and after infection with *L. major***

Ear tissue of C57BL/6 (▼) and BALB/c (▽) mice was harvested at different time points after infection with *L. major*, with  $n \geq 4$  ( $\geq 8$  ears) from three independent experiments per time point and strain. Single cell suspensions were generated from each ear by enzymatic and mechanical digestion. At weeks 0 (naïve mice) and 1.5, ear samples of two mice were pooled to enrich in cells in order to generate more valuable results. Cells were stained with surface staining and antigen expression of cells was assessed using flow cytometry. Myeloid cells were identified by expression of the surface marker CD45<sup>+</sup> and absence of the lineage markers CD19, CD90.2, CD49b/DX-5, NK1.1 and Ly6G, (lin<sup>neg</sup>). MHC II<sup>neg</sup> cells were further subdivided into four different subsets (IX-XII) based on their expression of the markers CD11b and Ly6C. **a)** Representative FACS density plots for the gating strategy used to subdivide MHC II<sup>neg</sup> cells into four cell subsets (IX-XII) in ear tissue of naïve mice (steady state) and 12 weeks after infection with *L. major* (w12) in C57BL/6 mice. **b)** Development of percentages and total cell numbers per ear of subsets IX-XII in C57BL/6 and BALB/c mice over time after infection with *L. major*. **c)** Mean percentages of subsets IX-XII of all CD45<sup>+</sup> lin<sup>neg</sup>, MHC II<sup>neg</sup> cells per time point and strain. Significance of differences between values in C57BL/6 and BALB/c mice was determined using Mann-Whitney test, with  $\alpha = 0.05$ ; \* =  $p < 0.05$ ; \*\* =  $p < 0.01$ ; \*\*\* =  $p < 0.001$ .

## 5. Discussion

The aim of this thesis was to evaluate whether the different behavior of C57BL/6 and BALB/c mice in terms of disease control<sup>137</sup>, also reflects in the myeloid cell landscape over time after infection with *L. major*. To this end, the phenotypic appearance of lesional and paralesional skin cells and also their inflammatory profile in terms of iNOS and arginase-1 expression was of interest.

In my study, I made an approach to characterize skin myeloid cell distribution and kinetics after low-dose *L. major* infection. By inoculation of highly infectious, metacyclic *L. major* parasites into the ear dermis of C57BL/6 and BALB/c mice, a cutaneous infection was achieved. Low-dose infection with approximately  $10^3$  parasites was used, because this occurs to be more similar to the actual number of parasites inoculated during a sand fly bite and therefore resembles the natural inoculation towards a dermal site.<sup>36,137</sup>

### 5.1 Evolution of ear lesion size of *L. major* infected mice differs between C57BL/6 and BALB/c mice

As was shown in previous work, resistant C57BL/6 mice present self-resolving lesions, whereas susceptible BALB/c mice develop progressive and even necrotic lesions when suffering from cutaneous leishmaniasis.<sup>36,131,134,137</sup> In order to demonstrate an ongoing infection in ear tissue, as well as differences in lesion evolution between the two genetic backgrounds of mice analyzed, ear lesion sizes of C57BL/6 and BALB/c mice were measured at different time points after inoculation of *L. major* parasites. In both mice, lesion size increased towards week 6, followed by shrinking lesions in C57BL/6 mice and progressing lesions in BALB/c mice. Around week 9, BALB/c mice also clinically began to suffer, which showed by reduced general condition. As a consequence, infected mice had to be killed at this time point to prevent them from suffering. Therefore, no comparison between C57BL/6 and BALB/c mice could be made at later time points, such as week 12 after infection with *L. major*. C57BL/6 mice only showed skin lesions, but no clinical signs of systemic inflammation at week 12 after infection with *L. major*.

The differences in lesion size between both genotypes were statistically significant in weeks 6 and 9 after infection. These differences in lesion size evolution found in C57BL/6 and BALB/c mice are in line with findings of previous investigators, such as Belkaid et al. (1998)<sup>137</sup>, Baldwin et al. (2004)<sup>131</sup> or Cangussu et al. (2009)<sup>134</sup> and therefore confirm the expected behavior of the two genotypes towards infection with leishmaniasis. Around 5 weeks after infection, growth of the lesion displays an inflammatory reaction with influx of immune cells, and in C57BL/6 was

shown to be coincident with parasite growth control.<sup>36,38</sup> In BALB/c mice, however, the disease continuously progresses, with increasing lesion sizes eventually leading to necrosis.<sup>131,134,137</sup>

Conclusively, here, lesion formation at the site of parasite inoculation proved successful infection as well as the resistant vs. susceptible behavior of C57BL/6 and BALB/c mice, respectively, which was the precondition for the following analyses.

## **5.2 *L. major* parasites found in ear tissue indicate successful (intra)dermal infection**

To monitor presence of parasites in intradermal cells, cytopsin centrifugation was performed on isolated ear cell samples in weeks 3, 6, 9 and 12 after infection with *L. major*. The resulting cells layered on microscope slides were then stained and each slide was analyzed for intracellular or free parasites.

In week 3, only the minority of slides obtained from C57BL/6 and BALB/c mice ear tissue contained *L. major* parasites. However, since at these early time points lower cell numbers were obtained from ear tissue, also less cells could be used for cytopsin centrifugation. This resulted in much lower cell density found on microscope slides. Fitting to this, in earlier studies by Lira et al. (2000), performed with low-dose infection of C57BL/6 mice, tissue was found to be negative for parasites in week 3 after infection.<sup>212</sup> Consequently, a low cell count, together with very low parasite presence or even absence of parasites would explain our findings at week 3 after infection with *L. major*. In week 6 after infection, all microscope slides contained *L. major* parasites. This also fits to the findings of Lira et al. (2000), which observed increased parasite counts in C57BL/6 mice tissue at week 7 after infection.<sup>212</sup> Also, in weeks 9 and 12 post-infection, in both mice, the majority of microscope slides contained *L. major* parasites, indicating successful infection.

However, the method used has limitations in that individual parasites can be missed, as only a representative proportion of each sample was analyzed instead of the entire sample and also, by microscopic examination investigator-related errors may occur. For example, a higher sensitivity could have been achieved by PCR analysis of the parasites.<sup>213</sup>

## **5.3 Comparison of IFN $\gamma$ release of LN cells after restimulation with SLA between C57BL/6 and BALB/c mice reflects their distinct immune reactions towards *L. major* infection**

The intradermal inoculation of parasites into the ear holds the advantage of harvesting the draining LN of the individuum, in order to analyze cytokine production.<sup>36,137</sup>

The restimulation of lymph node cells obtained from *L. major* infected mice with *Leishmania*-specific antigens and subsequent measurement of cytokine release by ELISA was used to examine the capability of cytokine release by T cells in response to that specific antigen, and thereby served as an indicator for the ongoing immune response.<sup>36,136,145</sup> IFN $\gamma$  release in supernatant of LN cells was measured after restimulation of these cells with SLA at three different time points after infection. Several analyses have confirmed the importance of IFN-gamma for healing.<sup>36,120,140,214,215</sup>

In line with these studies, our results showed significant higher IFN $\gamma$  release in resistant C57BL/6 mice than in susceptible BALB/c mice. Especially in week 6, there was a significant difference in release levels between the two genotypes. In addition, at this time point, levels of IFN $\gamma$  release inversely correlated with lesion size when compared between the mice: In C57BL/6 mice, where release of IFN $\gamma$  was significantly higher than in BALB/c mice, ear lesions were statistically significant smaller than lesions in BALB/c mice. Later, in week 9, where IFN $\gamma$  levels started to equalize at a higher level in both mice, the lesion volume had decreased in C57BL/6 mice, but further increased in BALB/c mice. These results represent the expected distinct reactions towards infection in C57BL/6 vs. BALB/c mice, as described in the literature, with higher Th<sub>1</sub> cell responses in C57BL/6 than in BALB/c mice, reflecting in higher levels of IFN $\gamma$  expression.<sup>120,136,139,140,142,214</sup>

#### **5.4 Gating strategy**

Successful infection with *L. major* in both mice was proved and the anticipated and observed different immune responses in both genotypes of mice justified the interpretability of the following analyses.

Next, we aimed to analyze potential cellular differences in these mice. To this end, first, different myeloid cell subsets were characterized based on their phenotypical appearance, identified by flow cytometry. Flow cytometry allows separation of cells by using fluorescence-conjugated antibodies and here, was used to characterize cells phenotypically by surface as well as functionally by intracellular marker expression. Due to the limited availability of channels, one channel was used for the viability dye as well as CD45 and the lineage markers. Therefore, in order to determine total cell numbers, we had to combine our gating strategy with the numbers determined by manual cell counting, which might lead to different cell counts than those obtained when using only flow cytometry. Therefore, this could be optimized using a flow cytometer with a higher number of channels available. This also limited us in the number of markers that we were able to apply. Consequently, in order to characterize myeloid cells as well as different myeloid cell populations, we applied markers that are well established in the literature and combined them in an order that we assumed would provide the greatest

selectivity between potentially distinct cell subsets. After defining the myeloid cell types found in infected ear tissue, their time kinetic behavior was analyzed and a comparison of the myeloid cell composition found at different time points after infection was performed between the two differently behaving genotypes of mice in terms of disease control. Still, the identification of different subsets was challenging sometimes, since there is no general classification or strategy to characterize the different myeloid subsets phenotypically. In addition, many investigations and classifications were not made in the skin, but in other tissues. Moreover, due to the limited amount of markers we were able to use, some characterizations made by other authors could only be substantiated on the basis of a proportion of markers.<sup>72,74,98,196,197,204</sup> Therefore, this analysis can provide an overview over the myeloid cell landscape, however, more informative data could probably be generated using lineage tracing tools.

## **5.5 Myeloid cells in C57BL/6 and BALB/c mice differ in their expression levels of Ly6C and CD64 at critical time points in the infection with *L. major***

Percentages and total cell numbers of viable, CD45<sup>+</sup> and lineage negative cells, therefore considered myeloid cells, were constantly increasing over time after infection, although a slight decrease was observed in week 6 after infection. Myeloid cells were found in statistically significant higher percentages in BALB/c mice than in C57BL/6 mice in week 3 after infection, whereas in week 9 after infection, statistically significant higher percentages were found in C57BL/6 mice. No difference between mice was found in total cell numbers per ear, therefore questioning to which extent these differences have an impact on the immune response.

### **5.5.1. MHC II<sup>neg</sup> cells**

MHC II<sup>neg</sup> cells were found in statistically significant higher percentages in BALB/c mice than in C57BL/6 mice in naïve mice as well as in weeks 3, 6 and 9 after infection with *L. major*. However, in total cell numbers per ear, a significant difference was only found in week 3 after infection with *L. major*. These cells are mainly considered to be monocytes and based on this hypothesis, we analyzed them for the expression of the markers Ly6C and CD11b.<sup>47,69,72,73,75,76,98,197,203</sup>

In naïve mice, the majority of MHC II<sup>neg</sup> cells did not express Ly6C or expressed low levels of Ly6C (Ly6C<sup>lo/neg</sup>, CD11b<sup>+</sup> mo; subset XI and MHC II<sup>neg</sup>, Ly6C<sup>lo/neg</sup>, CD11b<sup>lo/+</sup> mo; subset XII). This changed quickly, since at early time points, such as week 1.5 after infection, the majority of cells in the tissue presented high expression levels of Ly6C (Ly6C<sup>hi</sup>, CD11b<sup>+</sup> mo; subset IX). Sunderkötter et al. (2004) already described blood monocytes as heterogenic in their expression levels of Ly6C and stated that in inflammation, such as infection of C57BL/6 mice

with *L. major*, only monocytes expressing intermediate to high levels of Ly6C are recruited to affected sites in order to become MΦ, thereby inducing a shift towards Ly6C<sup>high</sup> monocytes in the blood.<sup>69</sup> In line with this, Geissmann et al. (2003) found Ly6C<sup>+</sup> monocytes, in contrast to their Ly6C<sup>neg</sup> counterparts, to be involved under inflammatory conditions.<sup>47</sup> Olekhovitch et al. (2014) also noticed recruitment of Ly6C<sup>+</sup> MHC II<sup>neg</sup> monocytes towards the infection site on day 1 to 2 after infection and consecutive differentiation of these cells into CD11c<sup>+</sup> MHC II<sup>+</sup> cells with downregulation of Ly6C at later time points.<sup>216</sup>

Goncalves et al. (2011) found monocytes at the lesion site even earlier: Within 30 minutes of infection with *L. major* they detected the accumulation of these cells.<sup>133</sup> In addition, they proposed that monocytes might be able to kill *L. major* parasites. This was based on observations which showed that early after high-dose *L. major* infection, monocytes contained parasites, which had been cleared a few hours later. This was also confirmed by in vitro experiments, where monocytes were shown to take up parasites as well as diminish parasite counts when incubated together.<sup>133</sup> Whether this rapid parasite invasion and killing by monocytes takes place *in vivo* also in low-dose *L. major* infection remains unclear: Using low-dose intradermal *L. major* infection in C57BL/6 and BALB/c mice, Cangussu et al. (2009) did not even detect any parasites at the lesion site until week 4-5.<sup>134</sup> In contrast, Belkaid et al. (2000) found rapidly increasing parasite counts until week 5 after infection, at which time a sudden reduction of parasite counts was observed.<sup>36</sup> However, our findings, together with what is known from the literature, reinforce the assumption that monocytes do infiltrate the tissue already at an early time point after infection with *L. major* in both, C57BL/6 and BALB/c mice. Most likely, Ly6C<sup>hi</sup>, CD11b<sup>+</sup> mo (subset IX) constituted of freshly recruited blood monocytes towards the site of inflammation, possibly ready to differentiate into other cell types. Fitting to a possible differentiation process or migration in and out of the tissue of these cells, the percentages of these cells had already decreased in week 3 after infection, to increase again later in week 6.

In week 3 after infection, expression levels had changed and the majority of cells were characterized by low to no expression of Ly6C (Ly6C<sup>lo/neg</sup>, CD11b<sup>+</sup> monocytes; subset XI and MHC II<sup>neg</sup>, Ly6C<sup>lo/neg</sup>, CD11b<sup>lo/+</sup> monocytes; subset XII). These dynamics found in the expression levels may indicate differentiation processes with downregulation of Ly6C in those cells found at earlier time points, which then expressed high levels of Ly6C. This process of marker downregulation has been described by Leon et al. (2004 and 2007) as well as Tamoutounour et al. (2013) to very likely take place, when monocytes differentiate into e.g. more mature DC.<sup>73,75,76</sup> In contrast, possibly there could also be an exchange in cells with migration of Ly6C<sup>hi</sup> cells out of the tissue and immigration of Ly6C<sup>neg</sup> cells into the tissue. Unfortunately, without lineage tracing, it cannot be said with certainty what exactly was the case in this analysis. However, as a consequence to what was described in the literature, it

seems more likely that downregulation of Ly6C was the case here. Later, in weeks 6, 9 and 12 after infection with *L. major*, more similar, but still varying levels of Ly6C expression were found among MHC II<sup>neg</sup> cells.

Regarding differences between C57BL/6 and BALB/c mice, the results indicate a stronger influx of Ly6C<sup>hi</sup> monocytes in C57BL/6 mice at early time points, such as week 1.5 and 3 (Ly6C<sup>hi</sup>, CD11b<sup>+</sup> mo; subset IX). Differences between mice were statistically significant at these time points. However, in this subset, already statistically significant higher percentages were found in naïve C57BL/6 mice than in naïve BALB/c mice and therefore, it remains unclear, whether this difference between genotypes really was a consequence of the inflammatory process in the tissue. Importantly, though, when analyzing all myeloid MHC II<sup>neg</sup> cells, statistically significant higher percentages were found in BALB/c mice than in C57BL/6 mice in week 3 after infection and therefore this might indicate that although overall MHC II<sup>neg</sup> cells predominate in BALB/c mice at this time point, when breaking it down to specific marker expression, the subset of Ly6C<sup>hi</sup>, CD11b<sup>+</sup> mo then predominates in C57BL/6 mice. Later on, in week 6 after infection, the downregulation of the marker Ly6C might be an explanation of the finding of statistically significant higher percentages of Ly6C<sup>lo/neg</sup> cells among MHC II<sup>neg</sup> cells (Ly6C<sup>lo/neg</sup>, CD11b<sup>lo/+</sup> mo; subset XII) in C57BL/6 compared to BALB/c mice. However, in week 9, higher percentages of these cells were found in BALB/c mice than in C57BL/6 mice, although not statistically significant. Importantly, it also has to be taken into consideration, that upregulation of MHC II in these cells, which very likely takes place in parallel to downregulation of Ly6C<sup>75,76</sup>, would lead to changes in their percentages among the MHC II<sup>neg</sup> population, a process that we were not able to track. The finding of statistically significant higher percentages of MHC II<sup>neg</sup> cells in BALB/c mice, but statistically significant higher percentages in MHC II<sup>+</sup> cells in C57BL/6 might either indicate a constantly stronger influx and supply of MHC II<sup>neg</sup> cells in BALB/c mice or a constantly stronger upregulation of MHC II in C57BL/6 mice, indicative of a stronger differentiation process towards activated cell types due to the infection with *L. major*.<sup>47,72,76,109,217</sup> However, this imbalance being present already in naïve mice might indicate a genotype-specific phenomenon.

Regarding total cell numbers per ear, higher numbers were found in BALB/c mice than in C57BL/6 mice in Ly6C<sup>lo/neg</sup>, CD11b<sup>+</sup> mo (subset XI) and Ly6C<sup>lo/neg</sup>, CD11b<sup>lo/+</sup> mo (subset XII) cells in week 3 after infection with *L. major*. These differences though, were not found in percentages and therefore might be a result of the overall higher cell counts in BALB/c ears. Also, in week 6 after infection, in Ly6C<sup>hi</sup>, CD11b<sup>+</sup> cells (subset IX), significant higher cell numbers per ear were found in BALB/c mice than in C57BL/6 mice. Although here, regarding their distribution, no statistically significant difference was found. Therefore, these results could also be due to a technical error, e.g. a counting error.

Although monocytes can be classified into Ly6C<sup>hi</sup> (classical and inflammatory) and Ly6C<sup>low</sup> (nonclassical and non-inflammatory) monocytes, Sunderkötter et al. (2004) also proposed that different expression levels of Ly6C in monocytes may represent different stages in their maturation process.<sup>69,47</sup> Since we did not find a strict division into low vs. high expression of Ly6C, but also intermediate values, we therefore used these markers to view the dynamics in their expression levels at the different time points after infection with *L. major* and subdivide different subsets based on this observation, in order to use this subdivision as a comparative tool between genotypes of mice.

Conclusively, our results show, that in infected tissue, CD45<sup>+</sup>, MHC II<sup>neg</sup> monocytes show a dynamic process during ongoing infection regarding their phenotypic appearance and possibly also their functionality when correlating their marker expression, especially of Ly6C (hi/low), to what is known from the literature regarding pro- and anti-inflammatory functions.<sup>47,69</sup> Importantly, although statistically significant differences between strains were found at specific time points regarding their marker expression, the dynamics in marker expression during the ongoing inflammation after infection with *L. major* were very similar between C57BL/6 and BALB/c mice.

Freshly recruited monocytes might infiltrate the tissue in order to serve as cell supply for increasing numbers of pro-inflammatory cells which are needed for ongoing immune responses. In addition, differentiation of MHC II<sup>neg</sup> blood monocytes into MHC II<sup>+</sup> cells might take place<sup>47,76</sup>, and therefore lineage-tracing might be useful in order to further investigate these processes.

### 5.5.2. MHC II<sup>+</sup> cells

MHC II<sup>+</sup> cells constantly increased after infection with *L. major* with a slight decrease in week 6 after infection. This fits to what is known from the literature regarding myeloid cell immigration and upregulation of this marker during infectious or immunogenic processes.<sup>47,72,76,85,109,193,217</sup>

We found statistically significant higher percentages of MHC II<sup>+</sup> myeloid cells in naïve mice, as well as in weeks 3, 6 and 9 after infection in C57BL/6 than in BALB/c mice .

When comparing the three myeloid cell groups among MHC II<sup>+</sup> cells between C57BL/6 and BALB/c mice, percentages per group were very similar between the mice, as well as their time point of appearance after *Leishmania*-infection. In both mice, percentages of cDC1 (group 1) remained low throughout all time points after infection. Percentages of Mo/MΦ/DC (group 2) also were rather low, compared to those obtained in Mo/MΦ (group 3). Especially in naïve mice and mice in week 1.5 after infection, Mo/MΦ/DC (group 2) showed very low percentages. With time after infection though, percentages of these cells increased, indicating that expansion or immigration into the tissue took place in this group. Mo/MΦ (group 3) made up the highest percentages of the three groups throughout all weeks after infection. A steady increase in cell

numbers of Mo/M $\Phi$  (group 3) was seen in lesional ear tissue, indicating that the associated subsets were of great importance for lesion formation and ongoing disease process. Difference between C57BL/6 and BALB/c mice was only found in percentages in week 3 after infection. In total cell numbers, no statistically significant difference was found.

To identify possible differences between these mice regarding the formation of a cellular landscape in response to the infection with *L. major*, we wanted to analyze these groups in more detail. In Mo/M $\Phi$ /DC (group 2) and Mo/M $\Phi$  (group 3) we were able to further differentiate these cells into eight different subsets, based on their phenotypic appearance. cDC1 (group 1) were not further differentiated, because their phenotypic appearance already allowed a more definitive interpretation and also, because their cell numbers were already quite low. In line with this, in a study by Henri et al. (2010), among DC found in the dermis, cells characterized by absence of CD11b made up lower frequencies as well.<sup>94</sup>

The eight different subsets were compared between C57BL/6 and BALB/c mice. First, it was focused on their time point of appearance, their relative share of the total cell population of the respective group, as well as their total cell number per ear. Starting with naïve mice, here, TR-M $\Phi$  (subset VI) were the dominant cell type found. Since at this time point, no infection was present, these cells might be interpreted as a non-inflammatory cell type. However, already between week 0 and week 1.5, the ratio between TR-M $\Phi$  (VI) vs. CD11c<sup>neg</sup> mo-M $\Phi$  (VII) or CD11c<sup>neg</sup> M $\Phi$  (VIII) shifted. At this early stage after infection, a short influx of CD11c<sup>neg</sup> mo-M $\Phi$  (VII) was observed, although these cells quickly disappeared afterwards. Whether this disappearance resulted from migration away from the tissue, differentiation into other cells with downregulation of specific marker expression or a short life span of these cells remains unclear.

However, as described in the previous chapter, a similar phenomenon with higher percentages of possibly monocytic cells with high expression of Ly6C at week 1.5 after infection was also found in MHC II<sup>neg</sup> cells. Therefore, this observation in MHC II<sup>+</sup> cells reinforces the assumption of an early response on the cellular level and these parallels might also indicate an interchange between MHC II<sup>neg</sup> and MHC II<sup>+</sup> cells. In a study by Glennie et al. (2017), for example, in mice with secondary *Leishmania* infection, which had resolved their primary lesion prior to the second infection and therefore were termed “*Leishmania*-immune mice”, the early recruitment of inflammatory Ly6C<sup>hi</sup> monocytes towards the site of infection was described.<sup>193</sup> These cells expressed iNOS and were assumed to be important for the early protective immune response.<sup>193</sup> Of course, in our study, next to a possible inflammatory reaction at this early time point, also a technical error should be taken into consideration as a cause of this observation. This would go along with the fact, that the cellular landscape found in week 3 resembled that one, which was already found in naïve mice: In week 3, TR-M $\Phi$  (VI) had expanded and almost completely replaced the two other subsets, and therefore again resembled the presumably

anti-inflammatory state which was found in naïve mice. Here, probably lineage tracing of the corresponding subsets would also be helpful, to determine whether an early pro-inflammatory response with monocyte influx in week 1.5 after infection with *L. major* really takes place at this time point or whether this rather made up a technical error.

However, among Mo/MΦ/DC (group 2), we also found an expansion of mo-DC (II) in week 3 after infection in both mice. This observation is in line with the results of a study by Heyde et al. (2018): Here, in C57BL/6 mice in week 3 after infection with *L. major*, CD11c<sup>+</sup>, Ly6C<sup>+</sup> cells, suspected to be mo-DCs, were found to be the main cells infected by high proliferating *L. major*. However, this analysis was not performed using low-dose, but high-dose infection.<sup>132</sup> Additionally, an expansion of cDC2 (I) was obtained in week 3. Regarding the immunological role of these cells in other skin diseases, e.g. in a study by Kim et al., cDC2 were found to drive psoriasis-like inflammation by production of IL-23.<sup>218</sup> The role of this cytokine in leishmaniasis was investigated by Dietze-Schwonberg et al. (2016), who found elevated levels of Th<sub>17</sub> inducing IL-23p19 in lymph node cells of *Leishmania*-infected BALB/c mice in comparison to those isolated from C57BL/6 mice. Here, CD4<sup>+</sup> Th<sub>17</sub> cells were found to promote parasite persistence and lesion growth in BALB/c mice.<sup>219</sup> In our analysis, percentages of cDC2 were statistically significant higher in C57BL/6 than in BALB/c mice in week 3 after infection, whereas at later time points, higher percentages of cDC2 were found in BALB/c mice. Together with what was described by the previously named authors, this would fit to a disease promoting role of cDC2 in *L. major* infected BALB/C mice.<sup>218,219</sup>

When comparing the timing of appearance or percentages of cDC1 (group 1) and cDC2 (I) between C57BL/6 and BALB/c mice, no huge differences were obtained. This is interesting, since in the literature it has been described, that CD11b<sup>+</sup> (cDC2-like) DC direct Th<sub>2</sub> pathways<sup>98-100</sup>, in contrast to CD11b<sup>neg</sup> (CD103<sup>+</sup> cDC1-like) DC, which rather direct Th<sub>1</sub> pathways.<sup>96,97,101,102</sup> Since in resistant individuals, the Th<sub>1</sub> answer has been described to be dominant, while the Th<sub>2</sub> answer is dominant in susceptible ones,<sup>136,139,142</sup> this could lead to the assumption of cDC1 being higher in C57BL/6 and cDC2 being higher in BALB/c mice. However, this was not found here. Similarly, in a study by Szulc-Dabrowska et al. (2023), cDC1 and cDC2 were analyzed in C57BL/6 and BALB/c mice following infection with mousepox. Interestingly, in BALB/c mice, both cDC1 and cDC2 were found to be generally reduced after infection, whereas in C57BL/6 mice, cDC2 rather increased. Also, the immune answer regarding Th<sub>1</sub> vs. Th<sub>2</sub> responses of specific cell subsets differed between C57BL/6 and BALB/c mice. Here, cDC1 and cDC2 in C57BL/6 mice produced higher levels of Th<sub>1</sub> cytokines than they did in BALB/c mice. In contrast, IL-4 was produced at statistically significant higher levels in cDC1 from BALB/c mice than from C57BL/6 mice.<sup>220</sup>

The expansion of cDC2 (I) and mo-DC (II) in week 3 after infection was followed by a decline in percentages obtained in week 6. Possibly, in week 6, DC had already migrated away from

the skin.<sup>73,75,109,221</sup> Fitting to these observations in terms of cell kinetics, in a study by Leon et al. (2007), mo-DC made up the most numerous cells at week 3 post-infection, whereas a decrease was observed afterwards.<sup>75</sup> Assumably, DC repopulated the tissue from week 6 onwards, as in week 9 cell numbers of cDC1 (group 1) and cDC2 (I) had increased again. This fits to observations made by Belkaid et al. (2000), who detected a huge increase of DCs at the lesion site around week 8 to week 10 after low-dose infection with *L. major*.<sup>36</sup> Also, cell numbers of mo-DC (II) had increased again in both mice in week 9 after infection. Leon et al. (2007) already described the immigration of monocytes into *L. major* infected tissue and their differentiation into DC.<sup>75</sup> In their studies, mo-DC were shown to migrate towards the draining LN and assumed to be of great importance for protective Th<sub>1</sub>-associated immune responses against *L. major*.<sup>75</sup> Surprisingly though, in our analysis, the percentages obtained in this subset (mo-DC, II) were higher in BALB/c mice than in C57BL/6 mice in week 9. As already mentioned, monocytes downregulate Ly6C upon differentiation into DC<sup>75,76,98</sup>, which might be one explanation for their lower percentages in C57BL/6 mice. Moreover, it has been described that not only the phenotypic appearance of cells, but also their way of generation determines their functionality. For example, Santini et al. (2000) found that DC differentiation from monocytes, induced by IFN- $\alpha$  led to higher IFN $\gamma$  production of these cells in contrast to those induced by IL-4, indicating a stronger capability of these cells to generate a Th<sub>1</sub> response.<sup>222</sup> In addition, since this analysis only represents a short period at each time point, without lineage tracing, it cannot be said with certainty what happened to these cells.

Later, in week 12 after infection, an increase in mo-DC was also found in C57BL/6 mice. Interestingly, Woelbing et al. (2006) found Fc $\gamma$ RI expression to be an important feature for the uptake of *L. major* parasites into DCs, a process needed for protective immunity with parasite killing and consecutive lesion resolution.<sup>223</sup> Therefore, the presence of these CD64-expressing (assumably dendritic) cells at this time point might indeed be critical for protective immunity. Importantly, high expression of CD64 may also identify cells involved in inflammatory processes, since it is upregulated under pro-inflammatory conditions and, in a study by Thepen et al. (2000), elimination of CD64 expressing M $\Phi$  lead to resolution of chronic cutaneous inflammation.<sup>224</sup> In general, it has been described by several authors, that mo-DC, which differ from cDC by higher expression of CD64, are especially generated during inflammation.<sup>47,73-75,98,204</sup> For example, in studies by Serbina et al., mo-DC, which were termed "Tip-DCs" due to their expression of TNF and iNOS were found to be crucial for control of bacterial replication and prevention of host death.<sup>205,206</sup>

Still, it remains unclear, whether cells characterized by low to no expression of Ly6C and CD64, which we defined as cDC2 (I), could rather be mo-DC that downregulated Ly6C.<sup>73,75,76,98</sup> Possibly though, mo-DCs, after their maturation process including Ly6C marker downregulation, would not be found in the tissue anymore, since this process has been

suspected to be completed in the LN.<sup>75</sup> In addition, conventional DC are CD64<sup>neg</sup>, in contrast to mo-DC, which would at least express low levels of CD64.<sup>73,74,98,204</sup>

Starting in week 6, a rise in percentages of mo-MΦ/MΦ (subset IV) and CD11c<sup>+</sup> MΦ (V) became obvious. CD11c<sup>+</sup> mo-MΦ (III) presented lower percentages in week 6, but had also increased in weeks 9 and 12, possibly due to monocyte recruitment from the circulation towards lesion site and differentiation into MΦ.<sup>69,72</sup>

In Mo/MΦ (group 3), in week 6, after their short influx in week 1.5 and their disappearance afterwards, CD11c<sup>neg</sup> mo-MΦ (VII) made up the majority of cells in terms of percentages in C57BL/6 and BALB/c mice. These cells, and CD11c<sup>+</sup> mo-MΦ (III), phenotypically resembled each other regarding their high expression of Ly6C and CD64. Their time point of expansion around 6 weeks after infection correlated with the time point that has been described by Belkaid et al. (2000) to mark the onset of lesion formation, the influx of myeloid cells as well as the time point where parasite depletion begins to take place in C57BL/6 mice.<sup>36</sup> However, at least in CD11c<sup>+</sup> mo-MΦ (III), no significant difference was found between C57BL/6 and BALB/c mice at any time point. In CD11c<sup>neg</sup> mo-MΦ (VII) though, in week 9 after infection, significant higher percentages were found in C57BL/6 than in BALB/c mice. This difference was also significant when analyzing total cell numbers of these cells, however, when analyzing whether they differed regarding their distribution, no significant difference was found, which might indicate a counting error.

All in all, according to their time point of appearance, these CD11c<sup>neg</sup>, CD11b<sup>+</sup>, Ly6C<sup>+/hi</sup> and CD64<sup>+</sup> cells could be relevant for the lesion resolution and associated processes, which is described to take place between week 6 and week 12 in C57BL/6 mice<sup>36</sup> and which also in our investigation took place between week 9 and week 12 in these mice. As a consequence, when correlating their time kinetic appearance as well as their high expression of CD64 and Ly6C, these cells could be considered as a rather pro-inflammatory cell type: As described earlier, by targeting and eliminating MΦ expressing CD64, a marker which is enhanced during inflammation, Thepen et al. (2000) found an improvement of chronic cutaneous inflammation.<sup>224</sup> Also, in other analyses in dermis under inflammatory conditions, such as atopic dermatitis, increased expression levels of CD64 were found in dermal cells, which was assumed to be due to upregulation of this marker on local cells rather than due to influx of new cells.<sup>225</sup> In addition, also their Ly6C<sup>high</sup> phenotype might indicate the pro-inflammatory nature of these cells, since 1) in inflammation, Ly6C<sup>high</sup> monocytes are found to immigrate towards tissue<sup>69</sup> and 2) in inflammation, Ly6C downregulation upon monocyte differentiation into MΦ was shown to be disrupted.<sup>197</sup> In contrast, TR-MΦ (VI), phenotypically presented the opposite of mo-MΦ, with no/low Ly6C and no/low CD64 expression. Therefore, in contrast to Ly6C<sup>+/hi</sup> and CD64<sup>+/hi</sup> cells, these cells were considered a rather anti-inflammatory cell type, also due to their early presence

in naïve mice. Interestingly, similar to what was described by Santini et al. (2000) for DC<sup>222</sup>, Luque-Martin et al. (2021) found that exposure to IFN $\gamma$  during differentiation of human monocytes to M $\Phi$  led to a hyperinflammatory phenotype and also, these M $\Phi$  expressed more CD64 when compared to M $\Phi$  stimulated by e.g. M-CSF or GM-CSF.<sup>226</sup> However, no specific surface marker indicative for this pro-inflammatory M $\Phi$  was identified in this study.<sup>226</sup> Therefore, environmental cues can influence cell functions, although this might not be displayed by the surface markers used.

In our investigation, TR-M $\Phi$  (VI) persisted at lower percentages during weeks 6-12 after infection in C57BL/6 mice but increased in BALB/c mice in week 9, where they, like in week 3, again made up the majority of cells in this group. Recently, Lee et al. (2020) described the interactions between eosinophils and dermal TR-M $\Phi$  in *L. major* infection. Here, eosinophil-derived IL-4 was found to be the major source for local proliferation of TR-M $\Phi$  and thereby important for maintaining their functional properties. Most importantly, in mice lacking IL-4/IL-13 from eosinophils, TR-M $\Phi$  shifted to a rather pro-inflammatory state, consequently improving disease outcome.<sup>227</sup> Possibly, this could be an explanation for the higher numbers of TR-M $\Phi$  in BALB/c mice, as these mice fail to downregulate IL-4 during *L. major* infection.<sup>113,140</sup>

Interestingly, in week 9, differences between C57BL/6 and BALB/c mice were observed regarding percentages of CD11c<sup>neg</sup> TR-M $\Phi$  (VI) and CD11c<sup>neg</sup> mo-M $\Phi$  (VII). BALB/c mice showed higher percentages of TR-M $\Phi$  (VI) in week 9 compared to C57BL/6 mice. In contrast, in C57BL/6 mice, percentages of CD11c<sup>neg</sup> mo-M $\Phi$  (VII) were higher than in BALB/c mice. The main phenotypically difference in these cells was their expression of Ly6C and CD64. Whereas CD11c<sup>neg</sup> mo-M $\Phi$  (VII) were defined by high expression of Ly6C and CD64, TR-M $\Phi$  (VI) were rather low in the expression of both. Although these differences only appeared in week 9, importantly, this is the time point where it has been described that lesions of C57BL/6 mice are already in the phase of healing<sup>36,134</sup>, whereas it is known that BALB/c mice do not resolve, but rather develop necrotic lesions<sup>134</sup>, which was also the case in our investigation.

Therefore, we found Ly6C and CD64 to be markers, whose expression by myeloid cells constituted the main difference in the cell landscape when comparing between C57BL/6 and BALB/c mice over time after infection with *L. major*. Expression of these markers could represent a decisive difference between C57BL/6 and BALB/c mice for the tendency of the immune response and the inflammatory process. Their enhancement at later time points in C57BL/6 mice, in contrast to low expression in BALB/c mice might be indicative for their importance for protective immunity. In addition, the high expression of Ly6C underlines the possible involvement of inflammatory monocytic cells in these processes.<sup>69,72,197,207</sup> Regarding the exact characterization of these cells, the Ly6C<sup>int to high</sup> monocyte-derived cells, which Leon

et al. (2007) claimed to be important for the protective Th<sub>1</sub> cell response<sup>75</sup> were CD11c<sup>+</sup> and assumed to be mo-DCs<sup>75</sup> and not mo-MΦ, in contrast to our CD11c<sup>neg</sup> mo-MΦ (VII). Besides their difference in CD11c expression, however, the expression of MHC II, CD11b as well as Ly6C was similar and, importantly, they were as well assumed to be monocyte-derived cells,<sup>75</sup> thus supporting the assumption of monocyte-involvement.

Therefore, our results are in line with what has been suspected in the literature before: The presence and assumable importance of monocytes and monocyte-derived cells in the infection with *L. major*.<sup>75,132,133</sup> These cells were shown to be recruited rapidly towards lesion sites, harboring high numbers of parasite and most importantly, involved in the protective immune response against the parasite.<sup>75,132,133</sup> It has to be mentioned though, that unfortunately not all results are equally comparable, since the studies described differed regarding low- or high-dose *L. major* infection.<sup>36,75,132,133</sup>

## **5.6 iNOS and Arginase-1 expression differs between C57BL/6 and BALB/c mice after infection with *L. major*, but is independent of cell type**

Previous studies indicated a disease-promoting role of arginase-1 in the infection with *L. major*.<sup>172,188,228</sup> In contrast, iNOS-derived NO is important for parasite killing.<sup>229-231</sup> Fitting to this, absence of iNOS in iNOS mutant mice was shown to lead to a diminished parasite controlling function and non-healing lesions<sup>36,232</sup>, while deletion of arginase-1 or inhibition of its activity led to improved control of disease in former susceptible mice.<sup>187,188</sup>

Here, we analyzed iNOS and arginase-1 expression in myeloid cells and compared this expression between C57BL/6 and BALB/c mice. iNOS and arginase-1 expression was determined by intracellular staining. By analyzing the presence of these enzymes at different time points after infection with *L. major* in myeloid cell subsets, we aimed to learn more about the functionality of the different cell types. We found that mean percentages of iNOS expressing myeloid cells constantly increased with weeks after infection in C57BL/6 mice, whereas in BALB/c mice, an increase was obtained only in week 9 after infection. In line with previous investigators<sup>126,134,172</sup>, percentages of iNOS expressing myeloid cells were much higher in C57BL/6 than in BALB/c mice. For example, in a study by Stenger et al (1994), expression of iNOS at the lesion site was found to be higher in resistant mice than in susceptible mice and its upregulation correlated with lesion resolution.<sup>126</sup>

The difference between percentages of myeloid cell iNOS expression in C57BL/6 vs. BALB/c mice in our study was especially prominent in weeks 6 and 9, where higher percentages of iNOS expressing myeloid cells were found in C57BL/6 mice than in BALB/c mice. Iniesta et al. (2005) also described iNOS expression to correlate with lesion resolution in resistant mice<sup>172</sup>, which is in line with our finding of a reduction of the lesion size taking place from week 6

onwards in C57BL/6 mice and therefore also correlated with the peak found in iNOS expression in week 9 after infection.

Regarding percentages of arginase-1-expressing myeloid cells, although we already found significant differences between the strains in week 6, here, in both mice, arginase-1 levels had increased when compared to week 3 after infection. Importantly, in BALB/c mice, these percentages further increased towards week 9, whereas in C57BL/6 mice they remained stable and then rather decreased towards week 12. Especially in week 9, higher percentages of arginase-1 expressing myeloid cells were obtained in BALB/c mice in contrast to percentages obtained in C57BL/6 mice. These results are also very similar to observations made by Iniesta et al. (2005), who found that in both, C57BL/6 and BALB/c mice after high-dose infection ( $10^6$ ) with *L. major*, the initial arginase-1 expression correlated with the onset of lesion formation and afterwards decreased in resistant C57BL/6 mice, but remained high in susceptible BALB/c mice.<sup>172</sup> Also, Kropf et al. (2005) found a decrease in arginase activity at the lesion site correlating with healing and lesion resolution in high-dose ( $2 \times 10^6$ ) *L. major*-infected resistant mice, whereas arginase activity further increased in non-healing BALB/c mice.<sup>188</sup>

Interestingly, in our investigation, week 6 marked a changing point in the expression of iNOS and arginase-1. From week 6 onwards, iNOS expression increased more strongly in C57BL/6 mice than in BALB/c mice. In contrast, arginase-1 expressing myeloid cells increased in BALB/c mice, but decreased in C57BL/6 mice. Overall, the differences in iNOS and arginase-1 expression in C57BL/6 vs. BALB/c mice seemed to evolve especially from week 6 onwards, to become most prominent in week 9. When correlating this development to ear lesion size development, the trends in arginase-1 expression, as well as lesion volume development resembled each other in each of the mice: The peak in percentages of arginase-1 expressing myeloid cells in C57BL/6 mice was obtained in week 6 and here, also highest mean lesion volume was measured in these mice. In contrast, in BALB/c mice, mean lesion volumes as well as percentages of arginase-1 expressing myeloid cells constantly increased towards week 9 after infection with *L. major*. Since no additional time points were examined in these mice, this trend was not assessed further.

Although regarding iNOS expression, highest percentages were reached in week 9 in both mice, in C57BL/6 mice this correlated with reduced lesion volume, whereas in BALB/c mice, increased lesion sizes were obtained. Interestingly, when analyzing whether cells expressed both iNOS and arginase-1 or only one of the enzymes, in C57BL/6 mice in week 9, percentages of iNOS SP cells were higher than percentages of iNOS and arginase-1 DP cells. In contrast, percentages of iNOS, arginase-1 DP cells in BALB/c mice exceeded those of iNOS-SP cells. In line with this, in a study by Schleicher et al. (2016), in C57BL/6 wild-type mice infected with *L. major*, only half of cells that expressed iNOS additionally co-expressed arginase-1. In addition, in skin lesions of BALB/c mice, arginase-1 levels were found to be higher compared

to levels obtained in C57BL/6 mice.<sup>187</sup> They also analyzed TNF-deficient mice (TNF<sup>-/-</sup> mice), where they found higher co-expression of iNOS and arginase-1, claiming this as a potential cause of susceptibility towards infection, which could also cause susceptibility in BALB/c mice. In situ, hyperexpression of arginase-1 was found to lead to impaired NO production and thereby, could possibly also lead to impaired *Leishmania* parasite control.<sup>187</sup> Importantly, regarding NO generation by iNOS, Rutschmann et al. (2001) pointed out that even though high iNOS levels might be detected in tissues, this would not necessarily correlate with NO production, since simultaneously high arginase-1 levels and high activity of the enzyme could lead to substrate depletion and therefore impair iNOS activity.<sup>189</sup> As a consequence of high arginase-1 activity, three different mechanisms were summarized by Schleicher et al. (2016), which include the impairment of NO generation by iNOS, as well as impairment of T cell functions, due to the lack of L-arginine.<sup>189,190,233-237</sup> The third mechanism summarizes the positive correlation between arginase-1 activity and parasite numbers<sup>172</sup> via the synthesis of polyamines from an product of arginase-1, which are an important source for parasite growth.<sup>238</sup> However, as Schleicher et al. (2016) brought into context, this third mechanism might not be as relevant, because *L. major* parasites command their own arginase<sup>238,239</sup> and therefore may not rely on exogenous sources.<sup>187</sup> Whether in this study higher arginase-1 levels in BALB/c mice correlated with higher parasite burden in these mice was not determined, since we were not able to examine the number of parasites by cytocentrifugation. However, in other studies, a positive correlation between arginase-1 expression/activity and parasite burden has been described<sup>187</sup> and therefore could likely be the case here as well. High expression of arginase-1 in BALB/c mice might have affected NO production by iNOS due to substrate depletion<sup>189,190</sup> and thereby lead to less efficient parasite control.<sup>187</sup> As stated above, our results confirm what other investigators have already described regarding iNOS and arginase-1 expression in infection with *L. major* and its correlation with lesion development.

To further investigate this, we analyzed iNOS and arginase-1 expression not only in the overall myeloid cell population, but also in our defined myeloid cell subsets in Mo/MΦ/DC (group 2) and Mo/MΦ (group 3) at the time points week 6 and 9 after infection, where the greatest differences in iNOS and arginase-1 expression among the myeloid cell population were found between mice. Unsurprisingly, again, in all subsets, percentages of iNOS-SP cells were higher in C57BL/6 than in BALB/c mice and in week 9, in the majority of subsets, this difference was statistically significant. In contrast, also statistically significant higher percentages of arginase-1-SP cells were found in all subsets in BALB/c mice compared to C57BL/6 mice in week 9. Some cell subsets were rather exclusively expressing iNOS, others expressed both, iNOS and arginase-1, but the expression of iNOS or Arginase-1 also differed per cell and mouse strain. Interestingly, the frequency of iNOS- or arginase-1-expressing cells did not show the same trends regarding subtype of cells, but seemed to depend on the mouse genotype.

For example, CD11c<sup>neg</sup> mo-MΦ (VII) showed statistically significant higher percentages of iNOS-SP cells in C57BL/6 than in BALB/c mice in week 9 after infection, whereas in this subset, percentages of arginase-1-SP cells were statistically significant higher in BALB/c mice than in C57BL/6 mice at this time point. The same trend was observed in cDC2 (II), mo-MΦ (III), MΦ (V), TR-Mac (VI) and CD11c<sup>neg</sup> MΦ (VIII) in week 9, although not as strong as in CD11c<sup>neg</sup> mo-MΦ (VII).

These findings are in contrast to the assumption made by Schleicher et al. (2016) that one major cell population would be responsible for arginase-1 expression, which in their analysis was claimed to be comprised of monocyte-derived DC or MΦ.<sup>187</sup> Also, in a study by Wilmes et al. (2023), tissue-resident MΦ were found to be the main iNOS expressing cells in infarcted myocardial tissue.<sup>240</sup> De Trez et al. (2009) claimed that inflammatory DC in the LN and in tissue sections are the main iNOS-producing cells.<sup>241</sup> However, in the tissue analyzed, this was only based on the expression of the markers MHC II, CD11c, CD11b and absence of Ly6G.<sup>241</sup> As already described earlier, on the basis of only these markers, characterization of DCs is not necessarily sufficient and therefore, it remains unclear, whether these cells were in fact constituted only of DC. Interestingly, in a study by Oleknovitch et al. (2014), iNOS expression was described to provide pathogen control at the tissue level, rather than having cell intrinsic effects, therefore allowing parasite killing even in phagocytes where intrinsic iNOS expression was absent.<sup>216</sup> In line with this, rather than identifying one specific subset responsible for NO production, we found a general tendency towards iNOS or arginase-1 expression, dependent on the genotype of mice. Therefore, our observations lead to the assumption, that the functionality of cells is determined by the genotype of the corresponding mice and the immunological imprinting in their cellular (micro-)environment by e.g. proinflammatory cytokines rather than linked to specific phenotypic attributes.

## 5.7 Conclusion/Outlook

In conclusion, this approach permitted us to generate a comprehensive skin myeloid cell landscape following *L. major* infection. It could be demonstrated that selected myeloid cell subsets may contribute to different disease stages, especially with regard to the influx of monocytes and the development of monocyte-derived myeloid cells in lesional ear tissue. Surprisingly, C57BL/6 and BALB/c mice did not show major differences in terms of the timing of overall myeloid cell landscape appearance and cellular distribution following *L. major* infection. However, when restricting the analysis to specific subsets at specific time points, especially at later time points, differences between the two genetic backgrounds were obtained. These differences particularly related to the surface expression of Ly6C and CD64 on cells, which according to the literature might indicate a monocytic origin. Cells with expression of

these markers were found in significantly higher percentages in resistant C57BL/6 than in BALB/c mice. The time point of appearance during the healing phase of C57BL/6 mice might indicate an important role for Ly6C and CD64 expressing myeloid cells in *L. major* infection. In addition, dynamic changes were found among the MHC II<sup>neg</sup> cell population, indicating cell supply by monocytes and differentiation processes during inflammation. Further, we confirmed that in C57BL/6 mice rather pro-inflammatory responses take place, with regard to higher levels of IFN $\gamma$  in weeks 3 and 6 and higher expression of iNOS in week 9, whereas in BALB/c mice, levels of IFN $\gamma$ - or iNOS-expression were much lower in favor of arginase-expression. The main differences between the mouse strains also coincided with the time points when lesion resolution appears in C57B/6 mice. Interestingly, the proinflammatory profile in C57BL/6 mice was not restricted to specific cell subsets but represented a general tendency in these mice.

Conclusively, this data might be helpful for future experiments, to further analyze origin and development of myeloid cells, to better understand the link between phenotypic appearance and functionality of cells. However, this method also beared weaknesses, e.g. in terms of non-exclusive marker expression for M $\Phi$  or DC. Therefore, to definitively study the complexity and heterogeneity of cell subsets, especially in inflammation, lineage-tracing experiments are required.<sup>73,242</sup> Specific tracing of subsets, to screen their developmental pathways and changes of marker expression, as well as functional distinct features in progressing disease might help to gain further information about manipulative effects of the parasite towards the immune system and the involvement of different myeloid cells in this process. Altogether, knowledge about the behavior of parasites and correlation to immune responses like cell development or cytokine expression might help to develop new approaches for future medication or even vaccines.

## 6. References

1. World Health O. Control of the leishmaniases. *World Health Organ Tech Rep Ser* 2010; (949): xii-xiii, 1-186, back cover.
2. Adler S, Ber M. Transmission of *Leishmania tropica* by the Bite of *Phlebotomus papatasi*. *Nature* 1941; **148**(3747): 227-.
3. Avari CR, Mackie FP. Canine Leishmaniasis in Bombay. *Ind Med Gaz* 1924; **59**(12): 604-5.
4. Burza S, Croft SL, Boelaert M. Leishmaniasis. *Lancet* 2018; **392**(10151): 951-70.
5. WHO Leishmaniasis. <https://www.who.int/news-room/fact-sheets/detail/leishmaniasis> (accessed April 24, 2023).
6. von Stebut E, Tenzer S. Cutaneous leishmaniasis: Distinct functions of dendritic cells and macrophages in the interaction of the host immune system with *Leishmania major*. *Int J Med Microbiol* 2018; **308**(1): 206-14.
7. Alvar J, Velez ID, Bern C, et al. Leishmaniasis worldwide and global estimates of its incidence. *PLoS One* 2012; **7**(5): e35671.
8. WHO Leishmaniasis Overview. [https://www.who.int/health-topics/leishmaniasis#tab=tab\\_1](https://www.who.int/health-topics/leishmaniasis#tab=tab_1) (accessed April 24, 2023).
9. Okwor I, Uzonna J. Social and Economic Burden of Human Leishmaniasis. *Am J Trop Med Hyg* 2016; **94**(3): 489-93.
10. Von Stebut E. Leishmaniasis. *J Dtsch Dermatol Ges* 2015; **13**(3): 191-200; quiz 1.
11. Aronson N, Herwaldt BL, Libman M, et al. Diagnosis and Treatment of Leishmaniasis: Clinical Practice Guidelines by the Infectious Diseases Society of America (IDSA) and the American Society of Tropical Medicine and Hygiene (ASTMH). *Clinical Infectious Diseases* 2016; **63**(12): 1539-57.
12. WHO Leishmaniasis Treatment. [https://www.who.int/health-topics/leishmaniasis#tab=tab\\_3](https://www.who.int/health-topics/leishmaniasis#tab=tab_3) (accessed May 03, 2023).
13. Aebischer T, Moody SF, Handman E. Persistence of virulent *Leishmania major* in murine cutaneous leishmaniasis: a possible hazard for the host. *Infect Immun* 1993; **61**(1): 220-6.
14. Muller I. Role of T cell subsets during the recall of immunologic memory to *Leishmania major*. *Eur J Immunol* 1992; **22**(12): 3063-9.
15. Hill JO, North RJ, Collins FM. Advantages of measuring changes in the number of viable parasites in murine models of experimental cutaneous leishmaniasis. *Infect Immun* 1983; **39**(3): 1087-94.
16. Schubach A, Haddad F, Oliveira-Neto MP, et al. Detection of *Leishmania* DNA by polymerase chain reaction in scars of treated human patients. *J Infect Dis* 1998; **178**(3): 911-4.
17. Belkaid Y, Hoffmann KF, Mendez S, et al. The role of interleukin (IL)-10 in the persistence of *Leishmania major* in the skin after healing and the therapeutic potential of anti-IL-10 receptor antibody for sterile cure. *J Exp Med* 2001; **194**(10): 1497-506.
18. Moll H, Flohe S, Rollinghoff M. Dendritic cells in *Leishmania major*-immune mice harbor persistent parasites and mediate an antigen-specific T cell immune response. *Eur J Immunol* 1995; **25**(3): 693-9.
19. Leclerc C, Modabber F, Deriaud E, Cheddid L. Systemic infection of *Leishmania tropica* (major) in various strains of mice. *Trans R Soc Trop Med Hyg* 1981; **75**(6): 851-4.
20. Lainson R, Shaw JJ. Observations on the development of *Leishmania* (L.) chagasi Cunha and Chagas in the midgut of the sandfly vector *Lutzomyia longipalpis* (Lutz and Neiva). *Ann Parasitol Hum Comp* 1988; **63**(2): 134-45.
21. Sacks DL, Perkins PV. Development of infective stage *Leishmania* promastigotes within phlebotomine sand flies. *Am J Trop Med Hyg* 1985; **34**(3): 456-9.
22. Sacks DL, Perkins PV. Identification of an infective stage of *Leishmania* promastigotes. *Science* 1984; **223**(4643): 1417-9.
23. Sacks D, Noben-Trauth N. The immunology of susceptibility and resistance to *Leishmania major* in mice. *Nat Rev Immunol* 2002; **2**(11): 845-58.

24. Gossage SM, Rogers ME, Bates PA. Two separate growth phases during the development of *Leishmania* in sand flies: implications for understanding the life cycle. *Int J Parasitol* 2003; **33**(10): 1027-34.
25. Beach R, Kiilu G, Leeuwenburg J. Modification of sand fly biting behavior by *Leishmania* leads to increased parasite transmission. *Am J Trop Med Hyg* 1985; **34**(2): 278-82.
26. Franke ED, Rowton ED, Perkins PV, McGreevy PB. Detection and enumeration of *Leishmania* in sand flies using agar-based media. *Am J Trop Med Hyg* 1987; **37**(3): 516-9.
27. Kimblin N, Peters N, Debrabant A, et al. Quantification of the infectious dose of *Leishmania* major transmitted to the skin by single sand flies. *Proc Natl Acad Sci U S A* 2008; **105**(29): 10125-30.
28. Peters NC, Egen JG, Secundino N, et al. In vivo imaging reveals an essential role for neutrophils in leishmaniasis transmitted by sand flies. *Science* 2008; **321**(5891): 970-4.
29. Antoine JC, Prina E, Jouanne C, Bongrand P. Parasitophorous vacuoles of *Leishmania amazonensis*-infected macrophages maintain an acidic pH. *Infect Immun* 1990; **58**(3): 779-87.
30. Alexander J, Vickerman K. Fusion of host cell secondary lysosomes with the parasitophorous vacuoles of *Leishmania mexicana*-infected macrophages. *J Protozool* 1975; **22**(4): 502-8.
31. Brazil RP. In vivo fusion of lysosomes with parasitophorous vacuoles of *Leishmania*-infected macrophages. *Ann Trop Med Parasitol* 1984; **78**(2): 87-91.
32. Locksley RM, Heinzl FP, Fankhauser JE, Nelson CS, Sadick MD. Cutaneous host defense in leishmaniasis: interaction of isolated dermal macrophages and epidermal Langerhans cells with the insect-stage promastigote. *Infect Immun* 1988; **56**(2): 336-42.
33. Chang KP, Dwyer DM. Multiplication of a human parasite (*Leishmania donovani*) in phagolysosomes of hamster macrophages in vitro. *Science* 1976; **193**(4254): 678-80.
34. Chang KP, Dwyer DM. *Leishmania donovani*. Hamster macrophage interactions in vitro: cell entry, intracellular survival, and multiplication of amastigotes. *J Exp Med* 1978; **147**(2): 515-30.
35. : Smart Servier Medical Art
36. Belkaid Y, Mendez S, Lira R, Kadambi N, Milon G, Sacks D. A natural model of *Leishmania* major infection reveals a prolonged "silent" phase of parasite amplification in the skin before the onset of lesion formation and immunity. *J Immunol* 2000; **165**(2): 969-77.
37. Maurer M, Dondji B, von Stebut E. What determines the success or failure of intracellular cutaneous parasites? Lessons learned from leishmaniasis. *Med Microbiol Immunol* 2009; **198**(3): 137-46.
38. Belkaid Y, Von Stebut E, Mendez S, et al. CD8+ T cells are required for primary immunity in C57BL/6 mice following low-dose, intradermal challenge with *Leishmania major*. *J Immunol* 2002; **168**(8): 3992-4000.
39. de Vries HJ, Reedijk SH, Schallig HD. Cutaneous leishmaniasis: recent developments in diagnosis and management. *Am J Clin Dermatol* 2015; **16**(2): 99-109.
40. Ben Salah A, Zakraoui H, Zaatour A, et al. A randomized, placebo-controlled trial in Tunisia treating cutaneous leishmaniasis with paromomycin ointment. *Am J Trop Med Hyg* 1995; **53**(2): 162-6.
41. Alrajhi AA, Ibrahim EA, De Vol EB, Khairat M, Faris RM, Maguire JH. Fluconazole for the treatment of cutaneous leishmaniasis caused by *Leishmania major*. *N Engl J Med* 2002; **346**(12): 891-5.
42. Asilian A, Jalayer T, Whitworth JA, Ghasemi RL, Nilforooshzadeh M, Oliaro P. A randomized, placebo-controlled trial of a two-week regimen of aminosidine (paromomycin) ointment for treatment of cutaneous leishmaniasis in Iran. *Am J Trop Med Hyg* 1995; **53**(6): 648-51.
43. Parkin J, Cohen B. An overview of the immune system. *Lancet* 2001; **357**(9270): 1777-89.
44. Chaplin DD. Overview of the immune response. *J Allergy Clin Immunol* 2010; **125**(2 Suppl 2): S3-23.

45. Steinman RM. Lasker Basic Medical Research Award. Dendritic cells: versatile controllers of the immune system. *Nat Med* 2007; **13**(10): 1155-9.
46. von Stebut E. Research in practice: Different dendritic cell types in skin with various functions - important implications for intradermal vaccines. *J Dtsch Dermatol Ges* 2011; **9**(7): 506-9.
47. Geissmann F, Jung S, Littman DR. Blood monocytes consist of two principal subsets with distinct migratory properties. *Immunity* 2003; **19**(1): 71-82.
48. Steinman RM, Witmer MD. Lymphoid dendritic cells are potent stimulators of the primary mixed leukocyte reaction in mice. *Proc Natl Acad Sci U S A* 1978; **75**(10): 5132-6.
49. Nussenzweig MC, Steinman RM. Contribution of dendritic cells to stimulation of the murine syngeneic mixed leukocyte reaction. *J Exp Med* 1980; **151**(5): 1196-212.
50. Nussenzweig MC, Steinman RM, Gutchinov B, Cohn ZA. Dendritic cells are accessory cells for the development of anti-trinitrophenyl cytotoxic T lymphocytes. *J Exp Med* 1980; **152**(4): 1070-84.
51. Steinman RM, Gutchinov B, Witmer MD, Nussenzweig MC. Dendritic cells are the principal stimulators of the primary mixed leukocyte reaction in mice. *J Exp Med* 1983; **157**(2): 613-27.
52. Van Voorhis WC, Valinsky J, Hoffman E, Luban J, Hair LS, Steinman RM. Relative efficacy of human monocytes and dendritic cells as accessory cells for T cell replication. *J Exp Med* 1983; **158**(1): 174-91.
53. Murray PJ, Wynn TA. Protective and pathogenic functions of macrophage subsets. *Nat Rev Immunol* 2011; **11**(11): 723-37.
54. De Kleer I, Willems F, Lambrecht B, Goriely S. Ontogeny of myeloid cells. *Front Immunol* 2014; **5**: 423.
55. Kashem SW, Haniffa M, Kaplan DH. Antigen-Presenting Cells in the Skin. *Annual Review of Immunology* 2017; **35**(1): 469-99.
56. van Furth R, Cohn ZA, Hirsch JG, Humphrey JH, Spector WG, Langevoort HL. The mononuclear phagocyte system: a new classification of macrophages, monocytes, and their precursor cells. *Bull World Health Organ* 1972; **46**(6): 845-52.
57. Guilliams M, Ginhoux F, Jakubzick C, et al. Dendritic cells, monocytes and macrophages: a unified nomenclature based on ontogeny. *Nat Rev Immunol* 2014; **14**(8): 571-8.
58. Gourko H, Williamson D, Tauber A. The Evolutionary Biology Papers of Elie Metchnikoff; 2000.
59. Wynn TA, Chawla A, Pollard JW. Macrophage biology in development, homeostasis and disease. *Nature* 2013; **496**(7446): 445-55.
60. Varol C, Mildner A, Jung S. Macrophages: development and tissue specialization. *Annu Rev Immunol* 2015; **33**: 643-75.
61. Crowley M, Inaba K, Witmerpack M, Steinman RM. The Cell-Surface of Mouse Dendritic Cells - Facs Analyses of Dendritic Cells from Different Tissues Including Thymus. *Cellular Immunology* 1989; **118**(1): 108-25.
62. Newman SL, Henson JE, Henson PM. Phagocytosis of senescent neutrophils by human monocyte-derived macrophages and rabbit inflammatory macrophages. *J Exp Med* 1982; **156**(2): 430-42.
63. Ross R, Benditt EP. Wound healing and collagen formation. I. Sequential changes in components of guinea pig skin wounds observed in the electron microscope. *J Biophys Biochem Cytol* 1961; **11**(3): 677-700.
64. van Furth R, Cohn ZA. The origin and kinetics of mononuclear phagocytes. *J Exp Med* 1968; **128**(3): 415-35.
65. Naito M, Yamamura F, Nishikawa S, Takahashi K. Development, differentiation, and maturation of fetal mouse yolk sac macrophages in cultures. *J Leukoc Biol* 1989; **46**(1): 1-10.
66. Naito M, Takahashi K, Nishikawa S. Development, differentiation, and maturation of macrophages in the fetal mouse liver. *J Leukoc Biol* 1990; **48**(1): 27-37.
67. Yona S, Kim KW, Wolf Y, et al. Fate mapping reveals origins and dynamics of monocytes and tissue macrophages under homeostasis. *Immunity* 2013; **38**(1): 79-91.

68. Hashimoto D, Chow A, Noizat C, et al. Tissue-resident macrophages self-maintain locally throughout adult life with minimal contribution from circulating monocytes. *Immunity* 2013; **38**(4): 792-804.
69. Sunderkotter C, Nikolic T, Dillon MJ, et al. Subpopulations of mouse blood monocytes differ in maturation stage and inflammatory response. *J Immunol* 2004; **172**(7): 4410-7.
70. Jutila MA, Kroese FG, Jutila KL, et al. Ly-6C is a monocyte/macrophage and endothelial cell differentiation antigen regulated by interferon-gamma. *Eur J Immunol* 1988; **18**(11): 1819-26.
71. Geissmann F, Manz MG, Jung S, Sieweke MH, Merad M, Ley K. Development of monocytes, macrophages, and dendritic cells. *Science* 2010; **327**(5966): 656-61.
72. Tamoutounour S, Henri S, Lelouard H, et al. CD64 distinguishes macrophages from dendritic cells in the gut and reveals the Th1-inducing role of mesenteric lymph node macrophages during colitis. *Eur J Immunol* 2012; **42**(12): 3150-66.
73. Tamoutounour S, Williams M, Montanana Sanchis F, et al. Origins and functional specialization of macrophages and of conventional and monocyte-derived dendritic cells in mouse skin. *Immunity* 2013; **39**(5): 925-38.
74. Chow KV, Lew AM, Sutherland RM, Zhan Y. Monocyte-Derived Dendritic Cells Promote Th Polarization, whereas Conventional Dendritic Cells Promote Th Proliferation. *J Immunol* 2016; **196**(2): 624-36.
75. Leon B, Lopez-Bravo M, Ardavin C. Monocyte-derived dendritic cells formed at the infection site control the induction of protective T helper 1 responses against Leishmania. *Immunity* 2007; **26**(4): 519-31.
76. Leon B, Martinez del Hoyo G, Parrillas V, et al. Dendritic cell differentiation potential of mouse monocytes: monocytes represent immediate precursors of CD8- and CD8+ splenic dendritic cells. *Blood* 2004; **103**(7): 2668-76.
77. Randolph GJ, Inaba K, Robbiani DF, Steinman RM, Muller WA. Differentiation of Phagocytic Monocytes into Lymph Node Dendritic Cells In Vivo. *Immunity* 1999; **11**(6): 753-61.
78. Ingersoll MA, Spanbroek R, Lottaz C, et al. Comparison of gene expression profiles between human and mouse monocyte subsets. *Blood* 2010; **115**(3): e10-9.
79. Jakubzick C, Gautier EL, Gibbins SL, et al. Minimal differentiation of classical monocytes as they survey steady-state tissues and transport antigen to lymph nodes. *Immunity* 2013; **39**(3): 599-610.
80. Shortman K, Naik SH. Steady-state and inflammatory dendritic-cell development. *Nat Rev Immunol* 2007; **7**(1): 19-30.
81. Randolph GJ, Ochando J, Partida-Sanchez S. Migration of dendritic cell subsets and their precursors. *Annu Rev Immunol* 2008; **26**: 293-316.
82. Steinman RM, Cohn ZA. Identification of a novel cell type in peripheral lymphoid organs of mice. I. Morphology, quantitation, tissue distribution. *J Exp Med* 1973; **137**(5): 1142-62.
83. Steinman RM, Lustig DS, Cohn ZA. Identification of a novel cell type in peripheral lymphoid organs of mice. 3. Functional properties in vivo. *J Exp Med* 1974; **139**(6): 1431-45.
84. Steinman RM, Kaplan G, Witmer MD, Cohn ZA. Identification of a novel cell type in peripheral lymphoid organs of mice. V. Purification of spleen dendritic cells, new surface markers, and maintenance in vitro. *J Exp Med* 1979; **149**(1): 1-16.
85. Nussenzweig MC, Steinman RM, Unkeless JC, Witmer MD, Gutchinov B, Cohn ZA. Studies of the cell surface of mouse dendritic cells and other leukocytes. *J Exp Med* 1981; **154**(1): 168-87.
86. Steinman RM, Cohn ZA. Identification of a novel cell type in peripheral lymphoid organs of mice. II. Functional properties in vitro. *J Exp Med* 1974; **139**(2): 380-97.
87. Merad M, Sathe P, Helft J, Miller J, Mortha A. The dendritic cell lineage: ontogeny and function of dendritic cells and their subsets in the steady state and the inflamed setting. *Annu Rev Immunol* 2013; **31**: 563-604.
88. Proietto AI, van Dommelen S, Zhou P, et al. Dendritic cells in the thymus contribute to T-regulatory cell induction. *Proc Natl Acad Sci U S A* 2008; **105**(50): 19869-74.

89. Liu K, Victora GD, Schwickert TA, et al. In vivo analysis of dendritic cell development and homeostasis. *Science* 2009; **324**(5925): 392-7.
90. Naik SH, Sathe P, Park HY, et al. Development of plasmacytoid and conventional dendritic cell subtypes from single precursor cells derived in vitro and in vivo. *Nat Immunol* 2007; **8**(11): 1217-26.
91. Nikolic T, de Bruijn MF, Lutz MB, Leenen PJ. Developmental stages of myeloid dendritic cells in mouse bone marrow. *Int Immunol* 2003; **15**(4): 515-24.
92. Onai N, Obata-Onai A, Schmid MA, Ohteki T, Jarrossay D, Manz MG. Identification of clonogenic common Flt3+M-CSFR+ plasmacytoid and conventional dendritic cell progenitors in mouse bone marrow. *Nat Immunol* 2007; **8**(11): 1207-16.
93. Fogg DK, Sibon C, Miled C, et al. A clonogenic bone marrow progenitor specific for macrophages and dendritic cells. *Science* 2006; **311**(5757): 83-7.
94. Henri S, Poulin LF, Tamoutounour S, et al. CD207+ CD103+ dermal dendritic cells cross-present keratinocyte-derived antigens irrespective of the presence of Langerhans cells. *J Exp Med* 2010; **207**(1): 189-206.
95. Schlitzer A, Sivakamasundari V, Chen J, et al. Identification of cDC1- and cDC2-committed DC progenitors reveals early lineage priming at the common DC progenitor stage in the bone marrow. *Nat Immunol* 2015; **16**(7): 718-28.
96. Maldonado-López R, De Smedt T, Michel P, et al. CD8alpha+ and CD8alpha-subclasses of dendritic cells direct the development of distinct T helper cells in vivo. *J Exp Med* 1999; **189**(3): 587-92.
97. Pulendran B, Smith JL, Caspary G, et al. Distinct dendritic cell subsets differentially regulate the class of immune response in vivo. *Proc Natl Acad Sci U S A* 1999; **96**(3): 1036-41.
98. Plantinga M, Guilliams M, Vanheerswynghels M, et al. Conventional and monocyte-derived CD11b(+) dendritic cells initiate and maintain T helper 2 cell-mediated immunity to house dust mite allergen. *Immunity* 2013; **38**(2): 322-35.
99. Redpath SA, Heieis GA, Reynolds LA, Fonseca NM, Kim SS, Perona-Wright G. Functional specialization of intestinal dendritic cell subsets during Th2 helminth infection in mice. *Eur J Immunol* 2018; **48**(1): 87-98.
100. Mesnil C, Sabatel CM, Marichal T, et al. Resident CD11b(+)Ly6C(-) lung dendritic cells are responsible for allergic airway sensitization to house dust mite in mice. *PLoS One* 2012; **7**(12): e53242.
101. Iwasaki A, Kelsall BL. Unique functions of CD11b+, CD8 alpha+, and double-negative Peyer's patch dendritic cells. *J Immunol* 2001; **166**(8): 4884-90.
102. Sulczewski FB, Martino LA, Almeida BDS, et al. Conventional type 1 dendritic cells induce T(H) 1, T(H) 1-like follicular helper T cells and regulatory T cells after antigen boost via DEC205 receptor. *Eur J Immunol* 2020; **50**(12): 1895-911.
103. Mosser DM, Edelson PJ. The mouse macrophage receptor for C3bi (CR3) is a major mechanism in the phagocytosis of Leishmania promastigotes. *J Immunol* 1985; **135**(4): 2785-9.
104. Schonlau F, Scharffetter-Kochanek K, Grabbe S, Pietz B, Sorg C, Sunderkotter C. In experimental leishmaniasis deficiency of CD18 results in parasite dissemination associated with altered macrophage functions and incomplete Th1 cell response. *Eur J Immunol* 2000; **30**(9): 2729-40.
105. Mattner F, Magram J, Ferrante J, et al. Genetically resistant mice lacking interleukin-12 are susceptible to infection with Leishmania major and mount a polarized Th2 cell response. *Eur J Immunol* 1996; **26**(7): 1553-9.
106. Mattner F, Di Padova K, Alber G. Interleukin-12 is indispensable for protective immunity against Leishmania major. *Infect Immun* 1997; **65**(11): 4378-83.
107. Heinzel FP, Schoenhaut DS, Rerko RM, Rosser LE, Gately MK. Recombinant interleukin 12 cures mice infected with Leishmania major. *J Exp Med* 1993; **177**(5): 1505-9.
108. Sypek JP, Chung CL, Mayor SE, et al. Resolution of cutaneous leishmaniasis: interleukin 12 initiates a protective T helper type 1 immune response. *J Exp Med* 1993; **177**(6): 1797-802.

109. von Stebut E, Belkaid Y, Jakob T, Sacks DL, Udey MC. Uptake of *Leishmania major* amastigotes results in activation and interleukin 12 release from murine skin-derived dendritic cells: implications for the initiation of anti-*Leishmania* immunity. *J Exp Med* 1998; **188**(8): 1547-52.
110. Belkaid Y, Butcher B, Sacks DL. Analysis of cytokine production by inflammatory mouse macrophages at the single-cell level: selective impairment of IL-12 induction in *Leishmania*-infected cells. *Eur J Immunol* 1998; **28**(4): 1389-400.
111. Carrera L, Gazzinelli RT, Badolato R, et al. *Leishmania* promastigotes selectively inhibit interleukin 12 induction in bone marrow-derived macrophages from susceptible and resistant mice. *J Exp Med* 1996; **183**(2): 515-26.
112. Weinheber N, Wolfram M, Harbecke D, Aebischer T. Phagocytosis of *Leishmania mexicana* amastigotes by macrophages leads to a sustained suppression of IL-12 production. *Eur J Immunol* 1998; **28**(8): 2467-77.
113. Reiner SL, Zheng S, Wang ZE, Stowring L, Locksley RM. *Leishmania* promastigotes evade interleukin 12 (IL-12) induction by macrophages and stimulate a broad range of cytokines from CD4<sup>+</sup> T cells during initiation of infection. *J Exp Med* 1994; **179**(2): 447-56.
114. Brittingham A, Morrison CJ, McMaster WR, McGwire BS, Chang KP, Mosser DM. Role of the *Leishmania* surface protease gp63 in complement fixation, cell adhesion, and resistance to complement-mediated lysis. *J Immunol* 1995; **155**(6): 3102-11.
115. Nandan D, Reiner NE. Attenuation of gamma interferon-induced tyrosine phosphorylation in mononuclear phagocytes infected with *Leishmania donovani*: selective inhibition of signaling through Janus kinases and Stat1. *Infect Immun* 1995; **63**(11): 4495-500.
116. von Stebut E, Schleicher U, Bogdan C. Kutane Leishmaniasis als Reisedermatose. *Der Hautarzt* 2012; **63**(3): 233-49.
117. Murray HW, Spitalny GL, Nathan CF. Activation of mouse peritoneal macrophages in vitro and in vivo by interferon-gamma. *J Immunol* 1985; **134**(3): 1619-22.
118. Titus RG, Kelso A, Louis JA. Intracellular destruction of *Leishmania tropica* by macrophages activated with macrophage activating factor/interferon. *Clin Exp Immunol* 1984; **55**(1): 157-65.
119. Murray HW, Rubin BY, Rothermel CD. Killing of intracellular *Leishmania donovani* by lymphokine-stimulated human mononuclear phagocytes. Evidence that interferon-gamma is the activating lymphokine. *J Clin Invest* 1983; **72**(4): 1506-10.
120. Sadick MD, Locksley RM, Tubbs C, Raff HV. Murine cutaneous leishmaniasis: resistance correlates with the capacity to generate interferon-gamma in response to *Leishmania* antigens in vitro. *J Immunol* 1986; **136**(2): 655-61.
121. Theodos CM, Povinelli L, Molina R, Sherry B, Titus RG. Role of tumor necrosis factor in macrophage leishmanicidal activity in vitro and resistance to cutaneous leishmaniasis in vivo. *Infect Immun* 1991; **59**(8): 2839-42.
122. Bogdan C, Moll H, Solbach W, Rollinghoff M. Tumor necrosis factor-alpha in combination with interferon-gamma, but not with interleukin 4 activates murine macrophages for elimination of *Leishmania major* amastigotes. *Eur J Immunol* 1990; **20**(5): 1131-5.
123. Liew FY, Li Y, Millott S. Tumor necrosis factor-alpha synergizes with IFN-gamma in mediating killing of *Leishmania major* through the induction of nitric oxide. *J Immunol* 1990; **145**(12): 4306-10.
124. Liew FY, Parkinson C, Millott S, Severn A, Carrier M. Tumour necrosis factor (TNF alpha) in leishmaniasis. I. TNF alpha mediates host protection against cutaneous leishmaniasis. *Immunology* 1990; **69**(4): 570-3.
125. Nacy CA, Fortier AH, Meltzer MS, Buchmeier NA, Schreiber RD. Macrophage activation to kill *Leishmania major*: activation of macrophages for intracellular destruction of amastigotes can be induced by both recombinant interferon-gamma and non-interferon lymphokines. *J Immunol* 1985; **135**(5): 3505-11.
126. Stenger S, Thuring H, Rollinghoff M, Bogdan C. Tissue expression of inducible nitric oxide synthase is closely associated with resistance to *Leishmania major*. *J Exp Med* 1994; **180**(3): 783-93.

127. Liew FY, Li Y, Moss D, Parkinson C, Rogers MV, Moncada S. Resistance to *Leishmania major* infection correlates with the induction of nitric oxide synthase in murine macrophages. *Eur J Immunol* 1991; **21**(12): 3009-14.
128. Titus RG, Sherry B, Cerami A. Tumor necrosis factor plays a protective role in experimental murine cutaneous leishmaniasis. *J Exp Med* 1989; **170**(6): 2097-104.
129. Moll H, Fuchs H, Blank C, Rollinghoff M. Langerhans cells transport *Leishmania major* from the infected skin to the draining lymph node for presentation to antigen-specific T cells. *Eur J Immunol* 1993; **23**(7): 1595-601.
130. Ritter U, Meissner A, Scheidig C, Korner H. CD8 alpha- and Langerin-negative dendritic cells, but not Langerhans cells, act as principal antigen-presenting cells in leishmaniasis. *Eur J Immunol* 2004; **34**(6): 1542-50.
131. Baldwin T, Henri S, Curtis J, et al. Dendritic cell populations in *Leishmania major*-infected skin and draining lymph nodes. *Infect Immun* 2004; **72**(4): 1991-2001.
132. Heyde S, Philipsen L, Formaglio P, et al. CD11c-expressing Ly6C+CCR2+ monocytes constitute a reservoir for efficient *Leishmania* proliferation and cell-to-cell transmission. *PLoS Pathog* 2018; **14**(10): e1007374.
133. Goncalves R, Zhang X, Cohen H, Debrabant A, Mosser DM. Platelet activation attracts a subpopulation of effector monocytes to sites of *Leishmania major* infection. *J Exp Med* 2011; **208**(6): 1253-65.
134. Cangussu SD, Souza CC, Campos CF, Vieira LQ, Afonso LC, Arantes RM. Histopathology of *Leishmania major* infection: revisiting *L. major* histopathology in the ear dermis infection model. *Mem Inst Oswaldo Cruz* 2009; **104**(6): 918-22.
135. Velasquez LG, Galuppo MK, E DER, et al. Distinct courses of infection with *Leishmania (L.) amazonensis* are observed in BALB/c, BALB/c nude and C57BL/6 mice. *Parasitology* 2016; **143**(6): 692-703.
136. Locksley RM, Heinzl FP, Sadick MD, Holaday BJ, Gardner KD, Jr. Murine cutaneous leishmaniasis: susceptibility correlates with differential expansion of helper T-cell subsets. *Ann Inst Pasteur Immunol* 1987; **138**(5): 744-9.
137. Belkaid Y, Kamhawi S, Modi G, et al. Development of a natural model of cutaneous leishmaniasis: powerful effects of vector saliva and saliva preexposure on the long-term outcome of *Leishmania major* infection in the mouse ear dermis. *J Exp Med* 1998; **188**(10): 1941-53.
138. Howard JG, Hale C, Chan-Liew WL. Immunological regulation of experimental cutaneous leishmaniasis. 1. Immunogenetic aspects of susceptibility to *Leishmania tropica* in mice. *Parasite Immunol* 1980; **2**(4): 303-14.
139. Scott P, Natovitz P, Coffman RL, Pearce E, Sher A. Immunoregulation of cutaneous leishmaniasis. T cell lines that transfer protective immunity or exacerbation belong to different T helper subsets and respond to distinct parasite antigens. *J Exp Med* 1988; **168**(5): 1675-84.
140. Sommer F, Meixner M, Mannherz M, Ogilvie AL, Rollinghoff M, Lohoff M. Analysis of cytokine patterns produced by individual CD4+ lymph node cells during experimental murine leishmaniasis in resistant and susceptible mice. *Int Immunol* 1998; **10**(12): 1853-61.
141. Malherbe L, Filippi C, Julia V, et al. Selective activation and expansion of high-affinity CD4+ T cells in resistant mice upon infection with *Leishmania major*. *Immunity* 2000; **13**(6): 771-82.
142. Heinzl FP, Sadick MD, Holaday BJ, Coffman RL, Locksley RM. Reciprocal expression of interferon gamma or interleukin 4 during the resolution or progression of murine leishmaniasis. Evidence for expansion of distinct helper T cell subsets. *J Exp Med* 1989; **169**(1): 59-72.
143. Morris L, Troutt AB, McLeod KS, Kelso A, Handman E, Aebischer T. Interleukin-4 but not gamma interferon production correlates with the severity of murine cutaneous leishmaniasis. *Infect Immun* 1993; **61**(8): 3459-65.
144. Kopf M, Brombacher F, Kohler G, et al. IL-4-deficient Balb/c mice resist infection with *Leishmania major*. *J Exp Med* 1996; **184**(3): 1127-36.

145. Lopez Kostka S, Dinges S, Griewank K, Iwakura Y, Udey MC, von Stebut E. IL-17 promotes progression of cutaneous leishmaniasis in susceptible mice. *J Immunol* 2009; **182**(5): 3039-46.
146. Caldwell RW, Rodriguez PC, Toque HA, Narayanan SP, Caldwell RB. Arginase: A Multifaceted Enzyme Important in Health and Disease. *Physiol Rev* 2018; **98**(2): 641-65.
147. Modolell M, Corraliza IM, Link F, Soler G, Eichmann K. Reciprocal regulation of the nitric oxide synthase/arginase balance in mouse bone marrow-derived macrophages by TH1 and TH2 cytokines. *Eur J Immunol* 1995; **25**(4): 1101-4.
148. Lowenstein CJ, Glatt CS, Bredt DS, Snyder SH. Cloned and expressed macrophage nitric oxide synthase contrasts with the brain enzyme. *Proc Natl Acad Sci U S A* 1992; **89**(15): 6711-5.
149. Hevel JM, White KA, Marletta MA. Purification of the inducible murine macrophage nitric oxide synthase. Identification as a flavoprotein. *J Biol Chem* 1991; **266**(34): 22789-91.
150. Stuehr DJ, Cho HJ, Kwon NS, Weise MF, Nathan CF. Purification and characterization of the cytokine-induced macrophage nitric oxide synthase: an FAD- and FMN-containing flavoprotein. *Proc Natl Acad Sci U S A* 1991; **88**(17): 7773-7.
151. Yui S, Mikami M, Yamazaki M. Purification and characterization of the cytotoxic factor in rat peritoneal exudate cells: its identification as the calcium binding protein complex, calprotectin. *J Leukoc Biol* 1995; **58**(3): 307-16.
152. Diefenbach A, Schindler H, Rollinghoff M, Yokoyama WM, Bogdan C. Requirement for type 2 NO synthase for IL-12 signaling in innate immunity. *Science* 1999; **284**(5416): 951-5.
153. Lu L, Bonham CA, Chambers FG, et al. Induction of nitric oxide synthase in mouse dendritic cells by IFN-gamma, endotoxin, and interaction with allogeneic T cells: nitric oxide production is associated with dendritic cell apoptosis. *J Immunol* 1996; **157**(8): 3577-86.
154. Qureshi AA, Hosoi J, Xu S, Takashima A, Granstein RD, Lerner EA. Langerhans cells express inducible nitric oxide synthase and produce nitric oxide. *J Invest Dermatol* 1996; **107**(6): 815-21.
155. Ross R, Gillitzer C, Kleinz R, et al. Involvement of NO in contact hypersensitivity. *Int Immunol* 1998; **10**(1): 61-9.
156. Robinson LJ, Weremowicz S, Morton CC, Michel T. Isolation and chromosomal localization of the human endothelial nitric oxide synthase (NOS3) gene. *Genomics* 1994; **19**(2): 350-7.
157. Lamas S, Marsden PA, Li GK, Tempst P, Michel T. Endothelial nitric oxide synthase: molecular cloning and characterization of a distinct constitutive enzyme isoform. *Proc Natl Acad Sci U S A* 1992; **89**(14): 6348-52.
158. Marsden PA, Heng HH, Scherer SW, et al. Structure and chromosomal localization of the human constitutive endothelial nitric oxide synthase gene. *J Biol Chem* 1993; **268**(23): 17478-88.
159. Forstermann U, Pollock JS, Schmidt HH, Heller M, Murad F. Calmodulin-dependent endothelium-derived relaxing factor/nitric oxide synthase activity is present in the particulate and cytosolic fractions of bovine aortic endothelial cells. *Proc Natl Acad Sci U S A* 1991; **88**(5): 1788-92.
160. Pollock JS, Forstermann U, Mitchell JA, et al. Purification and characterization of particulate endothelium-derived relaxing factor synthase from cultured and native bovine aortic endothelial cells. *Proc Natl Acad Sci U S A* 1991; **88**(23): 10480-4.
161. Fujisawa H, Ogura T, Kurashima Y, Yokoyama T, Yamashita J, Esumi H. Expression of two types of nitric oxide synthase mRNA in human neuroblastoma cell lines. *J Neurochem* 1994; **63**(1): 140-5.
162. Mayer B, John M, Bohme E. Purification of a Ca<sup>2+</sup>/calmodulin-dependent nitric oxide synthase from porcine cerebellum. Cofactor-role of tetrahydrobiopterin. *FEBS Lett* 1990; **277**(1-2): 215-9.
163. Bredt DS, Snyder SH. Isolation of nitric oxide synthetase, a calmodulin-requiring enzyme. *Proc Natl Acad Sci U S A* 1990; **87**(2): 682-5.
164. Karupiah G, Xie QW, Buller RM, Nathan C, Duarte C, MacMicking JD. Inhibition of viral replication by interferon-gamma-induced nitric oxide synthase. *Science* 1993; **261**(5127): 1445-8.

165. Heck DE, Laskin DL, Gardner CR, Laskin JD. Epidermal growth factor suppresses nitric oxide and hydrogen peroxide production by keratinocytes. Potential role for nitric oxide in the regulation of wound healing. *J Biol Chem* 1992; **267**(30): 21277-80.
166. Bogdan C. Nitric oxide and the immune response. *Nat Immunol* 2001; **2**(10): 907-16.
167. Lykens JE, Terrell CE, Zoller EE, et al. Mice with a selective impairment of IFN-gamma signaling in macrophage lineage cells demonstrate the critical role of IFN-gamma-activated macrophages for the control of protozoan parasitic infections in vivo. *J Immunol* 2010; **184**(2): 877-85.
168. Munder M, Eichmann K, Moran JM, Centeno F, Soler G, Modolell M. Th1/Th2-regulated expression of arginase isoforms in murine macrophages and dendritic cells. *J Immunol* 1999; **163**(7): 3771-7.
169. Munder M, Eichmann K, Modolell M. Alternative metabolic states in murine macrophages reflected by the nitric oxide synthase/arginase balance: competitive regulation by CD4+ T cells correlates with Th1/Th2 phenotype. *J Immunol* 1998; **160**(11): 5347-54.
170. MacMicking J, Xie QW, Nathan C. Nitric oxide and macrophage function. *Annu Rev Immunol* 1997; **15**: 323-50.
171. Xie QW, Cho HJ, Calaycay J, et al. Cloning and characterization of inducible nitric oxide synthase from mouse macrophages. *Science* 1992; **256**(5054): 225-8.
172. Iniesta V, Carcelen J, Molano I, et al. Arginase I induction during Leishmania major infection mediates the development of disease. *Infect Immun* 2005; **73**(9): 6085-90.
173. Stenger S, Donhauser N, Thuring H, Rollinghoff M, Bogdan C. Reactivation of latent leishmaniasis by inhibition of inducible nitric oxide synthase. *J Exp Med* 1996; **183**(4): 1501-14.
174. Witte MB, Barbul A, Schick MA, Vogt N, Becker HD. Upregulation of arginase expression in wound-derived fibroblasts. *J Surg Res* 2002; **105**(1): 35-42.
175. Campbell L, Saville CR, Murray PJ, Cruickshank SM, Hardman MJ. Local arginase 1 activity is required for cutaneous wound healing. *J Invest Dermatol* 2013; **133**(10): 2461-70.
176. Kampfer H, Pfeilschifter J, Frank S. Expression and activity of arginase isoenzymes during normal and diabetes-impaired skin repair. *J Invest Dermatol* 2003; **121**(6): 1544-51.
177. Corraliza IM, Soler G, Eichmann K, Modolell M. Arginase induction by suppressors of nitric oxide synthesis (IL-4, IL-10 and PGE2) in murine bone-marrow-derived macrophages. *Biochem Biophys Res Commun* 1995; **206**(2): 667-73.
178. Kossel A, Dakin HD. Über die Arginase. 1904; **41**(4): 321-31.
179. Krebs HA, Henseleit K. Untersuchungen über die Harnstoffbildung im Tierkörper. 1932; **210**(1-2): 33-66.
180. Meister A. Enzymatic transamination reactions involving arginine and ornithine. *J Biol Chem* 1954; **206**(2): 587-96.
181. Albina JE, Mills CD, Barbul A, et al. Arginine metabolism in wounds. *Am J Physiol* 1988; **254**(4 Pt 1): E459-67.
182. Wu G, Morris SM, Jr. Arginine metabolism: nitric oxide and beyond. *Biochem J* 1998; **336** ( Pt 1)(Pt 1): 1-17.
183. Rojkind M, Diaz de Leon L. Collagen biosynthesis in cirrhotic rat liver slices a regulatory mechanism. *Biochim Biophys Acta* 1970; **217**(2): 512-22.
184. Smith RJ, Phang JM. Proline metabolism in cartilage: the importance of proline biosynthesis. *Metabolism* 1978; **27**(6): 685-94.
185. Smith RJ, Phang JM. The importance of ornithine as a precursor for proline in mammalian cells. *J Cell Physiol* 1979; **98**(3): 475-81.
186. Paduch K, Debus A, Rai B, Schleicher U, Bogdan C. Resolution of Cutaneous Leishmaniasis and Persistence of Leishmania major in the Absence of Arginase 1. *J Immunol* 2019; **202**(5): 1453-64.
187. Schleicher U, Paduch K, Debus A, et al. TNF-Mediated Restriction of Arginase 1 Expression in Myeloid Cells Triggers Type 2 NO Synthase Activity at the Site of Infection. *Cell Rep* 2016; **15**(5): 1062-75.
188. Kropf P, Fuentes JM, Fahrnich E, et al. Arginase and polyamine synthesis are key factors in the regulation of experimental leishmaniasis in vivo. *FASEB J* 2005; **19**(8): 1000-2.

189. Rutschman R, Lang R, Hesse M, Ihle JN, Wynn TA, Murray PJ. Cutting edge: Stat6-dependent substrate depletion regulates nitric oxide production. *J Immunol* 2001; **166**(4): 2173-7.
190. El-Gayar S, Thuring-Nahler H, Pfeilschifter J, Rollinghoff M, Bogdan C. Translational control of inducible nitric oxide synthase by IL-13 and arginine availability in inflammatory macrophages. *J Immunol* 2003; **171**(9): 4561-8.
191. Marletta MA, Yoon PS, Iyengar R, Leaf CD, Wishnok JS. Macrophage oxidation of L-arginine to nitrite and nitrate: nitric oxide is an intermediate. *Biochemistry* 1988; **27**(24): 8706-11.
192. Dupasquier M, Stoitzner P, van Oudenaren A, Romani N, Leenen PJ. Macrophages and dendritic cells constitute a major subpopulation of cells in the mouse dermis. *J Invest Dermatol* 2004; **123**(5): 876-9.
193. Glennie ND, Volk SW, Scott P. Skin-resident CD4+ T cells protect against *Leishmania major* by recruiting and activating inflammatory monocytes. *PLoS Pathog* 2017; **13**(4): e1006349.
194. Metlay JP, Witmer-Pack MD, Agger R, Crowley MT, Lawless D, Steinman RM. The distinct leukocyte integrins of mouse spleen dendritic cells as identified with new hamster monoclonal antibodies. *J Exp Med* 1990; **171**(5): 1753-71.
195. Crowley MT, Inaba K, Witmer-Pack MD, Gezelter S, Steinman RM. Use of the fluorescence activated cell sorter to enrich dendritic cells from mouse spleen. *J Immunol Methods* 1990; **133**(1): 55-66.
196. Gautier EL, Shay T, Miller J, et al. Gene-expression profiles and transcriptional regulatory pathways that underlie the identity and diversity of mouse tissue macrophages. *Nat Immunol* 2012; **13**(11): 1118-28.
197. Bain CC, Scott CL, Uronen-Hansson H, et al. Resident and pro-inflammatory macrophages in the colon represent alternative context-dependent fates of the same Ly6Chi monocyte precursors. *Mucosal Immunol* 2013; **6**(3): 498-510.
198. Hashimoto D, Miller J, Merad M. Dendritic cell and macrophage heterogeneity in vivo. *Immunity* 2011; **35**(3): 323-35.
199. Hogg N, Takacs L, Palmer DG, Selvendran Y, Allen C. The p150,95 molecule is a marker of human mononuclear phagocytes: comparison with expression of class II molecules. *Eur J Immunol* 1986; **16**(3): 240-8.
200. Myones BL, Dalzell JG, Hogg N, Ross GD. Neutrophil and monocyte cell surface p150,95 has iC3b-receptor (CR4) activity resembling CR3. *J Clin Invest* 1988; **82**(2): 640-51.
201. Springer TA, Miller LJ, Anderson DC. p150,95, the third member of the Mac-1, LFA-1 human leukocyte adhesion glycoprotein family. *J Immunol* 1986; **136**(1): 240-5.
202. Sanchez-Madrid F, Simon P, Thompson S, Springer TA. Mapping of antigenic and functional epitopes on the alpha- and beta-subunits of two related mouse glycoproteins involved in cell interactions, LFA-1 and Mac-1. *J Exp Med* 1983; **158**(2): 586-602.
203. Springer T, Galfre G, Secher DS, Milstein C. Mac-1: a macrophage differentiation antigen identified by monoclonal antibody. *Eur J Immunol* 1979; **9**(4): 301-6.
204. Langlet C, Tamoutounour S, Henri S, et al. CD64 expression distinguishes monocyte-derived and conventional dendritic cells and reveals their distinct role during intramuscular immunization. *J Immunol* 2012; **188**(4): 1751-60.
205. Serbina NV, Pamer EG. Monocyte emigration from bone marrow during bacterial infection requires signals mediated by chemokine receptor CCR2. *Nat Immunol* 2006; **7**(3): 311-7.
206. Serbina NV, Salazar-Mather TP, Biron CA, Kuziel WA, Pamer EG. TNF/iNOS-producing dendritic cells mediate innate immune defense against bacterial infection. *Immunity* 2003; **19**(1): 59-70.
207. Crane MJ, Daley JM, van Houtte O, Brancato SK, Henry WL, Jr., Albina JE. The monocyte to macrophage transition in the murine sterile wound. *PLoS One* 2014; **9**(1): e86660.
208. Lagasse E, Weissman IL. Flow cytometric identification of murine neutrophils and monocytes. *J Immunol Methods* 1996; **197**(1-2): 139-50.

209. Barroca H. Cytospin Technique. In: Schmitt F, ed. *Cytopathology*. Cham: Springer International Publishing; 2017: 107-10.
210. RAL DIFF-QUIK, a fast variation of romanowsky stain. <https://www.ral-diagnostics.fr/en/solutions/human-biology-haematology-cytology/ral-diff-quick/>.
211. Ehrchen JM, Roebrock K, Foell D, et al. Keratinocytes determine Th1 immunity during early experimental leishmaniasis. *PLoS Pathog* 2010; **6**(4): e1000871.
212. Lira R, Doherty M, Modi G, Sacks D. Evolution of lesion formation, parasitic load, immune response, and reservoir potential in C57BL/6 mice following high- and low-dose challenge with *Leishmania major*. *Infect Immun* 2000; **68**(9): 5176-82.
213. Castelli G, Bruno F, Reale S, Catanzaro S, Valenza V, Vitale F. Molecular Diagnosis of Leishmaniasis: Quantification of Parasite Load by a Real-Time PCR Assay with High Sensitivity. *Pathogens* 2021; **10**(7).
214. Muller I, Pedrazzini T, Farrell JP, Louis J. T-cell responses and immunity to experimental infection with *leishmania major*. *Annu Rev Immunol* 1989; **7**: 561-78.
215. Swihart K, Fruth U, Messmer N, et al. Mice from a genetically resistant background lacking the interferon gamma receptor are susceptible to infection with *Leishmania major* but mount a polarized T helper cell 1-type CD4+ T cell response. *J Exp Med* 1995; **181**(3): 961-71.
216. Olekhnovitch R, Ryffel B, Müller AJ, Bousso P. Collective nitric oxide production provides tissue-wide immunity during *Leishmania* infection. *J Clin Invest* 2014; **124**(4): 1711-22.
217. Leon B, Ardavin C. Monocyte-derived dendritic cells in innate and adaptive immunity. *Immunol Cell Biol* 2008; **86**(4): 320-4.
218. Kim TG, Kim SH, Park J, et al. Skin-Specific CD301b(+) Dermal Dendritic Cells Drive IL-17-Mediated Psoriasis-Like Immune Response in Mice. *J Invest Dermatol* 2018; **138**(4): 844-53.
219. Dietze-Schwonberg K, Lorenz B, Lopez Kostka S, Waisman A, von Stebut E. Parasite Clearance in Leishmaniasis in Resistant Animals Is Independent of the IL-23/IL-17A Axis. *J Invest Dermatol* 2016; **136**(9): 1906-8.
220. Szulc-Dąbrowska L, Biernacka Z, Koper M, et al. Differential Activation of Splenic cDC1 and cDC2 Cell Subsets following Poxvirus Infection of BALB/c and C57BL/6 Mice. *Cells* 2023; **13**(1).
221. Kautz-Neu K, Schwonberg K, Fischer MR, Schermann AI, von Stebut E. Dendritic cells in *Leishmania major* infections: mechanisms of parasite uptake, cell activation and evidence for physiological relevance. *Med Microbiol Immunol* 2012; **201**(4): 581-92.
222. Santini SM, Lapenta C, Logozzi M, et al. Type I interferon as a powerful adjuvant for monocyte-derived dendritic cell development and activity in vitro and in Hu-PBL-SCID mice. *J Exp Med* 2000; **191**(10): 1777-88.
223. Woelbing F, Kostka SL, Moelle K, et al. Uptake of *Leishmania major* by dendritic cells is mediated by Fcγ receptors and facilitates acquisition of protective immunity. *J Exp Med* 2006; **203**(1): 177-88.
224. Thepen T, van Vuuren AJ, Kiekens RC, Damen CA, Vooijs WC, van De Winkel JG. Resolution of cutaneous inflammation after local elimination of macrophages. *Nat Biotechnol* 2000; **18**(1): 48-51.
225. Kiekens RC, Thepen T, Bihari IC, Knol EF, Van De Winkel JG, Bruijnzeel-Koomen CA. Expression of Fc receptors for IgG during acute and chronic cutaneous inflammation in atopic dermatitis. *Br J Dermatol* 2000; **142**(6): 1106-13.
226. Luque-Martin R, Angell DC, Kalxdorf M, et al. IFN-γ Drives Human Monocyte Differentiation into Highly Proinflammatory Macrophages That Resemble a Phenotype Relevant to Psoriasis. *J Immunol* 2021; **207**(2): 555-68.
227. Lee SH, Chaves MM, Kamenyeva O, et al. M2-like, dermal macrophages are maintained via IL-4/CCL24-mediated cooperative interaction with eosinophils in cutaneous leishmaniasis. *Sci Immunol* 2020; **5**(46).
228. Bogdan C. Macrophages as host, effector and immunoregulatory cells in leishmaniasis: impact of tissue micro-environment and metabolism. *Cytokine: X* 2020: 100041.

229. Vouldoukis I, Riveros-Moreno V, Dugas B, et al. The killing of *Leishmania major* by human macrophages is mediated by nitric oxide induced after ligation of the Fc epsilon RII/CD23 surface antigen. *Proc Natl Acad Sci U S A* 1995; **92**(17): 7804-8.
230. Liew FY, Millott S, Parkinson C, Palmer RM, Moncada S. Macrophage killing of *Leishmania* parasite in vivo is mediated by nitric oxide from L-arginine. *J Immunol* 1990; **144**(12): 4794-7.
231. Assreuy J, Cunha FQ, Epperlein M, et al. Production of nitric oxide and superoxide by activated macrophages and killing of *Leishmania major*. *Eur J Immunol* 1994; **24**(3): 672-6.
232. Wei XQ, Charles IG, Smith A, et al. Altered immune responses in mice lacking inducible nitric oxide synthase. *Nature* 1995; **375**(6530): 408-11.
233. Choi BS, Martinez-Falero IC, Corset C, et al. Differential impact of L-arginine deprivation on the activation and effector functions of T cells and macrophages. *J Leukoc Biol* 2009; **85**(2): 268-77.
234. Munder M, Schneider H, Luckner C, et al. Suppression of T-cell functions by human granulocyte arginase. *Blood* 2006; **108**(5): 1627-34.
235. Modolell M, Choi BS, Ryan RO, et al. Local suppression of T cell responses by arginase-induced L-arginine depletion in nonhealing leishmaniasis. *PLoS Negl Trop Dis* 2009; **3**(7): e480.
236. Rodriguez PC, Zea AH, DeSalvo J, et al. L-arginine consumption by macrophages modulates the expression of CD3 zeta chain in T lymphocytes. *J Immunol* 2003; **171**(3): 1232-9.
237. Rodriguez PC, Zea AH, Culotta KS, Zabaleta J, Ochoa JB, Ochoa AC. Regulation of T cell receptor CD3zeta chain expression by L-arginine. *J Biol Chem* 2002; **277**(24): 21123-9.
238. Roberts SC, Tancer MJ, Polinsky MR, Gibson KM, Heby O, Ullman B. Arginase plays a pivotal role in polyamine precursor metabolism in *Leishmania*. Characterization of gene deletion mutants. *J Biol Chem* 2004; **279**(22): 23668-78.
239. Reguera RM, Balana-Fouce R, Showalter M, Hickerson S, Beverley SM. *Leishmania major* lacking arginase (ARG) are auxotrophic for polyamines but retain infectivity to susceptible BALB/c mice. *Mol Biochem Parasitol* 2009; **165**(1): 48-56.
240. Wilmes V, Kur IM, Weigert A, Verhoff MA, Gradhand E, Kaufenstein S. iNOS expressing macrophages co-localize with nitrotyrosine staining after myocardial infarction in humans. *Front Cardiovasc Med* 2023; **10**: 1104019.
241. De Trez C, Magez S, Akira S, Ryffel B, Carlier Y, Muraille E. iNOS-producing inflammatory dendritic cells constitute the major infected cell type during the chronic *Leishmania major* infection phase of C57BL/6 resistant mice. *PLoS Pathog* 2009; **5**(6): e1000494.
242. Wu SH, Lee JH, Koo BK. Lineage Tracing: Computational Reconstruction Goes Beyond the Limit of Imaging. *Mol Cells* 2019; **42**(2): 104-12.

## 7. Appendix

### 7.1 List of Figures

Figure 1 Leishmania life cycle .....	15
Figure 2 Gating strategy .....	40
Figure 3 Ear lesion curve.....	48
Figure 4 Parasite uptake into a MΦ isolated from infected ear tissue .....	49
Figure 5 IFN $\gamma$ quantification in supernatant of LN cells restimulated with SLA at different time points after infection with <i>L. major</i> .....	52
Figure 6 Viable, CD45 <sup>+</sup> , lineage <sup>neg</sup> myeloid cells in naïve mice and after infection with <i>L. major</i> .....	53
Figure 7 MHC II <sup>+</sup> and MHC II <sup>neg</sup> myeloid ear tissue cells in naïve mice and after infection with <i>L. major</i> .....	55
Figure 8 Analysis of myeloid ear tissue cells in naïve mice and after infection with <i>L. major</i> based on CD11b and CD11c expression.....	57
Figure 9 Analysis of Ly6C and CD64 expression among myeloid cell group 2 in ear tissue of naïve mice and after infection with <i>L. major</i> .....	59
Figure 10 Analysis of Ly6C and CD64 expression among myeloid cell group 3 in ear tissue of naïve mice and after infection with <i>L. major</i> .....	61
Figure 11 iNOS and/or arginase-1 expression in MHC II <sup>+</sup> myeloid cells (1, 2 and 3) in ear tissue of naïve mice and after infection with <i>L. major</i> .....	63
Figure 12 iNOS and arginase-1 expression in MHC II <sup>+</sup> myeloid cells in ear tissue of naïve mice and after infection with <i>L. major</i> , specifically distributed into cells positive for iNOS and/or Arginase-1 expression.....	66
Figure 13 iNOS and arginase-1 expression in MHC II <sup>+</sup> myeloid cells subsets (I-VIII) in ear tissue of C57BL/6 and BALB/c mice at week 6 and 9 after infection with <i>L. major</i> , specifically distributed into cells expressing either iNOS or arginase-1 or both, iNOS and arginase-1.....	68
Figure 14 Analysis of CD11b and Ly6C expression in MHC II <sup>neg</sup> ear tissue cells in naïve mice and after infection with <i>L. major</i> .....	71

### 7.2 List of tables

Table 1 Number of mice analyzed per time point and strain.....	34
Table 2 Antibody panel used for surface staining .....	37
Table 3 Antibody panel used for intracellular staining.....	38
Table 4 Presence of <i>L. major</i> amastigotes in ear tissue of C57BL/6 and BALB/c mice at different time-points after infection with <i>L. major</i> .....	50

## **8. Vorabveröffentlichungen von Ergebnissen**